12-2018

Characterization of SIP68 for its Role in Plant Stress Signaling

Saroj Chandra Lohani
East Tennessee State University

Characterization of SIP68 for its Role in Plant Stress Signaling

---

A thesis

presented to

The faculty of the Department of Biological Sciences

East Tennessee State University

In partial fulfillment

of the requirement for the degree

Master of Science in Biology

---

by

Saroj Chandra Lohani

December 2018

Dhirendra Kumar, Chair, PhD

Cecilia McIntosh, PhD

Bert Lampson, PhD

Keywords: SABP2, SIP68, Glucosyltransferase, Subcellular localization, RNAi, CRISPR Cas9

ABSTRACT

Characterization of SIP68 for its Role in Plant Stress Signaling

by

Saroj Chandra Lohani

Glucosyltransferases catalyze the transfer of glucose molecules from an active donor to acceptor molecules and are involved in many plant processes. SIP68, a tobacco glucosyltransferase protein, is a SABP2-interacting protein. It was identified in a yeast two-hybrid screen using SABP2 as bait and tobacco proteins as prey. SABP2, converts methyl salicylate to salicylic acid (SA) as a part of the signal transduction pathways in SA-mediated defense signaling. Subcellular localization is a crucial aspect of protein functional analysis to assess its biological function. The recombinant SIP68 tagged with eGFP was expressed transiently in *Nicotiana benthamiana* and observed under confocal microscopy. Fluorescent signals were observed in the epidermal cells. Subcellular fractionation of the tobacco leaves transiently expressing SIP68-+eGFP confirmed that SIP68 is localized in the cytosol. To study the role of SIP68 in plant stress signaling, transgenic lines with altered SIP68 expression were generated using RNAi and CRISPR Cas9 and analyzed.

ACKNOWLEDGMENTS

Firstly, I would like to express my profound gratitude to my committee chair, Dr. Dhirendra Kumar, and committee members, Dr. Cecilia McIntosh, and Dr. Bert Lampson for their regular supervision and expert guidance during my research work. I am always indebted to them for their valuable suggestions and constructive criticisms. I would like to especially thank my advisor Dr. Dhirendra Kumar for his continuous support, inspiration and bringing best out of me. I would also like to thank the faculty and staff members of the Department of Biological Sciences, ETSU for their help, support and encouragement. I would also like to convey my gratefulness to my lab members Bal Krishna Chand Thakuri, Shantaya Andrews, Baylee Davenport and Sanjiv Das. I would also like to thank Dr. Hong-Gu Kang (Texas State University); Dr. Yiping Qi, and Dr. Levi Lowder (East Carolina University), and Dr. Johannes Stuttmann (Martin Luther University Halle-Wittenberg) for their suggestions on CRISPR Cas9. I would also like to thank Rolf Fritz for helping with confocal microscopy at the Confocal Microscopy Core Facility at Quillen College of Medicine, ETSU. I would also like to thank School of Graduate Studies ETSU for a graduate assistantship. I would also like to thank CSIRO (Australia) and Arabidopsis Biological Resource Center (ABRC) for providing plasmids used in this research. This research was supported by a grant from the National Science Foundation (MCB#1022077) to Dr. Dhirendra Kumar and funds from the Department of Biological Sciences, ETSU. I would also like to thank my family and friends for their unrelenting love, support, and care. Additionally, I sincerely acknowledge various authors and publishers to whom I have referred in the text.

TABLE OF CONTENTS

Page

LIST OF TABLES

Table Page

LIST OF FIGURES

Figure Page

CHAPTER 1

INTRODUCTION

Plants are universally recognized as the essential foundation of the living world. Their ability to produce food, recycle carbon dioxide and regenerate oxygen has played a pivotal role in the cycle of life on earth. From millions of years, their presence has become a cornerstone for survival, growth, and continuation of other living beings. Though very few plant species are utilized by humans as a food source, many thousands have proved to be culturally and economically important, providing materials for fuel, shelter, and clothing. In addition to this, a significant number of plants are used for the medicinal and aromatic purposes. An estimated figure of 50,000-80,000 flowering plants have medicinal utilities (Chen et al. 2016) making an essential contribution to healthcare and giving potential alternative enterprises for the farmer from developing countries.

With the immense importance and astonishing versatility, plants are always under threat. These threats come in different forms broadly classified as biotic and abiotic stressors. During their lifespan, plants are in constant interaction with various components of the ecosystem. Most of the interactions are essential for plant survival and proliferation, but in some cases, they are antagonistic resulting in either death or loss of yield. It is estimated that around 20-40% of crop yield is lost due to pathogens, animals, and weeds (Savary et al. 2012). This loss has significant impact on the global as well as individual country's economy. In the United States alone, approximately 40 billion dollars' is lost annually due to infections (Fang and Ramasamy 2015).

With an increase in the human population, the demand to increase food production is increasing tremendously. It is estimated that food production needs to be increased by 70-100% by 2050 to meet the needs of the growing human population (Godfray et al. 2010). This situation is compounded by the loss of agricultural land due to social, political and climate change related issues (Zabel et al. 2014). Due to all this, feeding the future generation seems very challenging. In such a demanding situation, minimizing the crop loss due to diseases and adverse environmental conditions is likely to play a crucial role in protecting crops against different stressors.

There are various methods for crop protection such as use of the chemical substances, biological control agents, physical methods such as biofumigation, solarization, hot water treatment, cultural practices such as the growth of resistant cultivar, crop rotation, multi-cropping, and soil amendment. (Yuliar et al. 2015). Use of pesticides has always been the most popular traditional approach (Ridgway et al. 1978). It provides a good control mechanism, but these chemicals find their way into our food chain and can cause serious health-related issues (Nicolopoulou-Stamati et al. 2016). At the same time there is always a possibility of development of resistance in the pathogen that significantly increases the lethal dose increasing the cost of application. In some instances, it requires the development of new pesticides that is expensive and time-consuming.

Use of bacteriophage has given an alternative technique in controlling pathogens in crops (Frampton et al. 2012). In recent years, it has been considered a realistic environmentally friendly approach to combat plant pathogens (Frampton et al. 2012). Use of high concentration of phage in close proximity to pathogen has been shown to

be an effective protective formulation to target specific pathogen (Jones et al. 2012). But UV light inactivation of phage and concern of potential rise of phage resistance are the major impeding factors still need to be fully addressed for effective phage therapy (Jones et al. 2012). Apart from these traditional methods of crop protection, in the past few decades there has been an increase in molecular approaches to protect and increase yield in the crops. For this, a better understanding of plant's natural defense mechanism is the first and foremost important step.

The Plant Immune System

Plants and microbes interact in various ways that impact plants' productivity, disease resistance, and stress tolerance. In some cases, those interactions are beneficial to both, but in many other cases, microbe interaction with the plant is detrimental. They two are in a constant arms race with each other; one tries to defend itself while other evolving to defend against existing defenses (Anderson et al. 2010).

Plant interaction with an intruding pathogen leads to several phases. In the initial phase, pattern recognition receptors in plants detect pathogen-associated molecular patterns (PAMP) such as flagellin, elicitin, lipopolysaccharides, peptidoglycans that result in PAMP-triggered immunity (PTI) (Chisholm et al. 2006; Jones and Dangl 2006). This triggers expression of defense genes, production of reactive oxygen species (ROS), and initiation of hormone-mediated defense signaling (Jones and Dangl 2006). In the next phase, if a pathogen can suppress PTI, it causes release of effector proteins by type III secretion systems that leads to the development of effector-triggered susceptibility (ETS) (Jones and Dangl 2006). In the third phase, the plant recognizes virulence proteins by deploying proteins nucleotide-binding-leucine rich repeat (NB-

LRR), which results in effector-triggered immunity (ETI) (Jones and Dangl 2006). In the final phase, pathogens either shed or diversify recognized effector gene or acquire additional effectors to bypass ETI (Jones and Dangl 2006).

Beside defense at the local level, the plant also transmits defense signals to the uninfected tissue resulting in broad-spectrum disease resistance known as systemic acquired resistance (SAR) that provides long-lasting immunity to other unrelated pathogen (Gao et al. 2015). Several studies have shown that salicylic acid (SA) and its derivative, methyl salicylate (MeSA) (Park et al. 2007) play a key role in the establishment of SAR that is not only confined in uninfected tissue within the plant but also has a role in neighboring plants (Shulaev et al. 1997). Apart from this, researcher have also reported trans-generational immune memory in plants (Luna et al. 2012). Plants pass on the inherited immunity to adapt against specific stress in the next generation (Imam et al. 2016).

Phytohormone

Phytohormones are structurally unrelated small molecules that act as chemical messengers. These molecules are synthesized in various metabolic and biosynthetic pathways. They coordinate and regulate various cellular activities in the plant's life, from seed-to-seed. They are actively involved in plant’s growth, development, and defense (Santner et al. 2009). Several of these hormones crosstalk with each other and orchestrate various physiological activities that convey different environmental outputs. Jasmonic acid, ethylene, abscisic acid, and salicylic acid are some of the important plant hormones among many other phytohormone that functions as a key signaling molecules (Leung and Giraudat 1998; Clarke et al. 2000).

A. Jasmonic Acid:

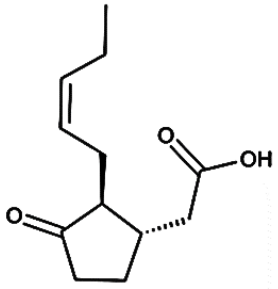

Figure 1: Chemical Structure of Jasmonic Acid. ChemDraw Direct was used to draw structure.

Jasmonic acid (JA) is synthesized from linolenic acid by the octadecanoid pathway (Vick and Zimmerman 1984). JA and its derivatives have a role in wound responses, secondary metabolite synthesis, and defense against biotic and abiotic stress (De Vleesschauwer et al. 2014). The level of JA increases locally within plants after pathogen infection and tissue damage (Lorenzo and Solano 2005; Wasternack 2007). It plays a prominent role in defense against the herbivore attack and necrotrophic pathogens (Glazebrook 2005). Apart from this, JA is also involved in seed germination, root growth, tuber formation, leaf senescence, fruit ripening and stomatal opening (Bari and Jones 2009). The role of JA in SAR is controversial. A study by Truman and colleagues showed that foliar administration of JA initiates SAR in Arabidopsis (Truman et al. 2007). While in another study in Arabidopsis, JA failed to act as a mobile signal in SAR (Chaturvedi et al. 2008).

JA signaling is also integrated with other defense signaling pathways. Three out of 41 JA-response genes are involved in signaling pathways for ethylene, auxin and SA (Sasaki et al. 2001). Crosstalk between SA and JA-mediated signaling pathways leads

to either synergistic or antagonistic relationship. Mostly it is found to be antagonistic and SA having a greater effect on JA pathway than another way (Proietti et al. 2013). The study showed that low-level application of both signal compounds resulted in a synergistic relationship while antagonistic relationship occurs upon application of higher doses and longer exposure (Mur et al. 2006). SA inhibits different genes that are involved in the biosynthesis of JA (Leon-Reyes et al. 2010). SA also degrades transcription factors that are involved in the activation of JA-signaling thereby affecting JA-induced transcription (Caarls et al. 2015). It sequesters JA-responsive transcription factors either in the nucleus by repressor proteins or interrupting them in the cytosol thereby making them unavailable for target genes (Caarls et al. 2015). SA and JA act reverse to each other in regulating *PR* gene expression. *PR1, PR2* and, *PR3* genes expression are upregulated by SA while JA suppresses them, and in case of *PR2, PR5* and, *PR6* genes, JA upregulates them while SA suppresses (Niki et al. 1998).

B. Ethylene:

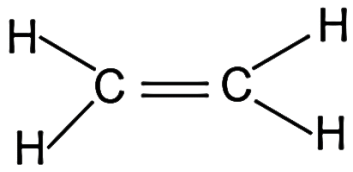

Figure 2: Chemical Structure of Ethylene. ChemDraw Direct was used to draw structure.

Ethylene (ET) is a simple plant hormone synthesized from the amino acid methionine. S-adenosyl-methionine (SAM), the precursor of ethylene biosynthesis, is synthesized from methionine by the enzyme SAM synthetase. The enzyme ACC

synthase that perform rate limiting step in ET biosynthesis (Bleecker et al. 1986) converts SAM to 1-aminocyclopropane-1carboxylic acid (ACC) which is finally oxidized to form ET, CO_2, and cyanide by the enzyme ACC oxidase (ACO). Cyanide thus produced is detoxified by being converted into amino acid β -cyanoalanine by the enzyme β-cyanoalanine synthase (Kende 1989; Wang et al. 2002). Ethylene is a gaseous hormone that regulates different physiological and developmental processes in the plant. It is an interesting hormone involving two contradictory processes, i.e., development, and senescence (Reviewed in Iqbal et al. 2017). It plays a role in seed germination, root hair development, nodulation, fruit ripening, leaves and flower senescence, organ abscission and defense against abiotic and biotic stresses (Wang et al. 2002; van Loon et al. 2006). It is known to play a role in regulating ROS homeostasis during salinity stress (Zhang et al. 2016). It is also associated with defense against nutrient stress conditions and hypoxia (Salazar et. al. 2015). In case of biotic stress, ethylene plays a dual role. Application of ethylene before pathogen infection stimulates resistance while application after the manifestation of symptoms enhances disease progression (van Loon et al. 2006). Studies have shown the role of ethylene in development of SAR. In Tobacco Mosaic Virus (TMV)infected tobacco leaves, the perception of ethylene is required for the synthesis of signal molecules that trigger SAR development (Verberne et al. 2003).

C. Abscisic Acid (ABA):

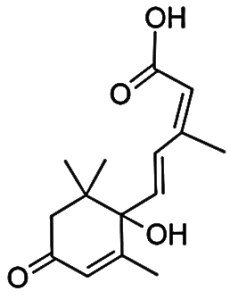

Figure 3: Chemical Structure of Abscisic Acid. ChemDraw Direct was used to draw structure.

Abscisic acid is an isoprenoid-based plant hormone synthesized indirectly from carotenoids (Finkelstein and Rock 2002). ABA is involved in many aspects of the plant like root growth, cell division, seed germination, embryo maturation, leaf senescence and adaptation to environmental stress (Finkelstein 2013). Studies show that ABA acts as both negative and positive regulators in plant defense depending upon the pathogen type and timing of induction of defenses (Ton et al. 2009). In the case of fungal and bacterial pathogens, at early stages of infection, ABA can enhance defenses by inducing callose deposition (Ton et al. 2009) and stomatal closure (Ellinger et al. 2013). Both act as a barrier against bacterial infection, limiting pathogen infectivity (Ton et al. 2009; Ellinger et al. 2013). But if the pathogen is successful in invading plant tissue, then ABA limits plant defenses by antagonizing along with other hormones (Yasuda et al. 2008). Contrary to it, in case of viral infection, several studies have shown enhancement of antiviral defense irrespective to stage of infection (Alazem and Lin

2017). ABA also acts as a negative regulator of SA dependent SAR while ABA biosynthesis is inhibited upon SAR induction (Yasuda et al. 2008).

D. Salicylic Acid:

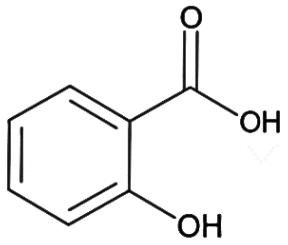

Figure 4: Chemical Structure of Salicylic Acid. ChemDraw Direct was used to draw structure.

Salicylic acid (2-hydroxy benzoic acid) is an important plant signaling molecule consisting of an aromatic ring with a hydroxyl group. SA is present in the free phenolic acid form or in the various conjugated forms in the plant (Malamy et al. 1992). It is another multifaceted hormone that plays a role in plant growth, development, and defense (Vlot et al. 2009). It influences different processes in the plant such as respiration, photosynthesis, seed germination, flowering, thermogenesis, senescence-associated gene expression, stomatal closure, cellular redox homeostasis maintenance, basal thermotolerance, biotic and abiotic stress signaling etc.(Vlot et al. 2009; Rivas-San Vicente and Plasencia 2011; Kumar et al. 2014; Kumar et al. 2015). SA in plants is synthesized via two pathways namely phenylalanine ammonia lyase (PAL) mediated pathway, and isochorismate synthase (ICS) mediated pathway; the latter contributes to more than 90% of SA production (Chen et al. 2009). Both pathways utilize chorismate,

the end product of shikimate pathway as an initial substrate. In the PAL-mediated pathway, cinnamate is converted to SA via benzoate while in the ICS-mediated pathway, chorismate is converted into SA via isochorismate (Dempsey et al. 2011). Depending upon plant species, early feeding studies using radio-labeled substrates suggested that trans-cinnamic acid formed from chorismic acid follows different route producing ortho-coumaric acid, benzaldehyde, and cinnamoyl-CoA which ultimately leads to salicylic acid synthesis (Dempsey et al. 2011). In case of the ICS-mediated pathway, the single route leads to SA biosynthesis through Isochorismate intermediate catalyzed by isochorismate synthase and isochorismate pyruvate lyase (Dempsey et al. 2011).

After synthesis, SA undergoes various chemical modifications that inactivates it in most cases but attributes properties which are required for its accumulation, mobility, and other additional functionality. Glucosylation, methylation, amino acid conjugation, hydroxylation and, sulfonation are the different known modifications of SA (Dempsey et al. 2011). Glucosylation can occur at the hydroxyl group or at the carboxyl group resulting in the formation of salicylic acid beta-glucoside (SAG) or salicylate glucose ester (SGE), respectively (Dean and Delaney 2008). Glucosylation reduces toxicity and enhances higher vacuolar storage (Dempsey et al. 2011). Methylation is catalyzed by carboxyl methyltransferase 1 (BSMT1) that transfers a methyl group to the carboxyl group of SA to form methyl salicylate (Chen et al. 2003). *BSMT1* is expressed in both normal and in stress conditions. In the normal condition, it helps in pollination by expressing in flowers to attract pollinators while in stress conditions it helps the plant to cope with unfavorable conditions (Chen et al. 2003; Effmert et al. 2005). Methylation of

SA results in loss of its ability to induce *PR-1* transcripts but increases its membrane permeability for efficient long-distance travel that acts as a critical mobile signal that triggers SAR (Park et al. 2007). Amino acid conjugation is another SA modification strategy. Salicyloyl-aspartate (SA-Asp), the only type of SA-amino acid conjugate reported in the plant, is presumably synthesized by GH3.5, a member of the GH3 (Gretchen Hagen 3) acyl adenylase family (Chen et al. 2013, Dempsey and Klessig 2017). GH3.5 synthetase catalyzes the amino acid conjugation reactions in which aspartic acid is conjugated with SA to form SA-Asp conjugate (Dempsey et al. 2011). The SA-Asp conjugate likely induces *pathogen-related* (*PR)* gene expression and defends against pathogenic *Pseudomonas syringae* infection (Chen et al. 2013). Sulfonation of SA has been observed only *in vitro*. Hydroxylation of SA results in the formation of benzoate derivatives 2,3 dihydroxybenzoate and 2,5 dihydroxybenzoate (Maskos et al. 1990). These benzoate derivatives are also the products of the isochorismate pathway, but it is unclear whether they are produced as a sole product of the isochorismate pathway only or also are produced from hydroxylation of SA (Dempsey et al. 2011).

Salicylic Acid and Systemic Acquired Resistance

The SA dependent pathway is an important defense pathway in plants. It provides defense at both local as well as in the distal uninfected plant tissue known as systemic acquired resistance (SAR) (Shah 2003). Plant infected with pathogens shows an increased level of endogenous SA as well as elevated expression of *PR* genes resulting in disease resistance (Malamy et al. 1990; Shah 2003). The essential role of SA in SAR was discovered through the experiments using transgenic plants expressing

the bacterial *salicylate hydroxylase* (*nahG*) gene (Gaffney et al. 1993). These transgenic plants were unable to express *PR* genes, and SAR induction was compromised as SA was readily converted to catechol (Delaney et al. 1994; Lawton et al. 1995). Other studies also support the role of SA in SAR. Here the exogenous application of SA, or its synthetic analog benzothiadiazole (Acibenzolar-s-methyl), induces disease resistance genes and activation of SAR (Klessig and Malamy 1994; Lawton et al. 1996). NPR1 (nonexpresser of pathogenesis related genes 1) is a key transcriptional regulator of SAR (Cao et al. 1994). Under normal conditions, NPR1 is expressed in low amounts and is localized as oligomers predominantly in the cytosol (Mou et al. 2003). In response to increase in SA levels, NPR1 expression increases by 2-3 fold (Cao et al. 1998). Increase in SA levels induces changes in cellular redox state in the cytosol resulting in the conversion of oligomeric forms of NPR1 into its monomers. Monomeric NPR1 is transported to the nucleus. In the nucleus, it activates immune-related genes thus activating SAR pathway (Mou et al. 2003). Mutants lacking functional *npr1* expression fail to induce SAR and exhibit increased susceptibility to fungal and bacterial infections (Cao et al. 1994). Apart from its role in SAR, NPR1 is also involved in cross talk between SA-JA in defense signaling pathways (Pieterse and Van Loon 2004).

SA-Binding Protein 2 (SABP2)

SABP2 is a 29 kDa (Kilo Dalton) soluble, low abundance protein (10 fmol/mg fwt) in tobacco leaves belonging to the α/β fold hydrolase superfamily with Ser-81, His-238, and Asp-210 as the catalytic triad (Du and Klessing 1997; Kumar and Klessig 2003; Forouhar et al. 2005; Park et al. 2007; Kumar and Klessig 2008). It binds SA with high affinity (equilibrium dissociation constant (K_d) = 90nM) (Kumar and Klessig 2003). It

cleaves off the methyl group of inactive MeSA, converting it to active SA (Kumar and Klessig 2003; Forouhar et al. 2005; Park et al. 2007; Kumar and Klessig 2008). In tobacco plants silenced in SABP2 expression, both the local resistance to tobacco mosaic virus (TMV) and SAR development are suppressed (Kumar and Klessig 2003). SABP2 is also capable of catalyzing the conversion of acibenzolar-S-methyl (ASM) (an ester), a functional analog of salicylic acid, into acibenzolar (an acid) to induce SAR (Tripathi et al. 2010). SABP2 is inhibited by a feedback mechanism by binding reversibly to its product, SA, that facilitates the accumulation of more MeSA in the uninfected parts of the plant (Forouhar et al. 2005; Park et al. 2007).

To further understand the role of SABP2 in plant defense, a yeast two-hybrid screening was performed to identify SABP2-interacting proteins (SIP). Using SABP2 as a bait protein and tobacco leaf proteins as prey, many interacting proteins were discovered (Odesina 2015). SIP68 is one of the several SABP2-interacting proteins identified in that study.

SIP68

SIP68 is a glucosyltransferase (GT) enzyme belonging to the family 1 of plant GTs (UDP glycosyltransferase) (Odesina 2015). It is encoded by tobacco *NtGT4* gene which has a protein coding region that is 1488 base pairs long that codes for 496 amino acids. It has a C-terminal consensus sequence, plant secondary product glycoslytransferase (PSPG) box that binds to the sugar donor substrate. *In silico* analysis using various prediction software predicted different subcellular localization for SIP68. It was predicated to be either as cytoplasmic protein or a secretory protein or an endoplasmic reticulum membrane-localized protein (Odesina 2015).

SIP68 was cloned and expressed recombinantly both in *E. coli* and *Pichia pastoris.* Ni-NTA affinity chromatography was used to purify the recombinant SIP68 from both the *E. coli* and yeast systems. The recombinant SIP68 expressed in yeast was further purified using Mono Q Anion exchange chromatography before testing for glucosyltransferase activity (Odesina, 2015).

Glucosyltransferase activity of recombinant SIP68 was determined using a radioactive-based assay (McIntosh et al. 1990). Out of 14 different synthetic substrates tested, the recombinant SIP68 glucosylated flavonols (kaempferol, quercetin, fisetin, gossypetin), flavones (apigenin, luteolin,) flavanones (hesperetin, naringenin), and isoflavones (4-acetone-7 hydroxy-6-methoxy-isoflavone) to a varying degree. The highest activity was detected with kaempferol followed by quercetin while negligible activity was detected in azelaic acid and the simple phenolic compounds SA, MeSA, benzoic acid, and p-hydroxybenzoic acid. To further confirm, a HPLC-based assay was performed to identify the products formed in the reaction involving kaempferol, quercetin, SA, hesperetin, and naringenin as acceptor which suggested that SIP68 was a flavonoid UDP-glucosyltransferase and not a SA glucosyltransferase (Odesina 2015).

Glycosyltransferase Protein and its Role in Plants

UDP-glycosyltransferase (UGT) catalyzes the formation of a glycosidic bond by transferring a glycosyl moiety from an activated donor containing a nucleoside phosphate or a lipid phosphate to an acceptor molecule (Campbell et al. 1997; Lairson et al. 2008). With some difference in acceptor and donor molecules, glycosylation reactions are similar in both plants and mammalian organisms. In case of plants UDP-

glucose is generally used and UDP glucuronic acid in mammals as a substrate in the transfer reactions (Lim and Bowles 2004).

Glycosyltransferase enzymes are widely distributed in nature. They are present in both eukaryotes and prokaryotes showing high specificity to donor and acceptor molecules. As of May 2018, according to the Carbohydrate-Active enZymes (CAZy) database, GTs were classified into 105 families (http://www.cazy.org). Classification is based upon experimentally characterized protein and sequence similarity (Cantarel et al. 2009). In *Arabidopsis thaliana* around 850, in peach 168, and in *Populus* more than 800 putative GTs have been reported (Lairson et al. 2008; Wu et al. 2017). The presence of such larger number of glycosyltransferase genes supports the diverse role of UGTs in plant physiology and development.

Glycosylation is a widespread reaction that regulates the bioactivity, solubility, and mobility of many aglycones in plants (Gachon et al. 2005; Ma et al. 2016). UGTs are involved in various functions such as cell wall biosynthesis, modification of secondary metabolites, enhancement of color and flavor (Li et al. 2001), maintaining cellular homeostasis and detoxification of pesticides and herbicides (Bock 2016). There is considerable information documented on glycosylation of plant hormones for maintaining the cellular homeostasis. Hormone such as abscisic acid, auxin, cytokinin, and brassinosteroids were reported to be glycosylated by UGTs. For example, *UGT71C5, UGT76C2, UGT74B1,* and *UGT73C5* of Arabidopsis glycosylates abscisic acid, cytokinin, auxin, and brassinosteroids, respectively and mediates their homeostasis (Grubb et al. 2004; Poppenberger et al. 2005; Wang et al. 2011; Liu et al. 2015). Another glucosyltransferase (*UGT74E2*) of Arabidopsis alter indole-3-acetic acid

(IAA) and indole-3-butyric acid(IBA) that are associated with different morphological changes in shoot and leaf resulting in improve survival in drought and salt stress, adding another role of UTG in defending abiotic stress (Tognetti et al. 2010).

Stabilization of secondary products and detoxification is another important role of glycosyltransferase protein in plants. Glycosylation decreases the toxicity of the potentially harmful secondary metabolites such as glucosinolates and cyanogenic glycodises, limits their interaction with other cellular components and enables their storage that later upon exposure to glycosidases, release reactive compounds to defend against pathogens or herbivores (Reviwed in Vogt and Jones 2000). Transgenic wheat expressing, barley UDP-glucosyltransferase (*HvUGT*13248) exhibited resistance to *Fusarium graminearum* that causes the devasting disease, fusarium head blight (Li et al. 2015). HvUGT13248 can metabolize deoxynivalenol; a toxic mycotoxin produced by this fungus to its glucoside form (Li et al. 2015). A similar result of detoxification of deoxynivalenol by Arabidopsis UGT73C5 has also been reported (Poppenberger et al. 2003).

Reports of UGTs helping the symbiotic association between plants and microbes are also documented. For example *Acromenium* sp., an endophytic fungus of the European yew, produces potential toxic compound leucinostatin A that is glycosylated by the host leucinostatin A glucosyltransferase, markedly reducing its toxicity (Strobel and Hess 1997).

Apart from reducing toxicity, UGTs are also involved in enhancing solubility. Addition of carbohydrate to hydrophobic substrates increases the polarity of resultant glycoside thereby increasing their solubility (Jones and Vogt 2001). For example,

glucosyltransferase from apple, UGT71A15 was able to increase the solubility of low water soluble phytochemical resveratrol by 1700-fold in its glucoside form, resveratrol 3,5-β-D-diglucoside (Lepak et al. 2015).

Glucosyltransferase enzymes are also involved in flavor, color, and aroma enhancement in plants (Daniel et al. 2011; Le Roy et al. 2016). For example, naringin, a flavanone glycoside present in high amount in young tissue is a well-known compound causing bitterness in *Citrus paradisi* andis due to UDP-glucosyltransferase activity (Jourdanet al. 1985; McIntosh et al. 1990). Similarly, the role of glucosyltransferase in pigmentation was well demonstrated in the study done on the expression pattern of seven genes of anthocyanin biosynthesis pathway in red and white grapes (Boss et al. 1996). Lack of expression of UDP glucose-flavonoid 3-O-glucosyltransferase (UFGT) resulted in loss of pigment in white grapes suggesting a role of UGTs in pigmentation in plants (Boss et al. 1996). Glycosyltransferases are also associated in aroma enhancement in plants. AdGT4, a UGT enzyme from *Actinidia deliciosa* (Kiwifruit) can glycosylate a range of terpenes and alcohols giving ‘grassy-green’ aroma notes in ripe kiwifruit. The same gene when over-expressed in petunia and tomato resulted in increased sequestration of a range of alcohols suggesting the role of UGTs to sequester volatile compounds to enhance aroma (Yauk et al. 2014).

Based upon all these diverse functions of glycosyltransferase proteins, undoubtedly this group of enzymes has an important role in plant’s growth, development, and survival. Studies on plant UGTs will enable us to better understand its role on plant physiology and may help us to protect plant and improve crop production. The focus of this study is to characterize tobacco SIP68. *NtGT4* that codes

for SIP68 has been shown to have a role in plant cell differentiation (Guo et al. 2016). We aim to understand its subcellular localization pattern and its role in plant defense signaling.

Hypothesis

Hypothesis 1: SIP68 is localized in the cytoplasm

Plant UGTs are most likely to function in the cytoplasm (Lim and Bowles 2004). UDP-glucose, the key substrate for glucosyltransferases is predominately present in the cytoplasm (Dancer et al. 1990). It is used as a sole source of glucose donor in the glucosylation of various plant secondary metabolites including flavonoids that are synthesized in the cytosol (Marinova et al. 2007). SIP68, a glucosyltransferase protein has the highest activity with flavonoids. Because both donor and acceptor molecules are present in the cytosol, it is arguable that SIP68 is likely to be localized in the cytoplasm.

Hypothesis 2: SIP68 has a role in the SABP2 mediated defense signaling pathway

SABP2 has an important role in SA-mediated defense signaling in the plant (Kumar and Klessig 2003; Park et al. 2007; Kumar 2014). Because SIP68 interacts with SABP2, an important protein of plant defense signaling, it might alter the SABP2 activity thereby affecting SABP2 mediated defense signaling pathway.

CHAPTER 2

MATERIALS AND METHODS

Materials

Plants Materials

Tobacco plants, *Nicotiana benthamiana* and *Nicotiana tabacum* cv. Xanthi-nc NN (XNN) were used for this research. In a controlled environment, both types of tobacco plants were grown from seed. The soil (Fafard F-15, Agawam, MA) purchased locally, was first autoclaved (Autoclave-Consolidated SSR-2A-PB) for 20 minutes and cooled down to room temperature. An average of 20 seeds per 4 x 4-inch square plastic container was sown and placed in a tray filled half with water (to maintain humidity during seed germination). The tray was kept covered, and seeds were allowed to germinate and grow at 22 °C at 16- hours light cycle (200 µmol m-2 sec-1) in a growth chamber (PGW 36, Conviron, Canada). After seedlings started to germinate, the plastic cover was removed, and the seedlings were allowed to grow. After 10-14 days two seedlings were transferred into each 4 x 4-inch square plastic container containing autoclaved soil saturated with water and allowed to grow for three weeks. During this period plants were watered regularly. After three weeks, young plants were transferred into 8-inch pots and allowed to grow for additional 2-4 weeks. Three days after transferring to the pot, fertilizer (Jack's professional 20:10:20 peat lite) was applied to the plants. Plants were watered regularly during the growing period.

Chemicals and Reagents

LE Agarose (SeaKem); Agar (Fisher Scientific); Luria Bertani (LB) Broth (Sigma-Aldrich), Oligo dT-20, Taq polymerase, platinum Pfx high fidelity Taq polymerase, proteinase K (Invitrogen); 100 bp DNA ladder 1 Kb DNA ladder (NEB); MMLV reverse transcriptase, DNase, RNase, RNAsin (Promega); Ethidium bromide (5 mg/ml), gel loading dye (Bio-Rad); QIAquick Gel extraction kit , Qiagen plasmid midi kit, QIA prep spin miniprep kit (Qiagen, CA); Restriction enzymes (NEB, Takara and Thermo fisher); lysozyme, T4 DNA ligase , T4 polynucleotide kinase , Alkaline phosphatase (NEB); X-gal (20 mg/ml), Dimethylformamide (DMF), diethylpyrocarbonate (DEPC), Dithiothreitol (DTT), Triton X, 100% ethanol, methanol (Fisher Scientific); Tween 20 (BioRad); Liquid nitrogen (Airgas, TN), Trizol reagent (Invitrogen); glycerol (Mallinckrodt); chloroform, isopropanol, phenol, isoamylalchol, glacial acetic acid, imidazole, Sodium dodecyl sulfate (SDS), Ammonium persulfate (APS), tetramethylethylenediamine (TEMED), β-mercaptoethanol (β-ME), phenylmethylsulfonyl fluoride (PMSF), Acetosyringone, morpholinoethanesulfonic acid(MES)-KOH, ponceau-S, sodium phosphate dibasic (Na_2HPO_4), magnesium chloride ($MgCl_2$), sodium chloride (NaCl), TRIS base, (Fisher Scientific); Guanidine hydrochloride, calcium chloride (Sigma-Aldrich); EDTA, 30% acrylamide (Bio-Rad); Polyvinylidene flouride (PVDF) membrane (Milipore); Low Molecular Weight (LMW) protein ladder (GE life Sciences); mouse monoclonal anit-PR1 antibody, rabbit monoclonal anti-eGFP antibody, mouse monoclonal anti-poly-Histidine antibody, rabbit monoclonal anti-GST antibody, HRP conjugated goat anti-mouse IgG, HRP conjugated goat anti-rabbit IgG, ECL western blotting substrate (Thermo Scientific); Murashige Skoog (MS) media (Plant Media); sucrose (BioWorld).

Antibiotics

Kanamycin, spectinomycin, tetracycline, cefotaxime, hygromycin (Sigma-Aldrich); carbenicillin (BioWorld); and (PhytoTechnology laboratories).

Other Materials/Instruments

Spectrophotometer Evolution 300 (Thermo scientific), ND-1000 Nanodrop spectrophotometer (Thermo scientific), Master cycler (Eppendorf, NY), UV imaging system (UVP Bioimaging Systems), French Press (Thermo scientific), Polyacrylamide gel electrophoresis apparatus (Biorad), microcentrifuge (Eppendorf), Ultracentrifuge (Thermo Scientific), centrifuge (Beckman, model J2-21 or Sorvall RC5B), LeicaTCSSP2 Spectral Confocal & Multiphoton System, Ultrasonicator (Fisher Scientific), pH meter (Beckman), growth chamber (PGW 36, Conviron, Canada), Autoclave (Consolidated SSR-2A-PB), Airegard Laminar air flow, Incubator (Fisher Scientific), shaker (Labline), and water bath (Fisher Scientific), FastPrep 24 (MP Bio).

Oligonucleotides (Primers)

All primers used in this research were custom synthesized by Eurofins MWG (Huntsville, AL). The lyophilized oligonucleotides were diluted to a final concentration of 10 µM by nuclease-free water. All primers and their purpose are listed in table 1.

Table 1: List of Primers with Their Sequence Used in This Research

Primer	Sequence (5'-3')	Purpose
M13-Forward	GTAAAACGACGGCCAG	Amplification of pDONR221-SIP68
M13-Reverse	CAGGAAACAGCTATGAC	Screening CRISPR final construct

DK518-Reverse	CTCGAGCTATTTTTCCTTGTGATTTTGTTG	Amplification of pDONR221-SIP68 and pSITE-2CA-SIP68
DK563-Forward	GGGGACAAGTTTGTACAAAAAAGCAGGCTCCATGGCAACTCAAGTGCAC	Adding aatB1 flanking sites in SIP68 sequence for BP reaction
DK564-Reverse	GGGGACCACTTTGTACAAGAAAGCTGGGTACTATTTTTCCTTGTGATTTTGTTG	Adding aatB2 flanking site in SIP68 sequence for BP reaction
DK643-Forward	GGATCCATGGCAACTCAAGTGCACAAACTTCATTTCATACTATTC	SIP68 silenced line screening
DK644-Reverse	CTCGAGCTATTTTTCCTTGTGATTTTGTTGCTCAATGATGTCTTC	SIP68 silenced line screening
DK677-Forward	AAGGAAGTTCATTTCATTTGGAGAG	Amplification of pSITE-2CA-SIP68
DK746-Forward	GATTGTGAGCAAATCAGATTAGCCG	Cloning the first gRNA in pYPQ131A
DK747-Reverse	AAACCGGCTAATCTGATTTGCTCAC	Cloning the first gRNA in pYPQ131A
DK748-Forward	GATTGTGTGAAGGTGCCTGTCAAA	Cloning the second gRNA in pYPQ132A
DK749-Reverse	AAACTTTGACAGGCACCTTCACAC	Cloning the second gRNA in pYPQ132A
DK750-Forward	GATTGCATGCTTCCTTCTCTTGACT	Cloning the third gRNA in pYPQ133A
DK751-Reverse	AAACAGTCAAGAGAAGGAAGCATGC	Cloning the third gRNA in pYPQ133A
DK752	ACGTGAGTGTGAGTGAGACT	Sequencing insertion of gRNAs in golden gate entry vector
DK755-Forward	CGAGAAGTTGAAGGGATCTCCA	Sequencing certain portion of Cas9 in the final construct
DK756-Forward	CTTCCGGAAAGGGCGAAT	Sequencing insertion of first gRNA in final construct

DK757-Reverse	GTACAAGAAAGCTGGGTCGAA	Sequencing insertion of last gRNA in final construct

List of Plasmids Used

All the plasmids used in this research are either purchased from Invitrogen or obtained from Arabidopsis Biological Resource Center (ABRC). All the plasmids and their purpose are listed in table 2.

Table 2: List of Plasmids Used in This Research

Vector	Purpose	Source
pDONR-221	Gateway cloning entry vector	Invitrogen
pSITE-2CA	Subcellular localization: Destination vector	Invitrogen
pYPQ131A	CRISPR: Cloning First gRNA oligos	TAIR
pYPQ132A	CRISPR: Cloning Second gRNA oligos	TAIR
pYPQ133A	CRISPR: Cloning Third gRNA oligos	TAIR
pYPQ142	CRISPR: Assembling 2gRNAs	TAIR
pYPQ143	CRISPR: Assembling 3gRNAs	TAIR
pYPQ150	CRISPR: Plant codon optimized Cas9 vector	TAIR
pMDC-32	CRISPR: Assembling gRNA construct and Cas9 for plant transformation	TAIR

The Arabidopsis Information Resource (TAIR)

Methods

Subcellular Localization of SIP68

To determine where SIP68 is localized in tobacco cells, a full-length SIP68 cDNA was cloned first into pDONR221 (Gateway Entry plasmid) and then subcloned into destination plasmid pSITE-2CA which has enhanced Green Fluorescent Protein (eGFP). The pSITE2CA plasmid tagged the eGFP on the N-terminal of the recombinant SIP68.

Cloning of Full-Length SIP68 in pDONR221

The primers, DK563 and DK564 (Table#1) were used to flank the SIP68 with attB1 and attB2 sites for cloning into pDONR221. The RT-PCR amplification mixture was prepared by adding 5 µl of 10X platinum Pfx amplification buffer, 1.5 µl of 10mM dNTP, 0.5 µl of 50mM $MgSO_4$, 0.75 µl of each forward and reverse primers, 0.4 µl of platinum Pfx DNA polymerase, 2 µl of template DNA (10 pg to 200 ng), and autoclaved milli-Q water to make final volume 50 µl. The PCR reaction was set for 35 cycles with two minutes extension and Tm of 68 °C.

Agarose Gel Electrophoresis

The PCR amplified product was detected using ethidium bromide stained 0.8 % agarose gel. Fifty microliters of PCR product was mixed with 10 µl of 6X DNA loading dye and gel was run for 90 minutes at 80 volts. One kb DNA ladder was used to compare the product size by visualizing on a UV transilluminator.

Gel Extraction and Purification

Using a clean surgical blade, expected amplified PCR fragment was excised from the gel. Qiagen gel extraction kit was used to extract DNA as described in the manufacturer's instruction manual and quantified using a Nanodrop.

Cloning of SIP68 into Gateway Entry Vector pDONR221

The gel purified SIP68 DNA was cloned into pDONR221. The reaction mixture for gateway cloning was prepared according to the manufacturer's instructions. The reaction mixture consists of 1 µl of the purified SIP68 with attB1 and attB2 sites (50 fmol), one µl of the pDONR221 plasmid, one µl of BP clonase enzyme and seven µl of TE buffer. The final ten µl reaction mixture was incubated at 37 °C, and after 2 hours one µl of proteinase K was added and incubated at 37 °C for 10 minutes to terminate the reaction. The total reaction mixture was centrifuged briefly and was maintained at 4 °C on ice before transforming into chemically competent top10 *E. coli* cells.

Preparation of Chemically Competent Top10 cells *E. coli*

Glycerol stock of Top10 *E. coli* cells from – 80 °C were streaked on LB media plate and incubated at 37 °C overnight. The following day, a single isolated colony was inoculated in 50 ml LB broth and allowed to grow at 37 °C at 250 rpm until the bacterial OD_{600} reached ~0.4-0.6. The culture was then transferred to pre-chilled (ice) falcon tube and then centrifuged at 3000 x g for 10 minutes at 4 °C. The resulting supernatant was discarded, and the pellet was resuspended with 0.1 M $CaCl_2$ (ice cold) by swirling gently with a sterile pipette. After suspending, cells were again centrifuged at 3000 x g for 10 minutes at 4 °C. The supernatant was discarded, and the pellet was gently resuspended in 2 ml of 0.1 M $CaCl_2$ (ice cold) by swirling gently with sterile pipette tips. All steps were

done in an ice bucket in a sterile condition. To prepare glycerol stock, chemically competent cells were mixed with sterilized glycerol to a final concentration of 25%, flash frozen in liquid nitrogen and stored at -80 °C for later use.

Transformation of pDONR221-SIP68 into Chemically Competent Top10 *E. coli*

Two µl of the reaction mixture was added into 100 µl of chemical competent Top10 *E. coli.* The mixture was mixed gently by tapping, and resulting mixture was incubated on ice. After 30 minutes the mixture was incubated at 42 °C in water bath for 45 seconds. Following heat shock, it was cooled on the ice for 2 minutes. Then 800 µl of SOC media (Appendix B) was added to the vial and sealed properly using parafilm. The tubes were then incubated at 37 °C at 250 rpm for 1 hour. After one hour, 50 µl, 100 µl and 150 µl of the transformed bacterial cells were plated on separate LB agar plates containing kanamycin (100 µg/ml) and incubated overnight at 37 °C.

Screening of Transformed pDONR221-SIP68 Clone Using Colony PCR

Colony PCR was used to screen the transformant colonies. Using a sterile toothpick single colony was picked and mixed in 30 µl of sterile water. As soon as solution looked cloudy, the tip was taken out and streaked on a fresh LB plate containing 100 µg /ml kanamycin plate. Ten µl of bacterial solution was used for PCR amplification. PCR mix was prepared by adding 4.8 µl of milli Q water, 2 µl of dNTP, 2 µl of 10X PCR buffer, 0.4 µl of Taq polymerase, 0.4 µl of forward primer (M13) and 0.4 µl of reverse primer (DK 518) (Table#1) in 10 µl of bacterial solution to make final volume of 20 µl. The PCR reaction was set for 30 cycles at 94 °C for 30 seconds, 55 °C for 30 seconds (annealing temperature), 72 °C for 2 minutes (extension temperature) and a final extension of 72 °C for 7 minutes. After PCR amplification, amplified products were

analyzed using 0.8 % agarose gel electrophoresis as described earlier. Positive colonies showing amplification of ~1581 bp were used for plasmid DNA isolation.

Plasmid DNA Isolation of Recombinant pDONR221-SIP68

PCR verified positive colonies were inoculated into 5 ml LB broth containing 100 µg/ml of kanamycin and incubated overnight at 37 °C shaker at 250 rpm. QIAprep Spin MiniPrep Kit (Qiagen) was used to extract recombinant pDONR221-SIP68 according to the manufacturer's instruction. The extracted plasmid DNA was quantified using a Nanodrop spectrpophotometer and was sent for DNA sequencing, and remaining was stored at -20 °C.

DNA Sequencing of pDONR221-SIP68 Clones

DNA Sequencing mixture of 10 µl was prepared by adding ~1000ng of purified recombinant plasmid and one µl each of M13 forward (5µM) and DK 518 reverse (5µM) (Table#1) sequencing primers. The mixture was sent to the Yale University DNA analysis facility for DNA sequencing using Sanger method.

Cloning of SIP68 into Destination Vector pSITE-2CA

The sequenced verified pDONR221-SIP68 construct was subcloned into destination vector pSITE-2CA using Gateway LR reaction (Invitrogen). The reaction mixture was prepared in 1.5 ml eppendorf tube by adding one µl of destination vector pSITE-2CA (150 ng/µl), one µl of entry clone pDONR221-SIP68 (50-150 ng), one µl of LR clonase, and TE buffer, pH 8.0 to make final eight µl reaction mixture. The reaction mixture was incubated at room temperature overnight and next morning one µl of proteinase K was added and incubated at 37 °C for 10 minutes to terminate the reaction. The reaction mixture was then maintained at 4 °C on ice before transforming

into chemically competent Top10 *E. coli*. The transformation was done as described above and transformed cells were grown on LB agar media plate containing selection antibiotic spectinomycin (100 µg/ml) by incubating at 37 °C overnight. Screening of successfully transformed colonies was done by colony PCR as described previously using DK677 forward and DK518 reverse primers (Table#1). Plasmid from the PCR verified clone was extracted using the boiling method and send for DNA Sequencing at Yale University sequencing facility as -described earlier. For DNA sequencing, primers DK677 and DK518 (Table # 1) were used.

Plasmid DNA Extraction

PCR verified positive colonies were grown in 5 ml LB broth containing spectinomycin (100 µg/ml) at 37 °C overnight. Next day, bacterial cells were pelleted by centrifuging at 18,800 x g for 60 seconds. The supernatant was discarded, and to the pellet, 500 µl of ice-cold STE solution (Appendix B) was added and mixed properly by vortexing. The bacterial suspension was then centrifuged at 4 °C at 13,600 x g for 60 seconds. Again, the supernatant was discarded completely, and 500 µl of STET solution (Appendix B) was added to the pellet and mixed properly by raking the tubes across the test tube rack followed by vortexing. To the completely mixed bacterial suspension, 25 µl of freshly prepared lysozyme (10mg/ml in 10mM Tris HCl, pH 8.0) was added and boiled in water bath for 45 seconds. The boiled bacterial solution was then kept at room temperature to cool down and after then centrifuged at 4 °C at 13,600 x g for 15 minutes. Cell debris were then removed by a sterile toothpick and an equal volume of Phenol:Chloroform:Isoamyl alcohol (25:24:1) was added to the supernatant. It was then mixed properly by vortexing for 10 seconds and then centrifuged for 10 minutes at 1606

x g at 4 °C. After centrifugation, the supernatant was transferred into fresh 1.5 ml eppendorf tube, and an equal volume of isopropanol was added, mixed by inverting the tube 5-6 times, and left in room temperature for 15 minutes. After then, it was centrifuged for 30 minutes at 18,800 x g in room temperature. Supernatant was then discarded, and the pellet was washed with ice-cold 70% ethanol by centrifuging for 10 minutes at 18,800 x g in room temperature (~25 °C). The supernatant was then carefully discarded, and tubes were placed under a lamp to dry the pellet. After 5-10 minutes each pellet was resuspended in 50 µl warmed sterile water (~55 °C), and concentration (A_{260}) was measured using Nanodrop spectrophotometer and extracted plasmid DNA was then stored at -20 °C for later use.

Preparation of Chemically Competent *Agrobacterium tumefaciens LBA4404* Cells

Agrobacterium tumefaciens LBA4404 was revived from -80 °C glycerol stock by streaking on a LB agar containing plate containing rifampicin (20 µg/ml) and spectinomycin (100 µg/ml). The plate was incubated at 28 °C for two days. After two days, a single isolated colony was grown overnight in 5 ml LB broth with rifampicin (20 µg/ml) and spectinomycin (100 µg/ml) at 250 rpm at 28 °C. Next day, 1 ml of growing culture was transferred to 100ml LB broth and incubated at 250 rpm at 28 °C until an OD_{600} =1.0 achieved. The bacterial suspension was then centrifuged at 4 °C for 10 minutes at 3,000 x g and resulting supernatant was discarded. Bacterial pellets were then resuspended in 5ml of cold, sterile $CaCl_2$ (20mM) and again centrifuged at 4 °C for 5 minutes at 3,000 x g. The resulting supernatant was discarded, and pellets were again resuspended in 1ml of ice cold, sterile $CaCl_2$ (20mM). During transportation and handling, bacterial cells were maintained on ice, and vigorous vortexing and pipetting

were avoided. Mixing of pellets was done by gentle swirling of the suspension. The glycerol stock was prepared and stored at -80 °C freezer as described earlier.

Transformation of *A. tumefaciens LBA4404* Cells with pSITE-2CA-SIP68

The sequenced verified pSITE-2CA-SIP68 plasmid DNA was transformed into *Agrobacterium tumefaciens LBA4404* cells by freeze/thaw shock method. Firstly, frozen competent cells from -80 °C stock were thawed on ice and 1000ng of verified pSITE-2CA-SIP68 was mixed gently by tapping with the index finger. Then, the tube was flash frozen in liquid nitrogen and thawed at 37 °C for 5 minutes. One ml of SOC media (Appendix B) was added to transformed cells and then incubated for 3 hours in 28 °C shaker at 250 rpm. After 3 hours three aliquots of 50 µl, 100 µl, and 150 µl of cultures were spread on three separate LB agar plates containing rifampicin (20 µg/ml) and spectinomycin (100 µg/ml). Plates were then incubated for two days at 28 °C and screened by colony PCR as described earlier using DK677 forward and DK518 reverse primers (Table#1).

Agrobacterium-Mediated Transient Expression of pSITE-2CA-SIP68 in *Nicotiana benthamiana Leaves*

Agrobacterium containing pSITE-2CA-SIP68 plasmid construct was grown in 5 ml LB broth containing antibiotics, rifampicin (20 µg/ml) and spectinomycin (100 µg/ml) at 28 °C shaking incubator (250 rpm) for 20 hours. Five hundred microliters of starter culture were transferred to 50 ml LB broth containing 20 µM acetosyringone, rifampicin (20 µg/ml) and spectinomycin (100 µg/ml) and incubated at 28 °C shaking incubator (250 rpm) for 20 hours. Acetosyringone was added to facilitate the DNA transfer by inducing *Agrobacterium* to move and attach to the plant and activate virulence genes on

the Ti plasmid (Gelvin 2003). The bacterial culture was then centrifuged at 3,000 x gat 4 °C for 5 minutes, and the pellet was resuspended into sterile infiltration medium (10 mM $MgCl_2$ + 10 mM MES; pH 5.7 adjusted with HCl). The bacterial suspension was washed by centrifuging at 3,000 x g at 4 °C for 5 minutes, and resulting pellet was again resuspended in 5 ml of infiltration medium, and OD was measured. In 20 ml of infiltration medium, bacterial OD_{600} = 0.6 was maintained and 150 µM final concentration of acetosyringone was added. Conical flask was wrapped with aluminum foil and incubated at 250 rpm in room temperature for 2 hours. Similarly, HCPro (Helper Component Proteinase) containing construct was prepared and 1 ml needleless syringe was used to infiltrate the lower side of *Nicotiana benthamiana* leaves. HCPro was used to suppress plant silencing mechanism and to enhance and prolong transient expression of pSITE-2CA-SIP68 (Peyret and Lomonossoff 2015). Two to three healthy leaves were chosen and infiltrated with and without HCPro. The plant was kept under 24 hours continuous lighting condition and five days after post infiltration, leaf samples were taken for confocal microscopy and subcellular fractionation.

Confocal Microscopy

Five days after infiltration, pSITE-2CA-SIP68 infiltrated plant was taken to the confocal microscopy core facility, Quillen College of Medicine, East Tennessee State University. Leaf discs were observed under Leica TCSSP2 Spectral Confocal & Multiphoton System.

Subcellular Fractionation

Five days after infiltration, leaves were washed with ice-cold water, blotted and cut into small pieces. Grinding buffer (Appendix B) stored at 4 °C was mixed with β-

mercaptoethanol (0.02% final concentration) and PMSF (1mM final concentration). Two grams of de-veined leaf tissue was ground in 10 ml grinding buffer containing β-mercaptoethanol and PMSF using sterile ice-cold mortar and pestle in cold chamber (4 °C). Four layers of cheesecloth were soaked in cold water, squeezed to remove extra water and used to filter plant homogenate in 4 °C cold chamber. The filtrate was centrifuged (Eppendorf centrifuge 5702; rotor: A-4-38) at 100 x g for 2 minutes at 4 °C. The resulting pellet was discarded, and the supernatant was centrifuged again at 600 x g for 10 minutes at 4 °C. The resulting supernatant was used for collecting chloroplast fraction and the pellet was washed three times with grinding buffer by centrifuging at 600 x g for 10 minutes at 4 °C to collect nuclei fraction. The supernatant from 600 x g centrifugation was further centrifuged at 2420 x g for 5 minutes at 4 °C. Pellet was washed three times with grinding buffer by centrifuging at the same condition to collect chloroplast fraction and supernatant was used to collect mitochondrial fraction by centrifuging (Sorvall RC5B; rotor: SA-300) at 16000 x g for 15 minutes at 4 °C. The resulting pellet was dissolved gently in 1-2 ml of grinding buffer without vortexing and centrifuged at 1100 x g for 10 minutes at 4°C. The resulting supernatant was transferred into a fresh centrifuged tube and the pellet was discarded. The supernatant was again centrifuged at 16,000 x g for 10 minutes at 4 °C to collect mitochondrial pellet. Washing step was repeated 2-3 times to collected, purified mitochondrial fraction. The supernatant from 16000 x g (step was centrifuged (Sorvall WX ultracentrifuge; rotor: T-865) at 100,000 x g for 1 hour at 4 °C. The resulting pellet was dissolved in 700 µl of grinding buffer to collect plasma membrane while the supernatant was again centrifuged at 100,000 x g for 1 hour at 4 °C to collect cytosolic fraction (supernatant). Sucrose step

gradient centrifugation was used to isolate purified plasma membrane. Sucrose step gradient was prepared by carefully layering 3 ml of 50%, 2 ml of 40%, 2 ml of 38%, 2 ml of 25%, and 2 ml of 18% sucrose respectively in a ultracentrifuge tube. Pellet dissolved in 700 µl of grinding buffer was carefully applied to the top layer and centrifuged at 100,000 x g for 1 hour at 4 °C. After centrifugation, 1-ml of plasma membrane solution from interphase between 40 % and 50 % was dissolved in 4-5 ml of grinding buffer and again centrifuged at 100,000 x g for 1 hour at 4 °C. The resulting supernatant was discarded, and the pellet was collected (plasma membrane fraction).

SDS-PAGE of Sub-Cellular Fractionated Samples

Each fraction (nuclei, chloroplast, mitochondria, and plasma membrane) was dissolved in 50 µl of 1x SDS plus 2.5% β-mercaptoethanol while 50 µl of the cytosolic fraction was dissolved in 50 µl of 2x SDS plus 5% β-mercaptoethanol and boiled in water bath for 5 minutes. After cooling at room temperature, samples were centrifuged at 16,200 x g for 10 minutes. Ten µl of supernatant was used for 12% SDS PAGE (acrylamide:bis-acrylamide= 30:1). Sample was run for ~1 hour at 20 mA constant current in 1x SDS running buffer until the blue dye reached the bottom of the gel. The gel was then processed for western transfer by rinsing and incubating in 1x western transfer buffer (Appendix B) until ready for transfer (5-10 minutes).

Western Blot Analysis of Sub-Cellular Fractions

At first, the PVDF membrane was prepared by soaking in 100% methanol for 15 seconds followed by washing with autoclave water twice for 2 minutes each followed by incubating in 1x western transfer buffer (Appendix B) for 5-10 minutes on a platform shaker. The gel following SDS-PAGE and PVDF membrane were sandwiched between

3mm Whatman papers pre-soaked in 1x western transfer buffer. Gel cassette was arranged in such a way that black side of the cassette is followed by foam pad, Whatman paper, SDS-gel, PVDF membrane, Whatman paper, foam pad and clear side of the cassette in an orderly manner. The sandwich was then placed in cassette holder facing black side of gel cassette in the black side of the holder and clear side on other way. A small magnetic stir and a cold ice pack were placed in the electrophoresis tank, and electroblotting was carried out for 1 hour at 94 volts at 4 °C. After transformation, PVDF membrane was soaked with 100% methanol for 10 seconds and allowed to dry for about 1 minute by placing the membrane in clean Whatman paper. After air drying, the membrane was again rinsed with 100% methanol for 10 seconds and then stained with ponceau-S stain for 1-2 minutes. After visual verification of transfer of proteins, the membrane was washed with milli Q water followed by washing twice with 1x PBS (Appendix B) for 3 minutes each. Then blocking buffer (3% BSA, 1 % non-fat dry milk in 1 X PBS) containing rabbit monoclonal anti-eGFP primary antibody (1:2,500) was applied to the membrane and incubated overnight at 4 °C. The next day, unbound primary antibody was removed by washing the membrane with 1x PBS, 1x PBS containing 0.3% tween 20, followed again by 1x PBS two times each for 5 minutes. The membrane was again incubated with anti-rabbit antibody in blocking buffer for 1 hour at room temperature on a shaker. The membrane was again washed as described above. To detect the presence of SIP68-eGFP, the blot was incubated in ECL substrate as described by the manufacturer. The signal from the blot was captured by exposing the blot to the X-ray film. To visualize the X-ray film was manually developed using developer and fixer. To visualized total protein loading, the blot was later stained with

coomassie blue. Protein loading was quantified by densitometric analysis and western blot was repeated with equal loading of protein mass if necessary.

Screening of RNAi-Silenced Transgenic SIP68-Silenced Lines

SIP68 transgenic tobacco lines silenced by RNAi-mediated silencing were screened using RT-PCR (Reverse Transcriptase PCR). Various transgenic lines were selected, and total RNA was extracted by Trizol, which was used to synthesize first strand cDNA for checking the levels of SIP68 transcripts. Wild-type tobacco plant was used as a control.

Total RNA Extraction from Tobacco Leaves

Using cork borer (# 6), three leaf discs were collected and transferred to an eppendorf tube and immediately frozen by immersing in liquid nitrogen. Leaf discs were then grounded into a fine powder using a clean blue pestle and a mechanical grinder in liquid nitrogen. For each sample, blue pestle was cleaned with 70% ethanol before using. To the homogenized leaf powder, 500 µl of Trizol was added and mixed properly by vortexing. After complete defrosting, an additional 500 µl of Trizol was added to the mixture and incubated at room temperature for 5 minutes. In 2 ml screw capped tubes, 2 mm autoclaved zirconia beads were added up to 0.2 ml, and leaf sample was then transferred which immediately homogenized using FastPrep 24 at 4.5 power setting for 45 seconds. To the extract, 200 µl of chloroform was added and mixed properly by inverting the tubes several times. The samples were then incubated for 5 minutes at room temperature. The samples were then centrifuged for 15 minutes at 12000 x g at 4 °C. After centrifugation, the upper aqueous phase was transferred to a new eppendorf tube, and 500 µl of isopropanol was added. The samples were mixed properly by

inverting the tubes several times and then incubated for 10 minutes at room temperature. After incubation, samples were centrifuged for 10 minutes at 12000 x g at 4 °C. The resulting supernatant was discarded, and the pellet was suspended in 1 ml of 75 % cold ethanol by vortexing. The samples were then centrifuged for 5 minutes at 7500 x g at 4 °C. The supernatant was discarded, and the pellet was air dried by placing under light for 10 minutes. Air dried pellets were then resuspended in 43 µl of 0.1% DEPC treated water (Appendix B) and incubated for 10 min at 55 °C. After incubation, samples were subjected to DNase treatment by adding five µl of DNase buffer and two µl of DNase (Promega) and incubated for 20 minutes at 37 °C. To remove DNase, the samples were again treated with half the volume of trizol, chloroform, isopropanol, and 75 % cold ethanol as described above. The resulting pellets were then air dried and resuspended in 20 µl DEPC treated water by incubating at 55 °C for 5-10 minutes. RNA concentration was quantified using nanodrop spectrophotometer at 260 nm and samples were stored at - 80 °C.

First Strand cDNA Synthesis

First strand complementary DNA (cDNA) was synthesized from the isolated total RNA using reverse transcriptase enzymes. In the first step, 1000 ng of total RNA was mixed with 2 µl of oligo-dT (0.5 µg/ml). The final volume was adjusted to 10 µl by DEPC treated water and incubated for 10 minutes at 75 °C in the thermocycler. The sample was then cooled down to 4 °C. For the second step, the reaction mixture was prepared by adding 0.25 µl maxima (RT), 4 µl of 5x RT buffer, 0.5 µl of RNAsin (RNase inhibitor), 1 µl of 10 mM dNTPs, and 4.25 µl of DEPC treated water to the sample from the first

step. The samples were then vortexed and incubated at 42 °C for 60 minutes followed by 10 minutes at 70 °C in the thermocycler. The samples were stored at -20 °C.

Reverse Transcriptase-Polymerase Chain Reaction (RT-PCR)

The synthesized cDNA was used to determine the expression of SIP68 in silenced tobacco lines. The reaction mixture was prepared by adding 6.4 µl of DEPC treated water, 1 µl of cDNA sample, 1 µl of 10X Taq polymerase buffer, 1 µl of 10x dNTP, 0.2 ul each of 10 µM forward and reverse primer, and 0.2 µl of Taq polymerase. DK643 and DK644 were used as a primer (Table#1). PCR product was analyzed by using gel electrophoresis as described earlier.

Generating SIP68 Knock out Transgenic Line Using CRISPR Cas9

CRISPR (Clustered Regularly Interspaced Short Palindromic Repeats) Cas9 system was used to knock out *SIP68* gene in *Nicotiana tabacum* and constructed using a protocol described by Lowder et al. (2015) with some modifications. The protocol allows to assemble multiple guide RNAs (gRNAs) to target at multiple sites in the *SIP68* gene. Two constructs, one targeting at two different sites and the other at three different sites were prepared along with their negative constructs (without gRNAs).

Site Selection and Design of gRNA Oligos

The online prediction platform CRISPR direct (https://crispr.dbcls.jp/) (Naito et. al 2015) was used to design unique sgRNA targeting *SIP68* gene only. *NtGT4* gene (codes SIP68) sequence was uploaded in the platform and specificity was checked against *Nicotiana tabacum* Cultivar *Basma Xanthi,* GeneBank assembly accession:

GCA_000715095.1. Three sites within *SIP68* gene were selected (Figure 6) according to result given by CRISPR direct (Figure 5).

position		target sequence	sequence information				number of target sites		
start - end	+ –	20mer+PAM (total 23mer)	GC% of 20mer	Tm of 20mer	TTTT in 20mer	restriction sites	20mer +PAM	12mer +PAM	8mer +PAM
574 - 596	+	CATGCTTCCTTCTCTTGACTTGG [gRNA]	45.00 %	69.26 °C	-		1 [detail]	18 [detail]	6651 [detail]
946 - 968	+	TGAGCAAATCAGATTAGCCGAGG [gRNA]	45.00 %	69.38 °C	-		1 [detail]	1 [detail]	1371 [detail]
2001 - 2023	+	GTGTGAAGGTGCCTGTCAAATGG [gRNA]	50.00 %	72.23 °C	-		1 [detail]	1 [detail]	6280 [detail]

Figure 5: Three Sequence Targets Predicted by CRISPRdirect

NtGT4 Gene

ACTTTAATACAAATATTAATAATTAATTCCACAATTCAAACTCGTTACCTGTAGGTAATACGAAAACAAC
TTTACCGTTGCTCTACTTTCCACCTATCATTATGATTATCACAAAAAAAGAAAGAAGTAAAAGTGTACAA
TTTGCTCACTTCTACCTACTTTGTTGTACTACCAAAGTGGACCACGATGTCCCTGGTATTTCCTCAATTG
GTGAACCAATTGCATCTATAACAACTGTATAGTTGAATTTTATAGCTTAAAATCAAGAATCCAAAACCCC
CAATACTAAGATCTTTGAGCATATCCTTCTTTTGCCATGGCAACTCAAGTGCACAAACTTCATTTCATAC
TATTCCCTTTAATGGCTCCAGGCCACATGATTCCTATGATAGACATAGCTAAACTTCTAGCAAATCGCGG
TGTCATTACCACTATCATCACCACTCCAGTAAACGCCAATCGTTTCAGTTCAACAATTACTCGTGCCATA
AAATCCGGTCTAAGAATCCAAATTCTTACACTCAAATTTCCAAGTGTAGAAGTAGGATTACCAGAAGGTT
GCGAAAATATTGA**CATGCTTCCTTCTCTTGACT**TGGCTTCAAAGTTTTTTGCTGCAATTAGT — 3gRNA
ATGCTGAAACAACAAGTTGAAAATCTCTTAGAAGGAATAAATCCAAGTCCAAGTTGTGTTATTTCAGATA
TGGGATTTCCTTGGACTACTCAAATTGCACAAAATTTTAATATCCCAAGAATTGTTTTTCATGGTACTTG
TTGTTTCTCACTTTTATGTTCCTATAAAATACTTTCCTCCAACATTCTTGAAAATATAACCTCAGATTCA
GAGTATTTTGTTGTTCCTGATTTACCCGATAGAGTTGAACTAACGAAAGCTCAGGTTTCAGGATCGACGA
AAAATACTACTTCTGTTAGTTCTTCTGTATTGAAAGAAGTTAC**TGAGCAAATCAGATTAGCCG** — 1gRNA
AGGAATCATCATATGGTGTAATTGTTAATAGTTTTGAGGAGTTGGAGCAAGTGTATGAGAAAGAATATAGG
AAAGCTAGAGGGAAAAAAGTTTGGTGTGTTGGTCCTGTTTCTTTGTGTAATAAGGAAATTGAAGATTTGGT
TACAAGGGGTAATAAAACTGCAATTGATAATCAAGATTGCTTGAAATGGTTAGATAATTTTGAAACAGAAT
CTGTGGTTTATGCAAGTCTTGGAAGTTTATCTCGTTTGACATTATTGCAAATGGTGGAACTTGGTCTTGGT
TTAGAAGAGTCAAATAGGCCTTTTGTATGGGTATTAGGAGGAGGTGATAAATTAAATGATTTAGAGAAATG
GATTCTTGAGAATGGATTTGAGCAAAGAATTAAAGAAAGAGGAGTTTTGATTAGAGGATGGGCTCCTCAAG — PSPG box
TGCTTATACTTTCACACCCTGCAATTGGTGGAGTATTGACTCATTGCGGATGGAATTCTACATTGGAAGGT
ACTATTCAATTGTGTGATCATCTTATCTAAAGTTTAAATTATTAGATATACCATGTTTTATTTACTTAATT
ATCTCTTGACTAGCGCCAAGTAAGTGGGGTGAGACTTGAATCTTGCCTGCTCTAATACCAATTAAATTGTG
TGACCAAAAAAAAGTGGACAATTCGGTGCACAAAGTATCATACGTTCACGCAGAGTCCGAGGAAAAGCCAC
ACCTAAAAGGTATGATTTAAGCAGACGACCCATATGCAGATATTAGTGGTTACTTCATGACTCGAACGTGT
GACCTATGGGCCCCCAAAGATAACTTTACCGAAATTAAACTATTATCTAAAAAAATTTAACTATTAGAGAT
AATATACTTTTATTTATCTTATCTAAAAATTCAAACTGTTAGAATAATATCATTTTAATTACTTAATTATG
TATTGTATAGGTATTTCAGCAGGATTACCAATGGTAACATGGCCACTATTTGCTGAGCAATTTTGCAATGA
GAAGTTAGTAGTCCAAGTGCTAAAAATTGGAGTGAGCCTAG**GTGTGAAGGTGCCTGTCAAA**TG — 2gRNA
GGGAGATGAGGAAAATGTTGGAGTTTTGGTAAAAAAGGATGATGTTAAGAAAGCATTAGACAAACTAATGG
ATGAAGGAGAAGAAGGACAAGTAAGAAGAACAAAAGCAAAAGAGTTAGGAGAATTGGCTAAAAAGGCATTT
GGAGAAGGTGGTTCTTCTTATGTTAACTTAACATCTCTGATTGAAGACATCATTGAGCAACAAAATCACAA
GGAAAAATAGTAAATTATGATTATTTTTTTTCTATATTTTTTTTTGTGGATTCTCTGTTACTAGTTTATCT
TACACATTTGCCTTGGATTGTTTGGGTTTAAGCTAAGA

Figure 6: Selection of Different Target Sites in *NtGT4* Gene. The magnified colored sequence represents unique gRNAs sites, the sequence in red represents putative plant secondary product glycosyltransferase (PSPG) box and underline sequence represents coding sequence.

For each of the target sites, oligos were designed by adding GATT in the forward and AAAC in the reverse primers. An additional ‘G’ (guanine) was added to the 5’ end in case of the target site (target site 1 and 3) that do not start with guanine, as U6 promoters strongly prefer guanine for the expression (Doench et al. 2014) and additional C (cytosine) at 3’ end of the complementary sequence.

Step1: Cloning of Guide RNA (gRNA) into Golden Gate Entry Plasmids

Linearization of pYPQ131A, pYPQ132A, and pYPQ133A Golden Gate Entry Plasmids

Golden Gate entry plasmids pYPQ131A, pYPQ132A, and pYPQ133A are guide RNA expressing entry plasmids. They consist of gRNA cloning site under the control of AtU6 promotor and gRNA scaffold region that binds to the Cas9 protein. All Golden Gate entry plasmids were first digested with restriction endonuclease BglII and SalI. A reaction mixture was prepared by adding 20 µl of golden gate entry vector (~100 ng/µl), 1 µl each of BglII (NEB; 10 u/ µl) and SalI (NEB; 10 u/ µl), 4 µl of 10X NEB buffer 3.1 and water 14 µl to make final volume 40 µl. The reaction mixture was incubated at 37 °C for 3 hours.

Linearized entry plasmids were purified by Qiagen PCR purification kit according to the manufacturer’s instructions and subjected to a second digestion using the restriction enzyme, BsmBI. The reaction mixture was prepared by adding 32 µl of digested entry vector from the first digestion, four µl of 10x NEB buffer 3.1, two µl of DTT (20 mM), and two µl of BsmBI (NEB; 10 u/ µl). The reaction mixture was incubated overnight at 55 °C and the following day the enzyme was inactivated by incubating at 80 °C for 20 minutes.

Dephosphorylation and Purification of Linearized Golden Gate Entry Plasmids

Linearized plasmid DNA from the second digestion were dephosphorylated by incubating one µg of the linearized vector with one unit of Alkaline phosphatase (calf intestinal) (NEB), two µl of cutSmart buffer (10X) and nuclease-free water to 20 µl final reaction volume for 30 minutes at 37 °C. Dephosphorylated plasmid DNA were then purified using Qiagen PCR purification kit and quantified using nanodrop spectrophotometer.

Oligo Phosphorylation and Annealing

Synthesized gRNA oligos were phosphorylated and annealed. For each CRISPR target site, the reaction mixture was prepared by adding 1 µl each of 100 µM concentration sgRNA oligo forward and reverse, 1 µl of 10X T4 polynucleotide kinase buffer, 0.5 µl of T4 polynucleotide kinase (10 U/ µl; NEB), and 6.5 µl of milli Q water to make final volume of 10 µl. The thermocycler was set at 37 °C for 30 minutes followed by 95 °C for 5 minutes. The reaction product was cooled down in boiled water.

Cloning of Annealed gRNAs Oligos into Golden Gate Entry Plasmid

Annealed gRNAs oligos were ligated into a linearized vector using T4 ligase. Annealed gRNAs oligos for the site first, second, and third sites were added to linearized pYPQ131A, pYPQ132A, and pYPQ133A, respectively. The reaction mixture was set up by adding one µl each of linearized entry vector (50 ng/µl), diluted annealed oligos (1:200 dilution), 10x NEB T4 ligase buffer, and 0.5 µl of T4 ligase. The final volume was adjusted to 10 µl by adding 6.5 µl of milli Q water. The reaction mixture was incubated at room temperature for 1 hour. After 1 hour, two µl of the reaction mixture was transferred to the competent cell as described earlier and bacterial cells were

grown on LB media containing tetracycline (5ng/µl) at 37 °C overnight. A simplified diagrammatic illustration of first step of cloning is represented in Figure 7.

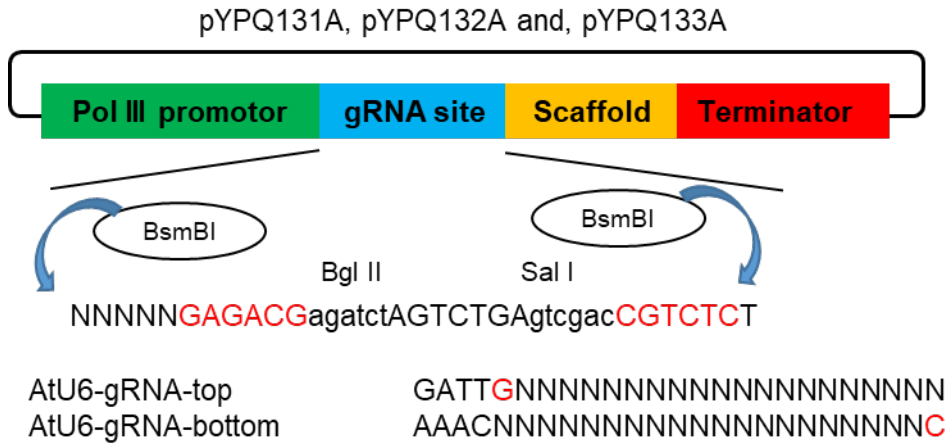

Figure 7: Step1: Cloning of Guide RNA (gRNA) into Golden Gate Entry Plasmids. Redrawn from Lowder et al. 2015.

PCR Screening of Ligation of Oligos into pYPQ131A, pYPQ132A, and pYPQ133A and Isolation of Plasmid for Sequencing

Next day, colony PCR was used to screen for the positive clone as described earlier. The primer, DK752 forward for all and DK747, DK749, and DK751 reverse (Table#1) for first gRNA vector (pYPQ131A), second gRNA vector (pYPQ132A), and third gRNA vector (pYPQ133A) was used, respectively. Plasmid DNA from PCR verified positive clones were extracted by boiling method as describe earlier and sent for DNA sequencing using a DK752 (5 mM) primer (Table#1).

Step 2: Golden Gate Assembly of two and three gRNAs in pYPQ142 and pYPQ143 Respectively

Sequenced verified clones were set up for assembly of two gRNAs in pYQP142 and three gRNAs in pYPQ143. For assembling two gRNAs, the reaction mixture was prepared by adding one µl each of pYPQ131-gRNA1 (100ng/µl), pYPQ132-gRNA2 (100 ng/µl), pYPQ142 (100ng/µl), and 10x T4 DNA ligase buffer (NEB) and 0.5 µl each of BsaI (NEB), and T4 DNA ligase (NEB). The final reaction volume of 10 µl was set by adding five µl of milli Q water. For assembling three gRNAs, the reaction mixture was prepared by adding one µl each of pYPQ131-gRNA1 (100ng/µl), pYPQ132-gRNA2 (100 ng/µl), pYPQ133-gRNA3(100/µl), pYPQ143 (100ng/µl), and 10x T4 DNA ligase buffer (NEB) and 0.5 µl each of BsaI (NEB), and T4 DNA ligase (NEB). The final reaction volume of 10 µl was set by adding 4 µl of milli Q water. Both reaction mixture was run through thermocycler set at ten cycles of 37 °C, 5 minutes and 16 °C, 10 minutes followed by 50 °C for 5 minutes, 80 °C for 5 min and a final hold at 10 °C.

Golden Gate Assembly of Negative two gRNAs-pYPQ142 and Negative three gRNAs-pYPQ143 Clone

Negative control two gRNAs-pYPQ142 constructs and negative control three gRNAs-pYPQ143 constructs were prepared using linearized empty (without gRNA) pYPQ131A, pYPQ132A, and pYPQ133 vector. The reaction mixture was prepared as same way as of positive construct, and thermocycler was run in same condition. Diagrammatic illustration showing the assembly of 3gRNA cassettes into Gateway entry vector pYPQ143 is represented in Figure 8.

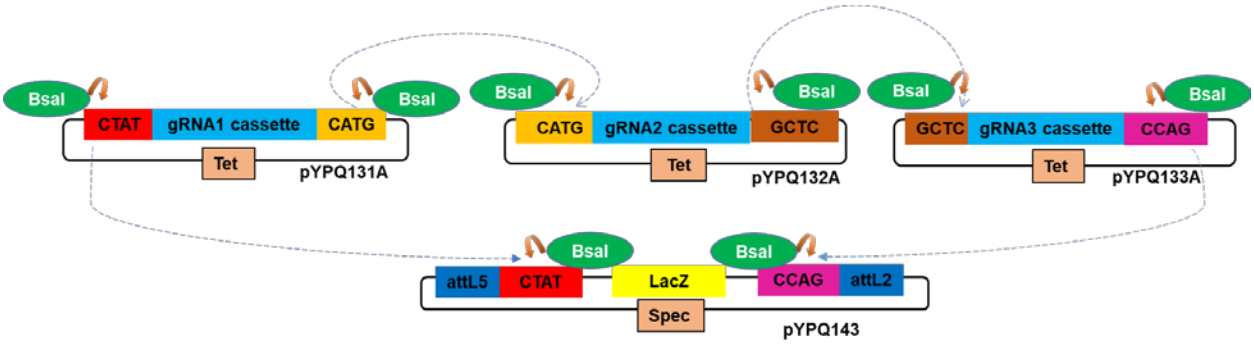

Figure 8: Step 2: Golden Gate Assembly of 3 gRNAS Cassettes into Gateway Entry Vector pYPQ143. Redrawn from Lowder et al. 2015.

Transformation and Screening of Assembly of two and three gRNAs Positive and Negative Construct in pYQP142 and pYPQ143

Two microliters of the reaction product were used to transform Top10 *E. coli* competent cells as described earlier and the bacterial cells were grown on an LB media plate containing spectinomycin (100 µg/ml) overnight at 37 °C. The blue-white screening was applied for easy detection of the positive clone. For this, 40 µl of IPGT (100mM) and 40 µl of X-gal solution (20 mg/ml) was spread on an LB media plate at least 30 minutes prior to plating transformed competent cells. The next day, an isolated colony from each construct (including one blue colony from each construct as a negative control) were grown in 5 ml LB broth with spectinomycin (100 µg/ml) overnight at 37 °C. Next day, plasmid DNA from each culture was extracted using the boiling method as described earlier.

Screening for successful assembly of constructs was done by restriction digestion of extracted plasmid from each construct. Restriction digestion mixture was prepared by adding 0.5 µl of each restriction enzyme BamHI (Takara) and EcoRV (Takara), one µl of Buffer K, 1000ng plasmid, and a final volume was adjusted to 10 µl

using autoclaved water. The reaction mixture was incubated at 37 °C for 3 hours, and digested products were analyzed by gel electrophoresis as described earlier.

Step3: Gateway Assembly of CRISPR-Cas9 System into a Binary Vector pMDC32

Gateway LR section was used to assemble two gRNAs, three gRNAs and Cas9 into a binary vector pMDC32. The reaction mixture for 2gRNA (+ve) construct was prepared by adding two µl each of pYQP150 (25 ng/µl), pYPQ142-2gRNA (25 ng/µl), and pMDC32 (100ng/µl) and one µl LR clonase II. Similarly, for 3gRNA (+ve) construct was prepared by adding pYPQ143-3gRNA plasmid instead of pYPQ143-2gRNA. Both 2gRNA (-ve) and 3gRNA (-ve) construct were prepared similarly as of positive construct using pYPQ142 (-ve) and pYPQ143 (-ve). The reaction mixtures were incubated overnight at room temperature. Next day, one µl of proteinase K was added in each reaction tubes and mixtures were incubated at 37 °C for 10 minutes to terminate the reaction. Simple diagrammatic illustration showing the assembly of gRNA cassettes and Cas9 represented by Figure 9.

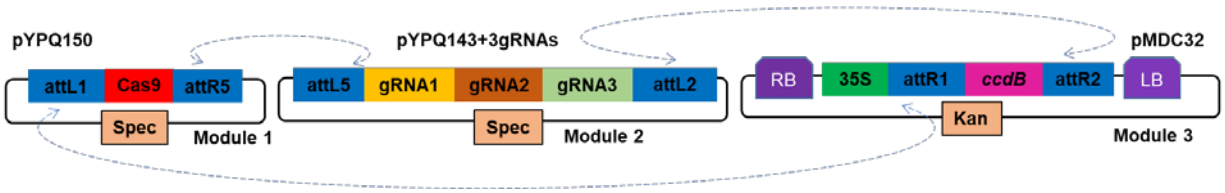

Figure 9: Step3: Gateway Assembly of CRISPR-Cas9 System into Binary Vector pMDC32. Redrawn from Lowder et al. 2015.

Transformation and Verification of Gateway Assembly in Binary Vector pMDC32

Two microliters of the reaction product were used to transform Top10 *E. coli* competent cells as described earlier and the bacterial cells were grown on an LB media

containing kanamycin (50 µg/ml) overnight at 37 °C. Following day, an isolated colony from each construct was grown in 5 ml LB broth with kanamycin (50 µg/ml) overnight at 37 °C. Next day, plasmid DNA from each culture was extracted using the boiling method as described earlier.

Successful assembly of CRISPR construct in the binary vector pMDCD32 was verified by restriction digestion of extracted plasmid from each construct. Restriction digestion mixture was prepared by adding one µl of each restriction enzyme XbaI (Fisher), one µl of Buffer D, 1000 ng plasmid, and final volume was adjusted to 10 µl using autoclaved water. The reaction mixture was incubated at 37 °C for 3 hours, and digested products were analyzed by gel electrophoresis as described earlier. Restriction verified construct was again sent for DNA sequencing to detect inserted gRNAs and Cas9.

Agrobacterium tumefaciens LBA4404 cells Transformation with Final Construct

The sequenced verified construct was used to transform chemically competent *Agrobacterium tumefaciens LBA4404* cells as described earlier. Colony PCR as described earlier was performed to confirm transformation into Agrobacterium using vector primer M13 (reverse) and gRNA specific primers (Table#1) DK746 forward for 2gRNA construct and DK748 forward for 3gRNA construct.

Transformation of *Nicotiana tabacum* with *Agrobacterium LBA4404* Containing 2gRNA and 3gRNA Constructs

Agrobacterium with sequence-verified constructs was grown in LB broth containing rifampicin (20 µg/ml) and kanamycin (100 µg/ml) for two days at 28 °C. After

two days, when the culture reached stationary phase, the culture was diluted with LB broth by transferring 20 ml of culture to 20 ml of fresh LB broth in sterile 50 ml falcon tube. Four to five young leaves from XNN (wild-type) tobacco plants were collected and surfaced sterilized by immersing in 20 % (v/v) commercial bleach with 0.1% Tween-80 for 15-20 minutes with occasional turning over the leaves. The leaves were then rinsed three times with sterile water to remove bleach. Leaf discs (~50) were punched out using a sterile cork borer (#6) and incubated with diluted *Agrobacterium* culture on a rocking platform for 15-20 minutes at room temperature. Using sterile forceps, leaf discs were then removed, blotted in sterile paper and plated on the shoot inducing media (SIM) (Appendix B) without antibiotic in an inverted position (dorsal surface up). Plates were then incubated in the dark for two days at 23 °C. After two days, all leaf discs were removed and incubated in 30 ml of MS medium containing 3% sucrose, cefatoxime (100 µg/ml) and carbenicillin (250 µg/ml) at room temperature in the rocking platform. After 2 hours, leaf discs were removed, blotted in sterile paper and plated on SIM media containing cefotaxime (100 µg/ml), carbenicillin (250 µg/ml) and hygromycin (10 µg/ml) in an inverted position. Plates were then incubated until calli development at 23 °C/ 16 hours light condition. After shoots developed to ~1-inch-tall, they were transferred into root inducing media (RIM) containing cefotaxime (100 µg/ml), carbenicillin (250 µg/ml) and hygromycin (10 µg/ml). Fully rooted plants were later transferred to soil. Carbenicillin and cefotaxime were used to kill the *Agrobacterium* and hygromycin was used for screening of transformed tobacco cells.

Screening of SIP68 Knock Out Transgenic Line Generated by CRISPR Cas9

CRISPR Cas9 system target DNA and introduces mutation in targeted gene. This results in a non-functional gene (Hsu et al. 2014). SIP68 knock out transgenic line generated by CRISPR Cas9 system was screened both by amplifying the edited genomic DNA (gDNA) and by RT-PCR. Amplification of SIP68 region in genomic DNA will help us to know section of *SIP68* gene deleted by 2gRNA and 3gRNA constructs while RT-PCR will help us to understand level of SIP68 transcription in transgenic line.

Extraction of Genomic DNA (gDNA) from Transgenic SIP68 Knock Out Line

Ten leaf discs from transgenic lines were collected using a cork borer (#6) and ground in 300 µl extraction buffer (Appendix B) using a mechanical grinder. Samples were then centrifuged to remove large debris and incubated at 65 °C for 15 minutes. Samples were then cooled to room temperature, and one µl of RNase (10mg/ml) was added and incubated at 37 °C for 15 minutes. After incubation, 250 µl of phenol:chloroform:isoamyl alcohol (25:24:1) was added to the sample and mixed by inverting tubes several times. The samples were then centrifuged for 7 minutes at 18,800 x g. Upper aqueous phase was transferred into a new eppendorf tube, and 100 µl of 5M ice-cold potassium acetate was added. The mixture was incubated on ice for 5 minutes and later centrifuged for 15 minutes at 16,200 x g. Four hundred microliters of supernatant were then added with 216 µl of ice-cold isopropanol and incubated in ice for 20 minutes. After incubation, samples were centrifuged for 10 minutes at 9,600 x g at room temperature. The resulting supernatant was discarded, and the pellet was washed with 500 µl of 70% ethanol. The resulting pellet was resuspended in 20 µl TE buffer (pH 8.0), and genomic DNA was quantified using nanodrop spectrophotometer.

PCR Amplification of Edited Genomic DNA

PCR amplification of *NtGT4* gene was performed to detect mutated *SIP68* gene in transgenic lines. The genomic DNA (1 µg) was first digested with restriction enzyme SpeI (NEB) and fragments thus generated were amplified by PCR. The PCR mixture was prepared by adding two µl of digested genomic DNA fragments, one µl of 10x dNTP, one µl of 10x PCR buffer, 0.2 µl each of forward and reverse primer, 0.2 µl of Taq polymerase and 5.4 µl of autoclaved milli-Q water. DK643 and DK644 (Table#1) were used as a primer. PCR product was analyzed by gel electrophoresis as described earlier.

Screening Using RT-PCR

Total RNA was extracted using a guanidine-HCl (GunHCl) buffer (Appendix B) and extracted RNA was used to synthesize cDNA. For this method, three leaf discs were collected using cork borer (#6) and grounded into a fine powder using the mechanical grinder in liquid nitrogen. To the powder, 500 µl of GunHCl buffer + 3.45 µl of β-mercaptoethanol was added and mixed by vortexing. The mixture was then incubated at room temperature for 10 minutes and centrifuged for 10 minutes at room temperature. The resulting supernatant was transferred into 2 ml screw capped tube and 500 µl of water-saturated phenol and 500 µl of chloroform: isoamyl alcohol (24:1) was added. The mixture was incubated at room temperature on a shaker for 10 minutes. After incubation, it was centrifuged for 10 minutes at 6,200 x g at room temperature. The resulting supernatant was transferred to another tube and an equal volume of chloroform: isoamyl alcohol (24:1) was added and incubated at room temperature in a shaker for 10 minutes. After incubation, the mixture was centrifuged at

4°C for 10 minutes at 9,500 x g. The resulting supernatant was again transferred to a fresh eppendorf tube, and 1/10 volume of 3 M sodium acetate and an equal volume of cold isopropanol was added. The mixture was then incubated at -20°C for at least 15 minutes and later centrifuged at 4°C for 10 minutes at 9,500 x g. The resulting supernatant was discarded, and the pellet was resuspended in 0.5ml of 75% ethanol and incubated on ice for 5 minutes. After incubation, it was centrifuged at 4°C for 5 minutes at 5,300 x g. The resulting supernatant was carefully removed, and the pellet was air dried by placing under light for 10-15 minutes. The air-dried pellet was again resuspended in 43 µl of DEPC treated water and incubated for 10 minutes at 55°C. Tubes were then vortex several times to dissolve pellet in the DEPC treated water and subjected to DNase treatment.

For DNase treatment, five µl of DNase buffer and two µl of DNase (Promega) was added to the solution and incubated for 20 minutes at 37°C. After incubation, 200 µl of trizol was added and mixed properly by inverting several times. After 5 minutes 100 µl of chloroform was added and mixed properly by inverting several times. The solution was then incubated for 3 minutes at room temperature and then centrifuged at 4°C for 15 minutes at 13,600 x g. After centrifugation, the upper aqueous phase was transferred to a new tube, and 200 µl of isopropanol was added. The solution was mixed properly and incubated at room temperature for 20 minutes. Following incubation, centrifugation was done at 4°C for 10 minutes at 13,600 x g. The resulting supernatant was discarded, and the pellet was resuspended in 500 µl of ice-cold 75% ethanol. The sample was again centrifuged at 4°C for 5 minutes at 5,300 x g. The supernatant was again discarded, and the pellet was air dried by placing under light for 10-15 minutes. Air dried

pellet was resuspended properly in 20 µl of 0.1% DEPC treated water, and RNA concentration was quantified using nanodrop spectrophotometer. One microgram of total RNA was used to synthesize cDNA as described earlier and remaining RNA was stored at -80°C. cDNA thus synthesized was used to check SIP68 expression using RT-PCR as described before.

CHAPTER 3

RESULTS

Subcellular Localization of SIP68

In silico Analysis of SIP68 Subcellular Localization

Various online signal peptide prediction software (Figure 10-12) predicted that SIP68 lacked the presence of any specific signal peptide. Signal peptide lacking protein is usually thought to localize in the cytoplasm (Moraga et al. 2009).

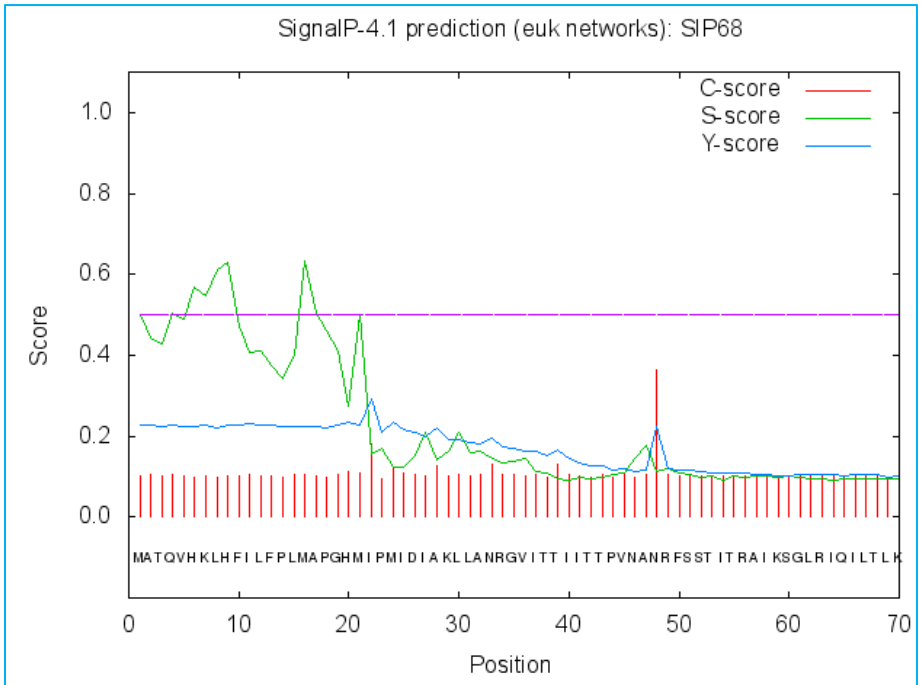

Figure 10: Signalp-4.1 Predicting SIP68 Lacking Signal Peptide. C-score is a raw cleavage site score that distinguish signal peptide cleavage sites from other. S-score is a signal peptide score that distinguish positions within signal peptides from positions in the mature part of the proteins and from proteins without signal peptides. Y-score is a combined cleavage site score that is geometric average of the slope of the S-score and C-score (Petersen et al. 2011).

```
Most Significant SValue:
>U73C1_ARATH
          Length = 60

 Score = 78.2 bits (191), Expect = 8e-16
 Identities = 35/52 (67%), Positives = 43/52 (82%)

Query: 1  MATQVHKLHFILFPLMAPGHMIPMIDIAKLLANRGVITTIITTPVNANRFSSTITRAIKS 60
                LHF+LFP MA GHMIPM+DIA+LLA RGV  TI+TTP NA RF + ++RAI+
Sbjct:        9  LHFVLFPFMAQGHMIPMVDIARLLAQRGVTITIVTTPQNAGRFKNVLSRAIQ 60

Result: Does NOT contain a Signal Peptide (by similarity to U73C1_ARATH)
```

Figure 11: Signal BLAST Predicting SIP68 Lacking Signal Peptide. Signal blast is based on sequence alignment techniques where Query is SIP68 mature protein sequence and Sbjct is a UDP-glycosyltransferase 73C1 (U73C1-ARATH) of Arabidopsis thaliana aligned by software itself (Frank and Sippl 2008).

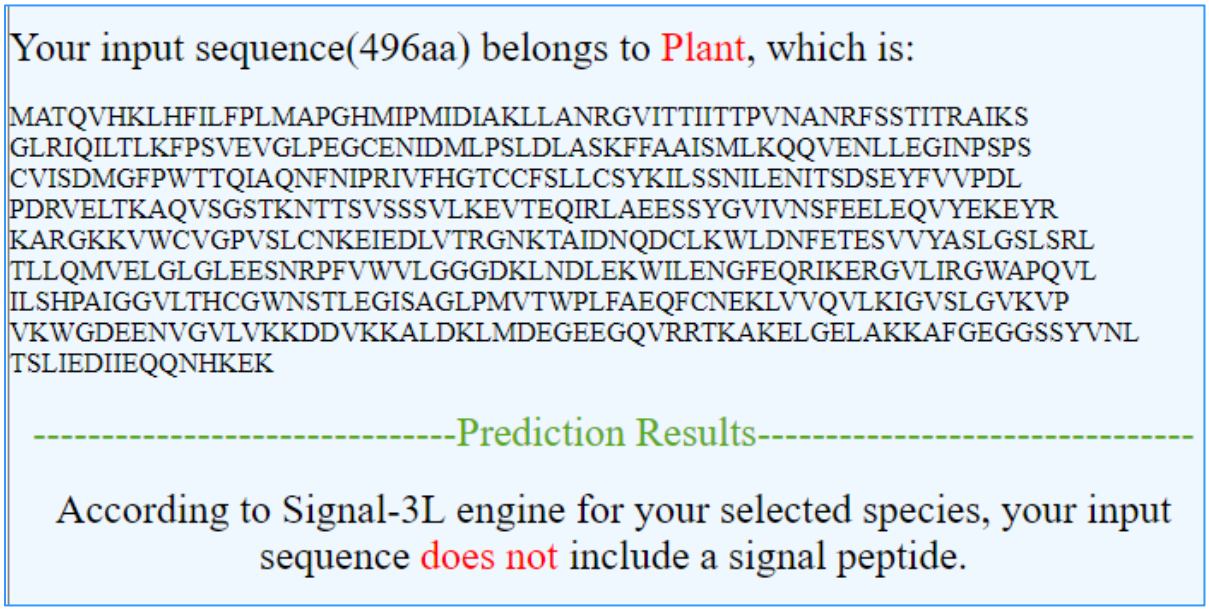

Figure 12: Signal-3L Predicting SIP68 Lacking Signal Peptide (Shen and Chou 2007)

Subcellular Localization Using Confocal Microscopy

Amplification of SIP68 Fragment

The full-length SIP68 fragment was RT-PCR amplified using primers DK563 and DK564 (Table#1) to add attB1 and attB2 sites for facilitating gateway cloning (Figure 13).

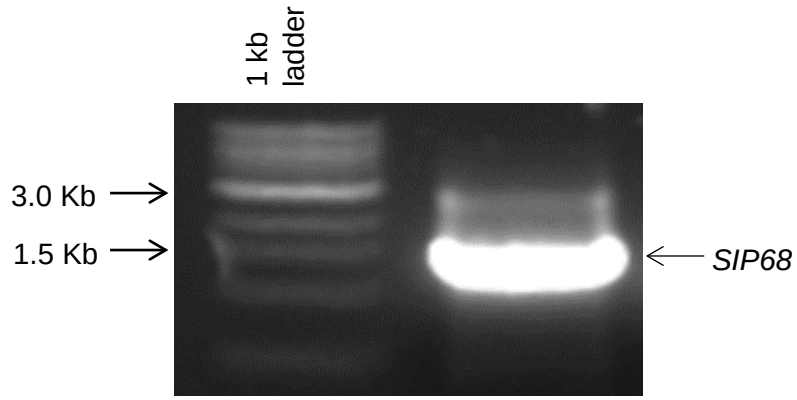

Figure 13: RT-PCR Amplification of SIP68 cDNA. Ethidium bromide stained 0.8% agarose gel showing ~1500bp amplified SIP68 cDNA. DNA ladder (1 kb) was used to compare the product size.

Cloning of SIP68 in Entry Clone pDONOR221

Gel extracted and purified SIP68 with attB1 and attB2 sites were cloned into entry plasmid, pDOR221, using the BP recombination reaction of gateway cloning system. BP reaction allows the recombination reaction between attP1 and attP2 sites present in entry clone (pDONR221) and attB1 and attB2 sites present in gel extracted SIP68. Colony PCR with M13 forward and DK518 reverse was used to detect a positive clone (Figure 14). The plasmid was extracted from PCR positive colonies and was sent for DNA sequencing. DNA sequencing result of one of the positive clones is shown below (Figure 15).

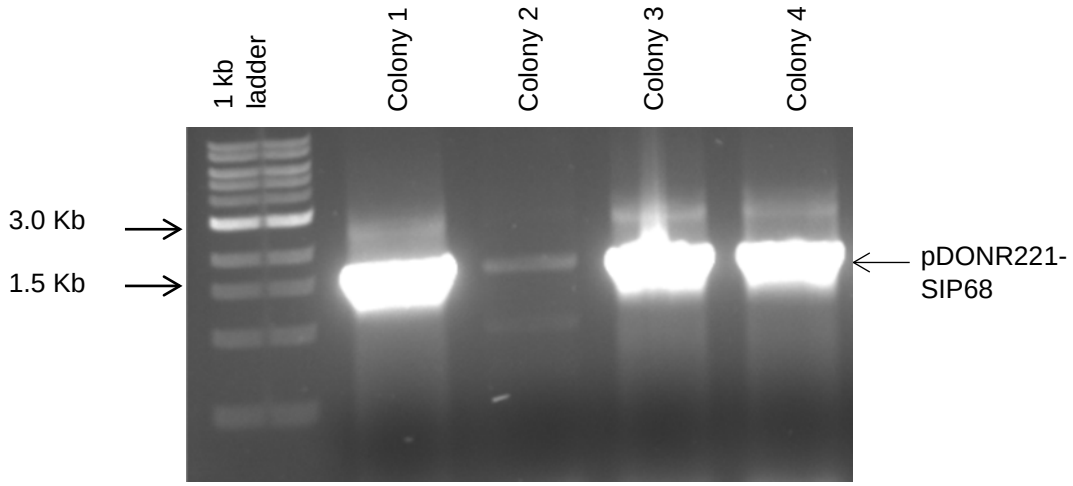

Figure 14: Colony PCR Amplification of pDONR221-SIP68. Ethidium bromide stained 0.8% agarose gel showing ~1581bp amplified pDONR-SIP68. DNA ladder (1 kb) was used to compare the product size.

```
Predicted      GTAAAACGACGGCCAGTCTTAAGCTCGGGCCCCAAATAATGATTTTATTTTGACTGATAG  60
Colony1        ----------------------------------CANATGATTTTATTTTGACTGATAG  25
                                                  **********************

Predicted      TGACCTGTTCGTTGCAACAAATTGATGAGCAATGCTTTTTTATAATGCCAACTTTGTACA 120
Colony1        TGACCTGTTCGTTGCAACAAATTGATGAGCAATGCTTTTTTATAATGCCAACTTTGTACA  85
               ************************************************************

Predicted      AAAAAGCAGGCTCCATGGCAACTCAAGTGCACAAACTTCATTTCATACTATTCCCTTTAA 180
Colony1        AAAAAGCAGGCTCCATGGCAACTCAAGTGCACAAACTTCATTTCATACTATTCCCTTTAA 145
               ************************************************************

Predicted      TGGCTCCAGGCCACATGATTCCTATGATAGACATAGCTAAACTTCTAGCAAATCGCGGTG 240
Colony1        TGGCTCCAGGCCACATGATTCCTATGATAGACATAGCTAAACTTCTAGCAAATCGCGGTG 205
               ************************************************************

Predicted      TCATTACCACTATCATCACCACTCCAGTAAACGCCAATCGTTTCAGTTCAACAATTACTC 300
Colony1        TCATTACCACTATCATCACCACTCCAGTAAACGCCAATCGTTTCAGTTCAACAATTACTC 265
               ************************************************************

Predicted      GTGCCATAAAATCCGGTCTAAGAATCCAAATTCTTACACTCAAATTTCCAAGTGTAGAAG 360
Colony1        GTGCCATAAAATCCGGTCTAAGAATCCAAATTCTTACACTCAAATTTCCAAGTGTAGAAG 325
               ************************************************************

Predicted      TAGGATTACCAGAAGGTTGCGAAAATATTGACATGCTTCCTTCTCTTGACTTGGCTTCAA 420
Colony1        TAGGATTACCAGAAGGTTGCGAAAATATTGACATGCTTCCTTCTCTTGACTTGGCTTCAA 385
               ************************************************************

Predicted      AGTTTTTTGCTGCAATTAGTATGCTGAAACAACAAGTTGAAAATCTCTTAGAAGGAATAA 480
Colony1        AGTTTTTTGCTGCAATTAGTATGCTGAAACAACAAGTTGAAAATCTCTTAGAAGGAATAA 445
               ************************************************************

Predicted      ATCCAAGTCCAAGTTGTGTTATTTCAGATATGGGATTTCCTTGGACTACTCAAATTGCAC 540
Colony1        ATCCAAGTCCAAGTTGTGTTATTTCAGATATGGGATTTCCTTGGACTACTCAAATTGCAC 505
               ************************************************************

Predicted      AAAATTTTAATATCCCAAGAATTGTTTTTCATGGTACTTGTTGTTTCTCACTTTTATGTT 600
Colony1        AAAATTTTAATATCCCAAGAATTGTTTTTCATGGTACTTGTTGTTTCTCACTTTTATGTT 565
               ************************************************************
```

```
Predicted       CCTATAAAATACTTTCCTCCAACATTCTTGAAAATATAACCTCAGATTCAGAGTATTTTG  660
Colony1         CCTATAAAATACTTTCCTCCAACATTCTTGAAAATATAACCTCAGATTCAGAGTATTTTG  625
                ************************************************************

Predicted       TTGTTCCTGATTTACCCGATAGAGTCGAACTAACGAAAGCTCAGGTTTCAGGATCGACGA  720
Colony1         TTGTTCCTGATTTACCCGATAGAGTCGAACTAACGAAAGCTCAGGTTTCAGGATCGACGA  685
                ************************************************************

Predicted       AAAATACTACTTCTGTTAGTTCTTCTGTATTGAAAGAAGTTACTGAGCAAATCAGATTAG  780
Colony1         AAAATACTACTTCTGTTAGTTCTTCTGTATTGAAAGAAGTTACTGAGCAAATCAGATTAG  745
                ************************************************************

Predicted       CCGAGGAATCATCATATGGTGTAATTGTTAATAGTTTTGAGGAGTTGGAGCAAGTGTATG  840
Colony1         CCGAGGAATCATCATATGGTGTAATTGTTAATAGTTTTGAGGAGTTGGAGCAAGTGTATG  805
                ************************************************************

Predicted       AGAAAGAATATAGGAAAGCTAGAGGGAAAAAAGTTTGGTGTGTTGGTCCTGTTTCTTTGT  900
Colony1         AGAAAGAATATAGGAAAGCTAGAGGGAAAAAAGTTTGGTGTGTTGGTCCTGTTTCTTTGT  865
                ************************************************************

Predicted       GTAATAAGGAAATTGAAGATTTGGTTACAAGGGGTAATAAAACTGCAATTGATAATCAAG  960
Colony1         GTAATAAGGAAATTGAAGATTTGGTTACAAGGGGTAATAAAACTGCAATTGATAATCAAG  925
                ************************************************************

Predicted       ATTGCTTGAAATGGTTAGATAATTTTGAAACAGAATCTGTGGTTTATGCAAGTCTTGGAA 1020
Colony1         ATTGCTTGAAATGGTTAGATAATTTTGAAACAGAATCTGTGGTTTATGCAAGTCTTGGAA  985
                ************************************************************

Predicted       GTTTATCTCGTTTGACATTATTGCAAATGGTGGAACTTGGTCTTGGTTTAGAAGAGTCAA 1080
Colony1         GTTTATCTCGTTTGACATTATTGCAAATGGTGGAACTTGGTCTTGGTTTAGAAGAGTCAA 1045
                ************************************************************

Predicted       ATAGGCCTTTTGTATGGGTATTAGGAGGAGGTGATAAATTAAATGATTTAGAGAAATGGA 1140
Colony1         ATAGGCCTTTTGTATGGGTATTAGGAGGAGGTGATAAATTAAATGATTTAGAGAAATGGA 1105
                ************************************************************

Predicted       TTCTTGAGAATGGATTTGAGCAAAGAATTAAAGAAAGAGGAGTTTTGATTAGAGGATGGG 1200
Colony1         TTCTTGAGAATGGATTTGAGCAAAGAATTAAAGAAAGAGGAGTTTTGATTAGAGGATGGG 1165
                ************************************************************

Predicted       CTCCTCAAGTGCTTATACTTTCACACCCTGCAATTGGTGGAGTATTGACTCATTGCGGAT 1260
Colony1         CTCCTCAAGTGCTTATACTTTCACACCCTGCAATTGGTGGAGTATTGACTCATTGCGGAT 1225
                ************************************************************

Predicted       GGAATTCTACATTGGAAGGTATTTCAGCAGGATTACCAATGGTAACATGGCCACTATTTG 1320
Colony1         GGAATTCTACATTGGAAGGTATTTCAGCAGGATTACCAATGGTAACATGGCCACTATTTG 1285
                ************************************************************

Predicted       CTGAGCAATTTTGCAATGAGAAGTTAGTAGTCCAAGTGCTAAAAATTGGAGTGAGCCTAG 1380
Colony1         CTGAGCAATTTTGCAATGAGAAGTTAGTAGTCCAAGTGCTAAAAATTGGAGTGAGCCTAG 1345
                ************************************************************

Predicted       GTGTGAAGGTGCCTGTCAAATGGGGAGATGAGGAAAATGTTGGAGTTTTGGTAAAAAAGG 1440
Colony1         GTGTGAAGGTGCCTGTCAAATGGGGAGATGAGGAAAATGTTGGAGTTTTGGTAAAAAAGG 1405
                ************************************************************

Predicted       ATGATGTTAAGAAAGCATTAGACAAACTAATGGATGAAGGAGAAGAAGGACAAGTAAGAA 1500
Colony1         ATGATGTTAAGAAAGCATTAGACAAACTAATGGATGAAGGAGAAGAAGGACAAGTAAGAA 1465
                ************************************************************

Predicted       GAACAAAAGCAAAAGAGTTAGGAGAATTGGCTAAAAAGGCATTTGGAGAAGGTGGTTCTT 1560
Colony1         GAACAAAAGCAAAAGAGTTAGGAGAATTGGCTAAAAAGGCATTTGGAGAAGGTGGTTCTT 1525
```

```
                ************************************************************

Predicted       CTTATGTTAACTTAACATCTCTGATTGAAGACATCATTGAGCAACAAAATCACAAGGAAA 1620
Colony1         CTTATGTTAACTTAACATCTCTGATTGAAGACATCATTGAGCAACAAAATCACAAGGAAA 1585
                ************************************************************

Predicted       AATAGTACCCAGCTTTCTTGTACAAAGTTGGCATTATAAGAAAGCATTGCTTATCAATTT 1680
Colony1         AATAGTACCCAGCTTTCTTGTACAAAGTTGGCATTATAAGAAAGCATTGCTTATCAATTT 1645
                ************************************************************

Predicted       GTTGCAACGAACAGGTCACTATCAGTCAAAATAAAATCATTATTTCAGCTTTCTTGTACA 1740
Colony1         GTTGCAACGAACAGGTCACTATCAGTCAAAATAAAATCATTATTT--------------- 1690
                *****************************************

Predicted       AAGTTGGCATTATAAGAAAGCATTGCTTATCAATTTGTTGCAACGAACAGG  1791
Colony1         -------------------------------------------------  1690
```

Figure 15: Nucleotide Sequence of a PCR Positive pDNOR221-SIP68-colony. Predicted sequence is the computer generated expected sequence containing full length SIP68 sequence and part of vector sequence that is expected to be sequenced by sequencing primer used.

Cloning of pDONR221-SIP68 in Destination Vector pSITE-2CA

Plasmid DNA from sequence verified positive colony was isolated and used for LR reaction to generate pSITE-2CA-SIP68 clone. LR recombination reaction allows transfer of DNA fragment containing attL1 and attL2 sites in entry vector pDONR221 into destination vector pSITE-2CA containing attR1 and attR2 sites. Positive clones were detected by colony PCR using DK677 (forward) and DK518 (reverse) primers (Table#1) (Figure 16). The plasmid DNA was extracted from PCR positive colony and was sent for DNA sequencing (Figure 17).

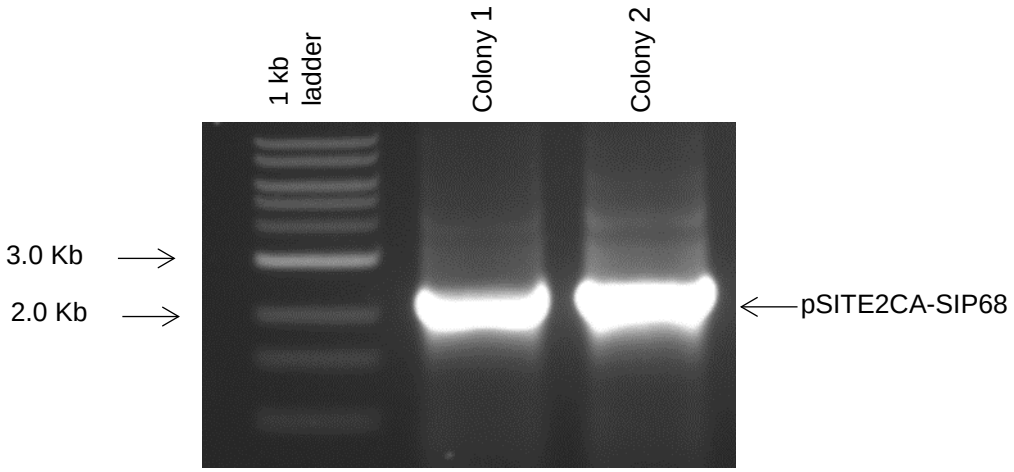

Figure 16: Colony PCR Amplification of SIP68 Cloned into pSITE-2CA. Ethidium bromide stained 0.8% agarose gel showing ~2208 bp amplified pSITE2CA-SIP68. DNA ladder (1 kb) is used to compare the product size.

```
Sequence      CATGGACGAGCTGTACAAGTCCGGACTCAGATCTATCACAAGTTTGTACAAAAAAGCAGG  60
SIP68         ------------------------------------------------------------  0

Sequence      CTCCATGGCAACTCAAGTGCACAAACTTCATTTCATACTATTCCCTTTAATGGCTCCAGG  120
SIP68         ----ATGGCAACTCAAGTGCACAAACTTCATTTCATACTATTCCCTTTAATGGCTCCAGG  56
                  ************************************************************

Sequence      CCACATGATTCCTATGATAGACATAGCTAAACTTCTAGCAAATCGCGGTGTCATTACCAC  180
SIP68         CCACATGATTCCTATGATAGACATAGCTAAACTTCTAGCAAATCGCGGTGTCATTACCAC  116
              ************************************************************

Sequence      TATCATCACCACTCCAGTAAACGCCAATCGTTTCAGTTCAACAATTACTCGTGCCATAAA  240
SIP68         TATCATCACCACTCCAGTAAACGCCAATCGTTTCAGTTCAACAATTACTCGTGCCATAAA  176
              ************************************************************

Sequence      ATCCGGTCTAAGAATCCAAATTCTTACACTCAAATTTCCAAGTGTAGAAGTAGGATTACC  300
SIP68         ATCCGGTCTAAGAATCCAAATTCTTACACTCAAATTTCCAAGTGTAGAAGTAGGATTACC  236
              ************************************************************

Sequence      AGAAGGTTGCGAAAATATTGACATGCTTCCTTCTCTTGACTTGGCTTCAAAGTTTTTTGC  360
SIP68         AGAAGGTTGCGAAAATATTGACATGCTTCCTTCTCTTGACTTGGCTTCAAAGTTTTTTGC  296
              ************************************************************

Sequence      TGCAATTAGTATGCTGAAACAACAAGTTGAAAATCTCTTAGAAGGAATAAATCCAAGTCC  420
SIP68         TGCAATTAGTATGCTGAAACAACAAGTTGAAAATCTCTTAGAAGGAATAAATCCAAGTCC  356
              ************************************************************

Sequence      AAGTTGTGTTATTTCAGATATGGGATTTCCTTGGACTACTCAAATTGCACAAAATTTTAA  480
SIP68         AAGTTGTGTTATTTCAGATATGGGATTTCCTTGGACTACTCAAATTGCACAAAATTTTAA  416
              ************************************************************

Sequence      TATCCCAAGAATTGTTTTTCATGGTACTTGTTGTTTCTCACTTTTATGTTCCTATAAAAT  540
SIP68         TATCCCAAGAATTGTTTTTCATGGTACTTGTTGTTTCTCACTTTTATGTTCCTATAAAAT  476
              ************************************************************
```

```
Sequence    ACTTTCCTCCAACATTCTTGAAAATATAACCTCAGATTCAGAGTATTTTGTTGTTCCTGA  600
SIP68       ACTTTCCTCCAACATTCTTGAAAATATAACCTCAGATTCAGAGTATTTTGTTGTTCCTGA  536
            ************************************************************

Sequence    TTTACCCGATAGAGTCGAACTAACGAAAGCTCAGGTTTCAGGATCGACGAAAAATACTAC  660
SIP68       TTTACCCGATAGAGTCGAACTAACGAAAGCTCAGGTTTCAGGATCGACGAAAAATACTAC  596
            ************************************************************

Sequence    TTCTGTTAGTTCTTCTGTATTGAAAGAAGTTACTGAGCAAATCAGATTAGCCGAGGAATC  720
SIP68       TTCTGTTAGTTCTTCTGTATTGAAAGAAGTTACTGAGCAAATCAGATTAGCCGAGGAATC  656
            ************************************************************

Sequence    ATCATATGGTGTAATTGTTAATAGTTTTGAGGAGTTGGAGCAAGTGTATGAGAAAGAATA  780
SIP68       ATCATATGGTGTAATTGTTAATAGTTTTGAGGAGTTGGAGCAAGTGTATGAGAAAGAATA  716
            ************************************************************

Sequence    TAGGAAAGCTAGAGGGAAAAAAGTTTGGTGTGTTGGTCCTGTTTCTTTGTGTAATAAGGA  840
SIP68       TAGGAAAGCTAGAGGGAAAAAAGTTTGGTGTGTTGGTCCTGTTTCTTTGTGTAATAAGGA  776
            ************************************************************

Sequence    AATTGAAGATTTGGTTACAAGGGGTAATAAAACTGCAATTGATAATCAAGATTGCTTGAA  900
SIP68       AATTGAAGATTTGGTTACAAGGGGTAATAAAACTGCAATTGATAATCAAGATTGCTTGAA  836
            ************************************************************

Sequence    ATGGTTAGATAATTTTGAAACAGAATCTGTGGTTTATGCAAGTCTTGGAAGTTTATCTCG  960
SIP68       ATGGTTAGATAATTTTGAAACAGAATCTGTGGTTTATGCAAGTCTTGGAAGTTTATCTCG  896
            ************************************************************

Sequence    TTTGACATTATTGCAAATGGTGGAACTTGGTCTTGGTTTAGAAGAGTCAAATAGGCCTTT 1020
SIP68       TTTGACATTATTGCAAATGGTGGAACTTGGTCTTGGTTTAGAAGAGTCAAATAGGCCTTT  956
            ************************************************************

Sequence    TGTATGGGTATTAGGAGGAGGTGATAAATTAAATGATTTAGAGAAATGGATTCTTGAGAA 1080
SIP68       TGTATGGGTATTAGGAGGAGGTGATAAATTAAATGATTTAGAGAAATGGATTCTTGAGAA 1016
            ************************************************************

Sequence    TGGATTTGAGCAAAGAATTAAAGAAAGAGGAGTTTTGATTAGAGGATGGGCTCCTCAAGT 1140
SIP68       TGGATTTGAGCAAAGAATTAAAGAAAGAGGAGTTTTGATTAGAGGATGGGCTCCTCAAGT 1076
            ************************************************************

Sequence    GCTTATACTTTCACACCCTGCAATTGGTGGAGTATTGACTCATTGCGGATGGAATTCTAC 1200
SIP68       GCTTATACTTTCACACCCTGCAATTGGTGGAGTATTGACTCATTGCGGATGGAATTCTAC 1136
            ************************************************************

Sequence    ATTGGAAGGTATTTCAGCAGGATTACCAATGGTAACATGGCCACTATTTGCTGAGCAATT 1260
SIP68       ATTGGAAGGTATTTCAGCAGGATTACCAATGGTAACATGGCCACTATTTGCTGAGCAATT 1196
            ************************************************************

Sequence    TTGCAATGAGAAGTTAGTAGTCCAAGTGCTAAAAATTGGAGTGAGCCTAGGTGTGAAGGT 1320
SIP68       TTGCAATGAGAAGTTAGTAGTCCAAGTGCTAAAAATTGGAGTGAGCCTAGGTGTGAAGGT 1256
            ************************************************************

Sequence    GCCTGTCAAATGGGGAGATGAGGAAAATGTTGGAGTTTTGGTAAAAAAGGATGATGTTAA 1380
SIP68       GCCTGTCAAATGGGGAGATGAGGAAAATGTTGGAGTTTTGGTAAAAAAGGATGATGTTAA 1316
            ************************************************************

Sequence    GAAAGCATTAGACAAACTAATGGATGAAGGAGAAGAAGGACAAGTAAGAAGAACAAAAGC 1440
SIP68       GAAAGCATTAGACAAACTAATGGATGAAGGAGAAGAAGGACAAGTAAGAAGAACAAAAGC 1376
            ************************************************************

Sequence    AAAAGAGTTAGGAGAATTGGCTAAAAAGGCATTTGGAGAAGGTGGTTCTTCTTATGTTAA 1500
SIP68       AAAAGAGTTAGGAGAATTGGCTAAAAAGGCATTTGGAGAAGGTGGTTCTTCTTATGTTAA 1436
            ************************************************************
```

```
Sequence        CTTAACATCTCTGATTGAAGACATCATTGAGCAACAAAATCACAAGGAAAAATAGAC      1557
SIP68           CTTAACATCTCTGATTGAAGACATCATTGAGCAACAAAATCACAAGGAAAAATAG--      1491
                **************************************************
```

Figure 17: Sequencing Result of pSITE-2CA-68-Colony#1.

Transformation of pSITE-2CA-SIP68 into *Agrobacterium tumefaciens LBA4404*

Sequenced positive pSITE-2CA-SIP68 plasmid was used to transform *A. tumefaciens LBA4404.* Colony PCR was performed to detect positive clones using DK677 (forward) and DK518 (reverse) primers (Table#1) (Figure 18).

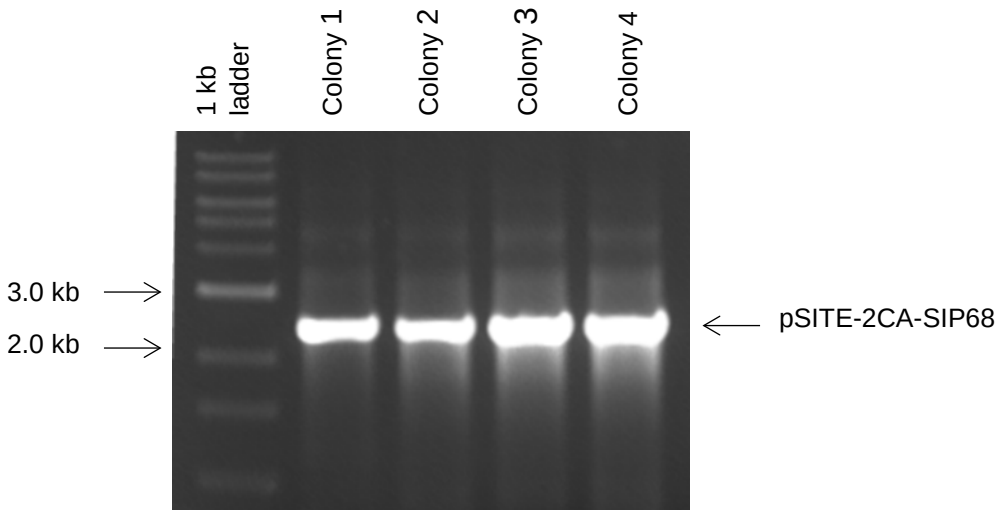

Figure 18: Colony PCR Amplification of pSITE-2CA-SIP68 in *LBA4404*. Ethidium bromide stained 0.8% agarose gel showing ~2208 bp amplified pSITE-2CA-SIP68. DNA ladder (1 kb) was used to compare the product size.

Time Course Expression of SIP68+eGFP

Agrobacterium LBA4404 containing pSITE-2CA-SIP68 plasmid was expressed transiently in *Nicotiana benthamiana* leaves with and without HCPro as described in the methods section to produce SIP68+eGFP protein in tobacco. HCPro was used to suppress plant silencing mechanism and to prolong and enhance SIP68+eGFP protein expression, SIP68+eGFP protein expression pattern over seven days post infiltration

(DPI) is shown in Figure 19. A slight tilt in the band at SIP68+eGFP is due to improper alignment of the polyvinylidene difluoride (PVDF) membrane with gel. SIP68+eGFP production was enhanced and prolonged in case of leaf co-infiltrated with HCPro while in case of leaf without HCPro co-infiltration, SIP68+eGFP production started diminishing after 5 DPI and by 7 DPI no SIP68+eGFP protein was detected.

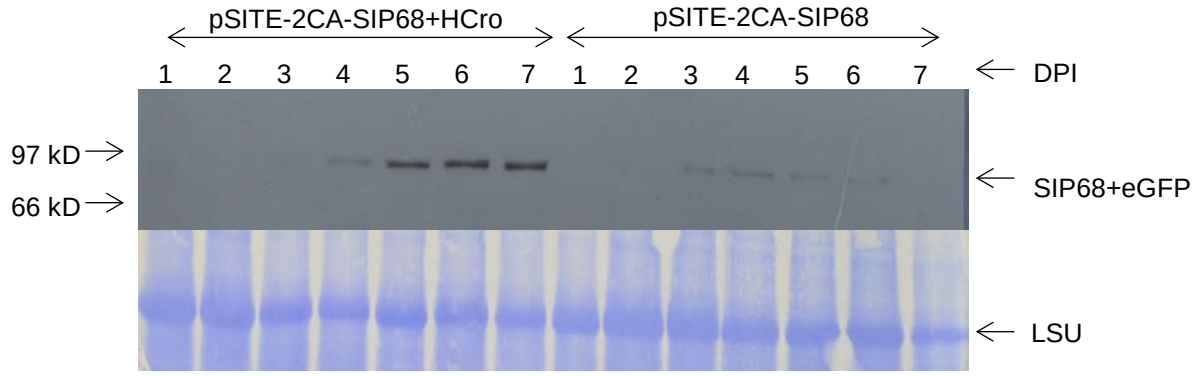

Figure 19: Time Course Expression of SIP68+eGFP Protein Over 7 DPI. Western blot analysis showing upper X ray film of SIP68+eGFP protein expression with and without HCPro infiltration and corresponding commassie blue stained blot of large subunit of RuBisCo (LSU).

Time Course Expression of PR1 Protein

Pathogenesis-related protein 1(PR-1), a member of PR protein family is expressed most abundantly during infection and is used as a marker protein for SA-mediated disease resistance (Seo et al. 2008). Time course expression of pSITE-2CA-SIP68 with HCPro revealed enhanced and prolonged expression of SIP68+eGFP recombinant protein in *N. benthamiana* leaves. To know whether this construct could be used for biotic stress test experiments, PR1 protein expression by *Agrobacterium* only, HCPro only, and pSITE-2CA-SIP68 with and without HCPro was determined. For this, each of the constructs were transiently expressed in *Nicotiana benthamiana* leaves to

check the PR1 protein expression at the different time points. PR1 protein expression was detected by western blot (Figure 20) and corresponding densitometric analysis was performed with respect to PR1 protein expression at 2-day sample (Figure 21). Because the level of PR1 protein expression was significantly high in *Agrobacterium* strain (*LBA4404)* and HCPro only, it was not used for a biotic stress test as resistance exhibited by plant due to PR1 protein production will be difficult to infer whether it was due to *A. tumefaciens* or HCPro or SIP68.

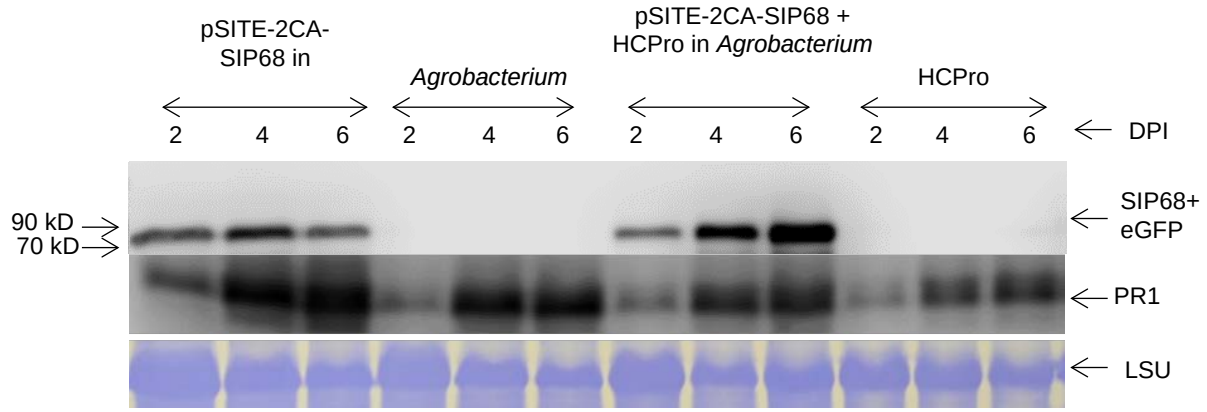

Figure 20: PR1 Protein Expressed by Agrobacterium, HCPro and Agrobacterium+pSITE-2CA-SIP68 With and Without HCPro at Different Time Points. Western blot analysis showing upper SIP68+eGFP protein expression (~82.53 kD), middle blot representing PR1 protein expression and the third representing corresponding coomassie blue stained blot showing large subunit of RuBisCo.

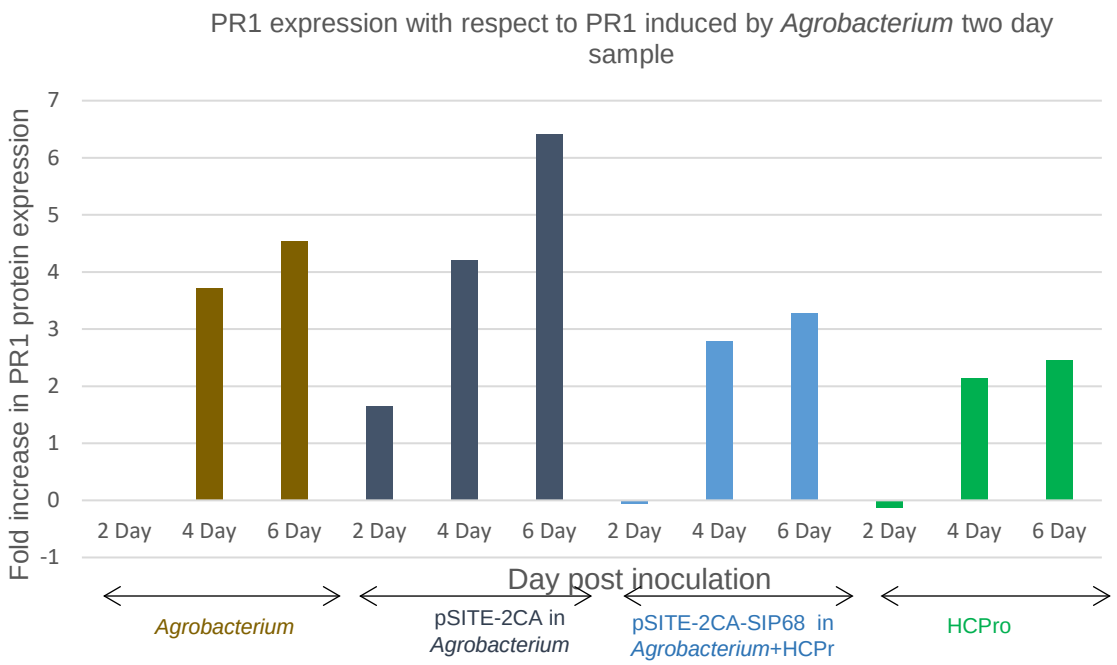

Figure 21: Densitometric Analysis of PR1 Expression at 2, 4 and 6 Days Post Infiltration of *Agrobacterium*, *Agrobacterium*+SIP68+ eGFP With and Without HCPro, and HCPro Only With Respect to *Agrobacterium* two-day Sample.

Confocal Microscopy of SIP68+eGFP Expression

Confocal microscopy as described in methods was done to detect SIP68+eGFP protein expression in tobacco cell with and without HCPro (Figure 22 and 23). Confocal microscopy optically sections the epidermal layers of plants. SIP68+eGFP seems to be sequestered prominently towards the cell periphery and in/around the nucleus. Typically a leaf epidermal cell has a large sized vacuole, and it occupies a greater portion of the cell volume (Speth et al. 2009). The arge sized vacuole pushes the other cell contents toward the edge of the cell forming a thin layer of cytoplasm between the vacuolar membrane (tonoplast) and the plasma membrane (Kost and Chua 2002) . The fluorescent signal detected towards the edge of the cell could be the signal coming from the tonoplast or plasma membrane or cytoplasm or cytoplasmic content. Since the

signal is diffused, it most likely is coming from the cytoplasm and not from either plasma membrane or vacuolar membrane. Tobacco leaf inoculated along with HCPro has much more intensified fluorescent signal than without HCPro.

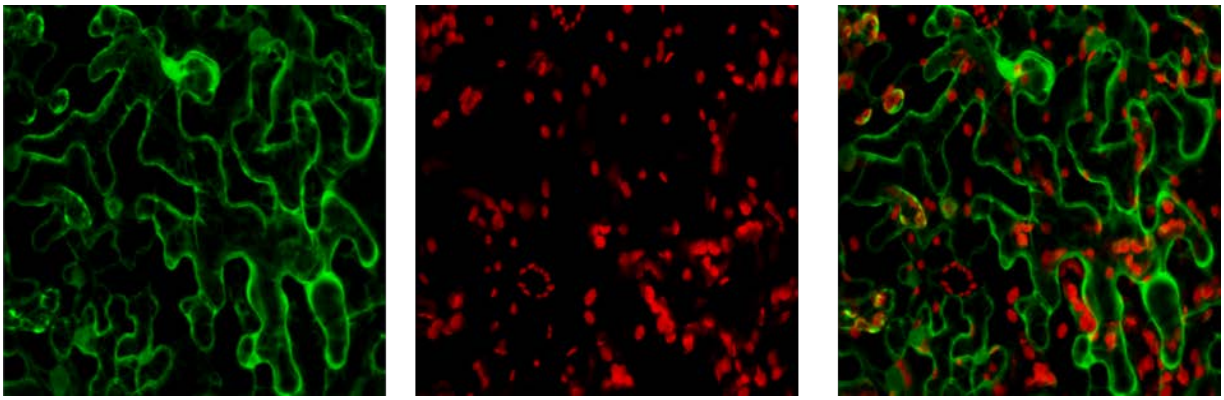

A. SIP68+eGFP B. Chlorophyll C. Merged

Figure 22: Confocal Microscopy Image of SIP68+eGFP and Auto Fluorescence Protein in Tobacco Leaf. A. Sip68+eGFP expression in tobacco cell. B. Chlorophyll autofluorescence in red channel. C. SIP68+eGFP and Chlorophyll fluorescing merged.

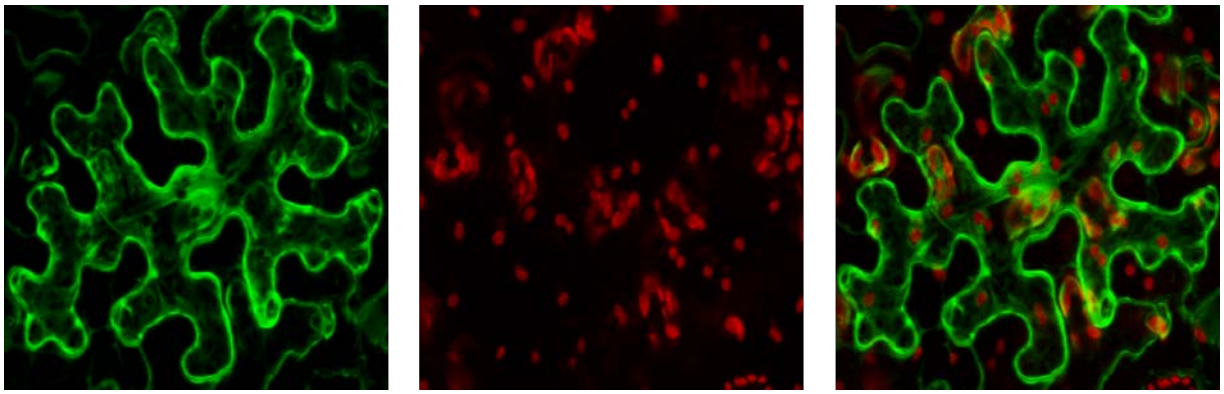

A. SIP68+eGFP with HcPro B. Chlorophyll C. Merged

Figure 23: Confocal Microscopy Image of SIP68+eGFP With HCPro and Auto Fluorescence Protein in Tobacco Leaf. A. SIP68+eGFP expression in tobacco cell. B. Chlorophyll fluorescing red. C. SIP68+eGFP and Chlorophyll expression merged.

Subcellular Fractionation of SIP68+eGFP

SIP68+eGFP with HCPro was express transiently in *Nicotiana benthamiana* for subcellular fractionation. On the 5th day post-infiltration, leaf samples were collected, and subcellular fractionation was performed as described in methods section. An equal amount of protein was used for western blot analysis (Figure 24). SIP68+eGFP expression was detected in the cytosolic fraction with the expected size of ~82.53 kD. Electrophoretic Relative migration distance (Rf) of the standards and SIP68+eGFP were plotted versus log MW to generate a standard curve. A linear fit to the data points and cofficient of determination (R^2) was determined, and molecular weight of SIP68+eGFP was determined using generated equation (Appendix D). The molecular weight of SIP68+eGFP was calculated as 81.23 kD which is similar to the expected size 82.53 kD.

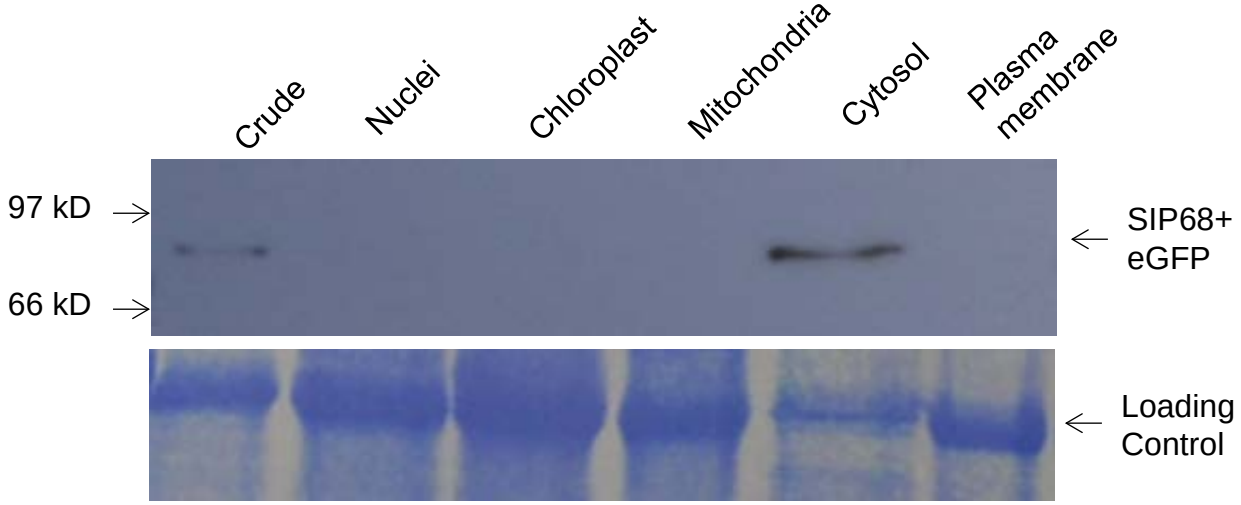

Figure 24: Subcellular Fraction of SIP68+eGFP. Western blot analysis showing upper X ray film of SIP68+eGFP protein expressed in different fractions and lower coomassie blue stained blot showing loading control.

Screening of RNAi Transgenic Lines

Screening T1 Generation

T1-generation of transgenic *Nicotiana tabacum* silenced lines using RNAi system (Kumar et al. 2017 unpublished) was screened for the expression level of the SIP68 transcripts (Figure 25 and Figure 26). Total RNA was extracted from the leaf samples collected from transgenic lines, and RT-PCR was performed as described earlier. Synthetic primers, DK643 and DK644 (Table#1) were used to detect the expression level of SIP68 transcripts. For amplification, a 30X PCR cycle with a 1-minute extension for *Actin* (housekeeping) gene and 2 minutes for SIP68 was set. Transgenic line B, E, G, and M showed a significant level of silencing as compared to wild-type plant (XNN1). Second wild-type control sample, XNN2 did not show any amplification. This is likely to be an error in PCR mixture preparation. *Actin* gene was used to determine the quality of cDNA synthesized and loading control.

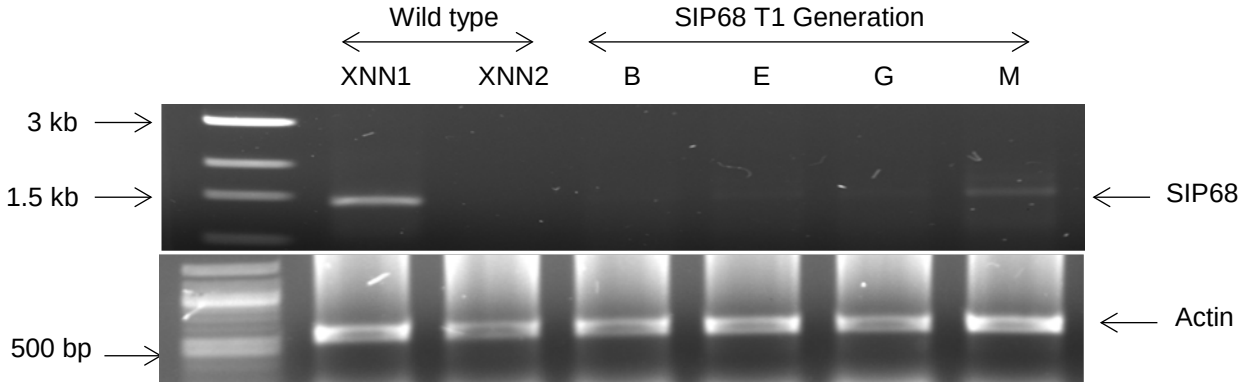

Figure 25: Screening of T1 RNAi Silenced Transgenic Lines. Ethidium bromide stained 0.8% and 1% agarose gel showing expression of SIP68 and actin, respectively. DNA ladder (1 kb) for SIP68 (~1491bp) and 100 bp ladder for actin (~550) was used to compare product size.

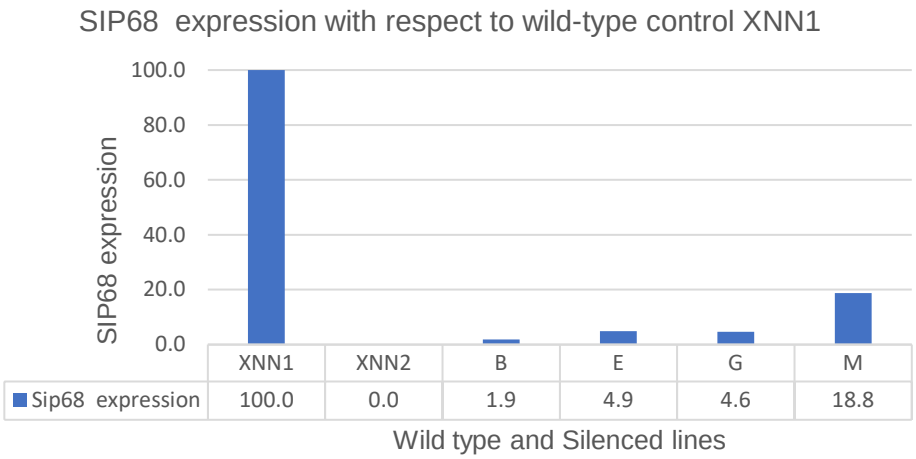

Figure 26: Densitometric Analysis of SIP68 Expression With Respect to XNN1. Signal is normalized to actin intensity in each lane.

Screening T2 Generation of Line #B

T1 silenced transgenic line # B line was grown for seed collection. Seed pods were comparatively smaller in size as compared to wild-type and most of them didn't bore seeds. Around 50 seeds were collected, and they were grown in antibiotic selection media (Kanamycin 100µg/ml) in tissue culture and screened for SIP68 expression. Briefly, total RNA from 12 silenced lines and 2 XNN (wild-type control) were collected and cDNA was synthesized using RT-PCR as described earlier. DK643 and DK644 were used to detect the expression level of SIP68 (Figure 27). The PCR amplification (30X cycle) with a 1-minute extension for *Ef1α* and 2 minutes for *SIP68* was set. Except for transgenic line #B1 (~93%), all (# B2-B12) are more than 96% silenced as compared to wild type control XNN1 (Figure 28). *Ef1α* gene was used to determine the quality of cDNA synthesized and loading control.

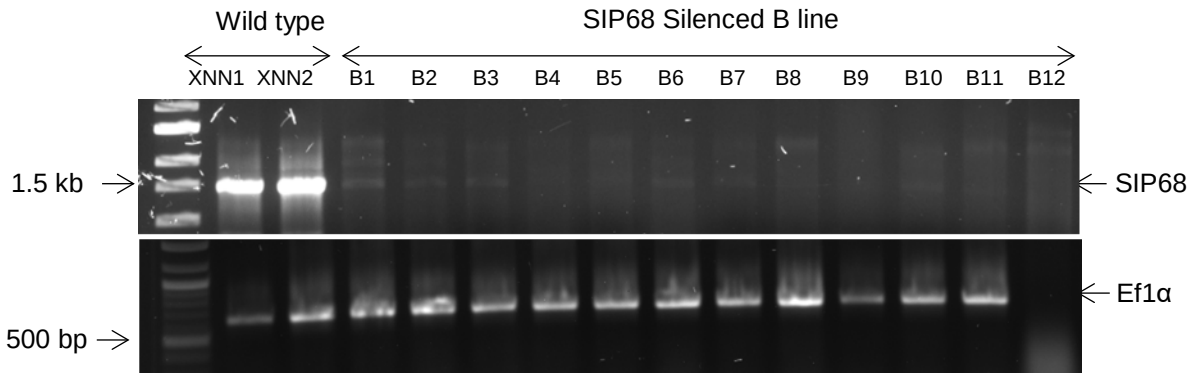

Figure 27: Screening of T2 RNAi Silenced #B Lines. Ethidium bromide stained 0.8% and 1% agarose gel showing expression of SIP68 and Ef1α respectively. DNA ladder (1 kb) for SIP68 (~1491bp) and 100 bp ladder for Ef1α (~600) was used to compare a product size.

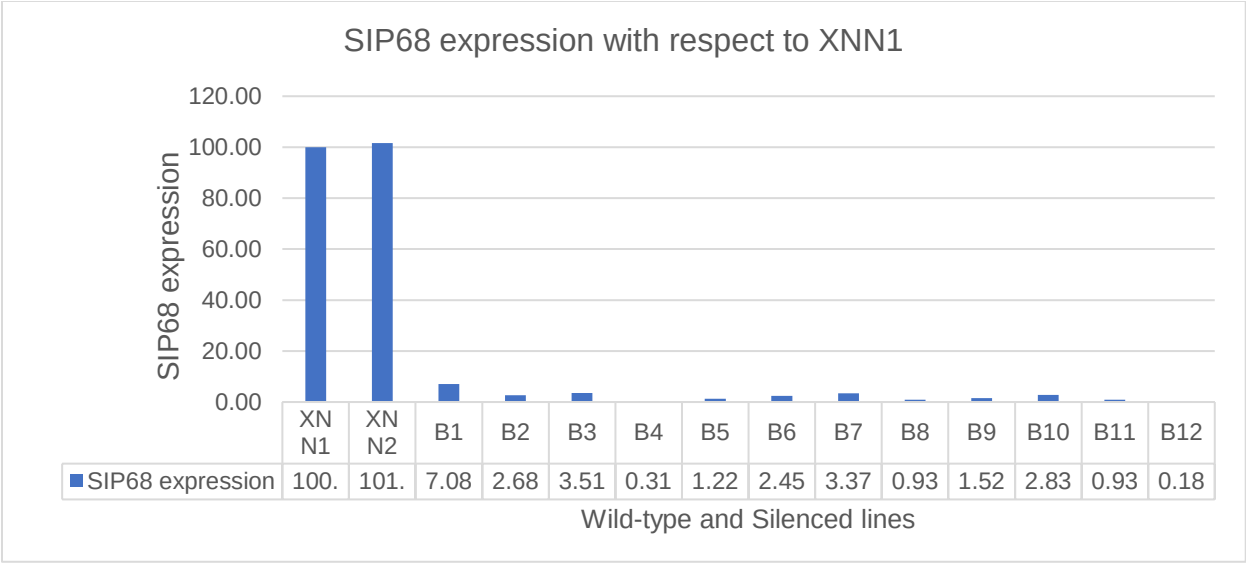

Figure 28: Densitometric Analysis of SIP68 Expression of T2 #B Line With Respect to XNN1. Signal is normalized to Ef1α intensity in each lane.

Screening T2 Generation of Lines #E and #G

T1 silenced transgenic lines # E and #G lines were grown for seed collection. Line #E seed pods were comparatively smaller in size as compared to wild type plant while #G were of normal size. Around 30 seeds were collected from #E line and seed

production in #G line was normal. Seeds were grown under antibiotic selection medium (Kanamycin 100ug/ml) in MS media and seedlings were later screened for SIP68 expression. Briefly total RNA from transgenic #E lines (11 plants), #G silenced lines (2 plants) and XNN (wild-type control) (two plants) were collected, and RT-PCR performed as described earlier DK643 and DK644 were used to detect the expression level of SIP68 (Figure 29). PCR cycle (30X) with a 1-minute extension for *Ef1α* and 2 minutes for SIP68 was set. All transgenic lines expect E8 (~18.25) were more than 98% silenced as compared to XNN1 (Figure 30). *Ef1α* gene was used to determine the quality of cDNA synthesized and loading control.

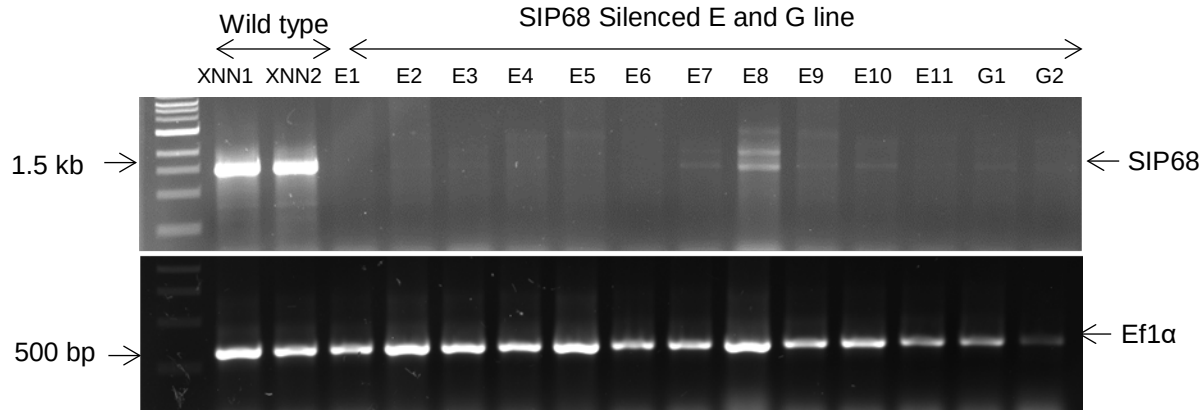

Figure 29: Screening of T2 RNAi Silenced #E and #G Lines. Ethidium bromide stained 0.8% and 1% agarose gel showing expression of SIP68 and Ef1α respectively. DNA ladder (1 kb) for SIP68 (~1491bp) and 100 bp ladder for Ef1α (~600) was used to compare a product size.

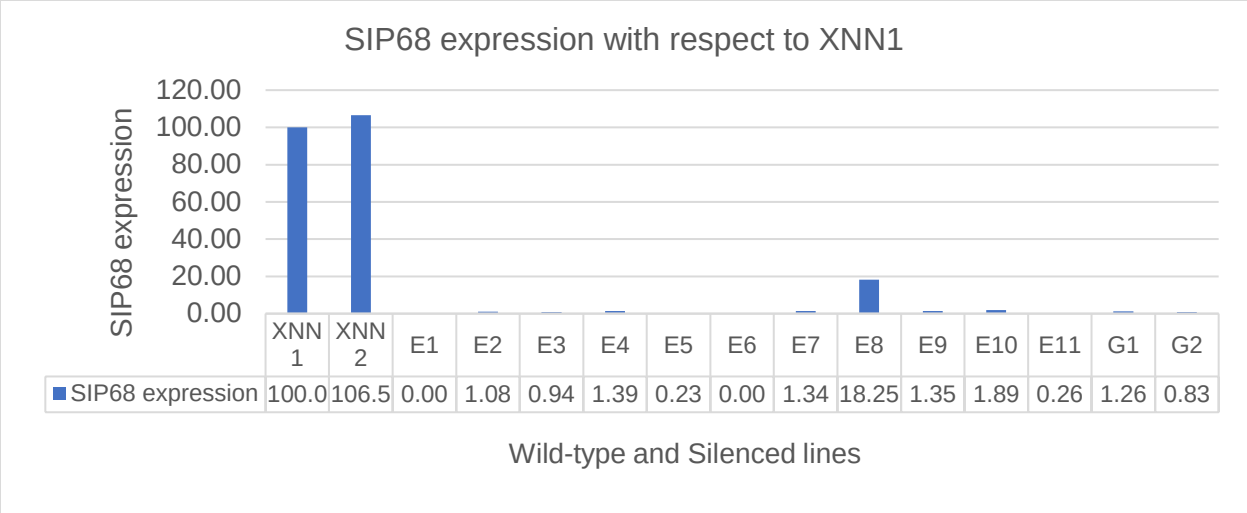

Figure 30: Densitometric Analysis of SIP68 Expression of T2 #E and #G Lines With Respect to Control (XNN1). Signal is normalized to Ef1α intensity in each lane.

CRISPR Cas9 Knock out of SIP68 Gene

First Digestion of Golden Gate Entry Plasmids

Golden Gate entry plasmids pYPQ131A, 132A, and 133A were first digested with BglII and SalI to linearize them (Figure 31).

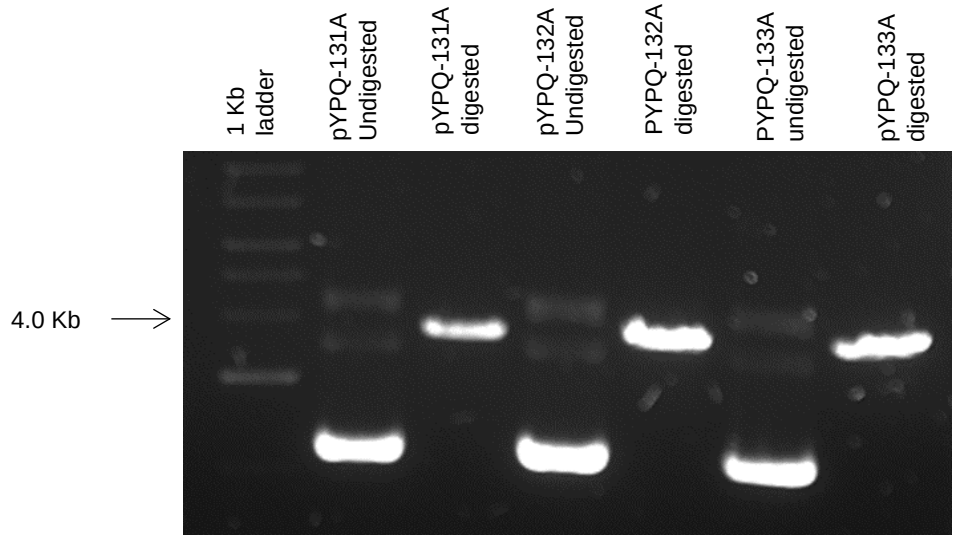

Figure 31: Golden Gate Entry Vector pYPQ131A, 132A, and 133A Digested by BglII and SalI. DNA ladder (1 kb) ladder was used to compare product size (3808 bp).

Second Digestion of Golden Gate Entry Plasmids

Linearized Golden Gate entry plasmids pYPQ131A, 132A, and 1331A digested by BglII and SalI were purified using Qiagen PCR purification kit and again digested by BsmBI (Figure 32). First digestion is optional but recommended step while second digestion with BsmB produces overhangs containing GTTT and AATC, complementary to the annealed gRNAs oligos.

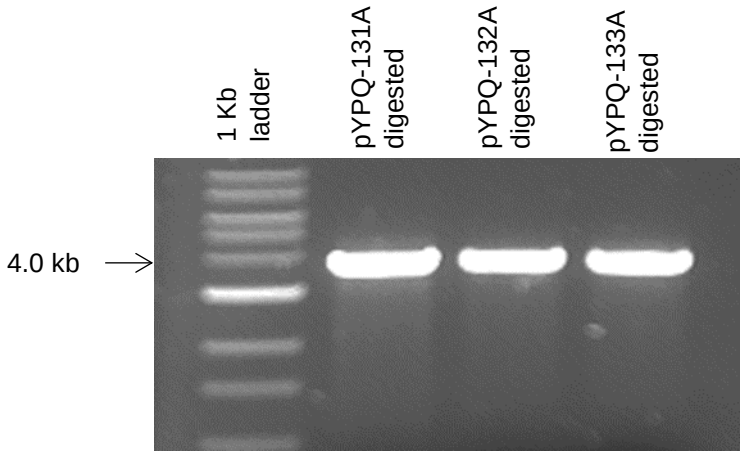

Figure 32: Second Digestion of Golden Gate Entry Plasmid DNA by BsmBI. DNA ladder (1kb) was used to estimate a product size 3808 bp.

PCR Screening of Cloning of Oligos into Linearized Golden Gate Entry Plasmids

gRNAs oligos were ligated into linearized plasmids and transformed into chemically competent TOP10 *E. coli,* and positive clones were screened by PCR amplification (Figure 33) before sending for DNA sequencing (Figure 34-36). DK752 forward primer for all and DK747, DK749, and DK751 reverse primers (Table#1) for first gRNA vector, second gRNA vector, and third gRNA vector were used respectively.

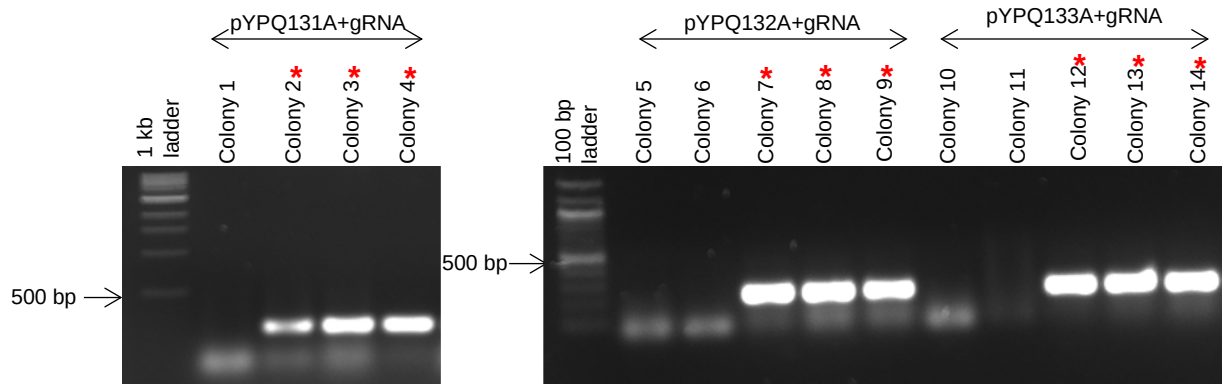

Figure 33: Colony PCR Screening of Recombinant Golden Gate Plasmids Containing SIP68 gRNA. Ethidium bromide stained agarose gel showing the ligation of first, second, and third gRNA oligos into pYPQ131A, pYPQ132A, and pYPQ133A respectively. DNA ladder (100 bp) ladder for pYPQ131A+gRNA and 1kb ladder for pYPQ132A+gRNA and pYPQ133A+gRNA was used to compare a product size (~270 bp). Positive clones were indicated by red asterisk.

```
Predicted       TAAGCTATTAACAATCTTCAAAAGTACCACAGCGCTTAGGTAAAGAAAGCAGCTGAGTTT        180
Colony-2        TAAGCTATTAACAATCTTCAAAAGTACCACAGCGCTTAGGTAAAGAAAGCAGCTGAGTTT        180
                ************************************************************

Predicted       ATATATGGTTAGAcACGAAGTAGTGATTGTGAGCAAATCAGATTAGCCGGTTTTAGAGCT        240
Colony-2        ATATATGGTTAGAcACGAAGTAGTGATTGTGAGCAAATCAGATTAGCCGGTTTTAGAGCT        240
                ************************************************************

Predicted       AGAAATAGCAAGTTAAAATAAGGCTAGTCCGTTATCAACTTGAAAAAGTGGCACCGAGTC        300
Colony-2        AGAAATAGCAAGTTAAAATAAGGCTAGTCCGTTATCAACTTGAAAAAGTGGCACCGAGTC        300
                ************************************************************
```

Figure 34: Portion of Sequencing Result Showing Ligation of Second gRNA Oligos in pYPQ132A. gRNA sequence indicated by blue. Predicted sequence is the computer generated expected sequence containing gRNA sequence and part of vector sequence that is expected to be sequenced by sequencing primer used.

```
Predicted       TAAGCTATTAACAATCTTCAAAAGTACCACAGCGCTTAGGTAAAGAAAGCAGCTGAGTTT     180
Colony-7        TAAGCTATTAACAATCTTCAAAAGTACCACAGCGCTTAGGTAAAGAAAGCAGCTGAGTTT     180
                ************************************************************

Predicted       ATATATGGTTAGAcACGAAGTAGTGATTGTGTGAAGGTGCCTGTCAAAGTTTTAGAGCTA     240
Colony-7        ATATATGGTTAGAcACGAAGTAGTGATTGTGTGAAGGTGCCTGTCAAAGTTTTAGAGCTA     240
                ************************************************************

Predicted       GAAATAGCAAGTTAAAATAAGGCTAGTCCGTTATCAACTTGAAAAAGTGGCACCGAGTCG     300
Colony-7        GAAATAGCAAGTTAAAATAAGGCTAGTCCGTTATCAACTTGAAAAAGTGGCACCGAGTCG     300
                ************************************************************
```

Figure 35: Portion of Sequencing Result Showing Ligation of Second gRNA Oligos in pYPQ132A. gRNA sequence indicated by blue. Predicted sequence is the computer generated expected sequence containing gRNA sequence and part of vector sequence that is expected to be sequenced by sequencing primer used.

```
Predicted       TAAGCTATTAACAATCTTCAAAAGTACCACAGCGCTTAGGTAAAGAAAGCAGCTGAGTTT     180
Colony-12       TAAGCTATTAACAATCTTCAAAAGTACCACAGCGCTTAGGTAAAGAAAGCAGCTGAGTTT     180
                ************************************************************

Predicted       ATATATGGTTAGAcACGAAGTAGTGATTGCATGCTTCCTTCTCTTGACTGTTTTAGAGCT     240
Colony-12       ATATATGGTTAGAcACGAAGTAGTGATTGCATGCTTCCTTCTCTTGACTGTTTTAGAGCT     240
                ************************************************************

Predicted       AGAAATAGCAAGTTAAAATAAGGCTAGTCCGTTATCAACTTGAAAAAGTGGCACCGAGTC     300
Colony-12       AGAAATAGCAAGTTAAAATAAGGCTAGTCCGTTATCAACTTGAAAAAGTGGCACCGAGTC     300
                ************************************************************
```

Figure 36: Portion of Sequencing Result Showing Ligation of Third gRNA Oligos in pYPQ133A. gRNA sequence indicated by blue. Predicted sequence is expected sequence containing gRNA sequence and part of vector sequence that is expected to be sequenced by sequencing primer used.

Golden Gate Assembly of Two or Three gRNAs

Golden Gate reaction as described earlier was performed to assemble two and three gRNAs into Golden Gate recipient plasmids pYPQ142 and pYPQ143 respectively. Golden Gate assembly uses Type IIS restriction endonucleases that cleave outside the recognition sequence producing a fragment specific overhangs allowing simultaneous assembly of multiple fragments. Restriction endonuclease BsaI was used to cut the pYPQ131A producing CTAT and CATG over hangs, pYPQ132A producing CATG and

GGAC over hangs, pYPQ133A producing GGAC and CCAG over hangs, pYPQ142 producing CTAT and GGAC over hangs and pYPQ143 producing CTAT and CCAG overhangs. The overhang thus produced are a complementary sequence in the sequential order allowing assembly of fragments generated from pYPQ131A and pYPQ132A in pYPQ142 and pYPQ131A, pYPQ132A and pYPQ133A in pYPQ143. pYPQ142 and pYPQ143 have a LacZ gene that is replaced by gRNA expression cassettes producing white colonies in blue-white screening. Negative control constructs were constructed using empty plasmids (without gRNA sequence) pYPQ131A, pYPQ132A, and pYPQ133A.

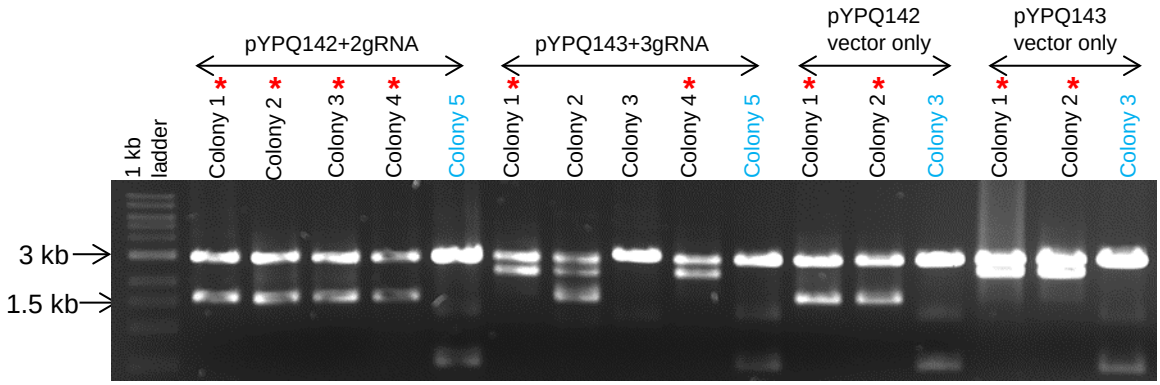

Figure 37: Restriction Digestion Screening of Golden Gate Assembly of Two and Three gRNAs Using BamHI and EcoRV. Positive clones are indicated by red asterisk giving 2737 bp vector backbone in all constructs and 1707 bp in pYPQ142 and 2485 bp in pYPQ143. Blue colony (indicated by blue color) from the blue-white screening was used as negative control.

Gateway Assembly of CRISPR-Cas9 System into a Binary Vector pMDC32

Two gRNAs bearing plasmid construct pYPQ142 and three gRNAs bearing construct pYPQ143 each were assembled into binary vector pMDC32 along with Cas9 from pYPQ150 using the Gateway cloning system as described in the methods section.

Positive clones were screened by restriction digestion using XbaI. All constructs produced fragments of size 4879bp, and 9970bp along with 1657bp for 2gRNA positive construct, 1694bp for 2gRNA negative construct, 2472bp for 3gRNA negative construct, and 2435bp for 3gRNA positive construct (Figure 38). The final CRISPR construct was first verified by restriction digestion as suggested by protocol and again additional verification was done by sequencing. DNA sequencing was done to detect inserted gRNAs and Cas9 sequence (Appendix C). Vector map of the final construct is represented in Figure 39-42. Map is generated using SnapGene® software (from GSL Biotech; available at snapgene.com).

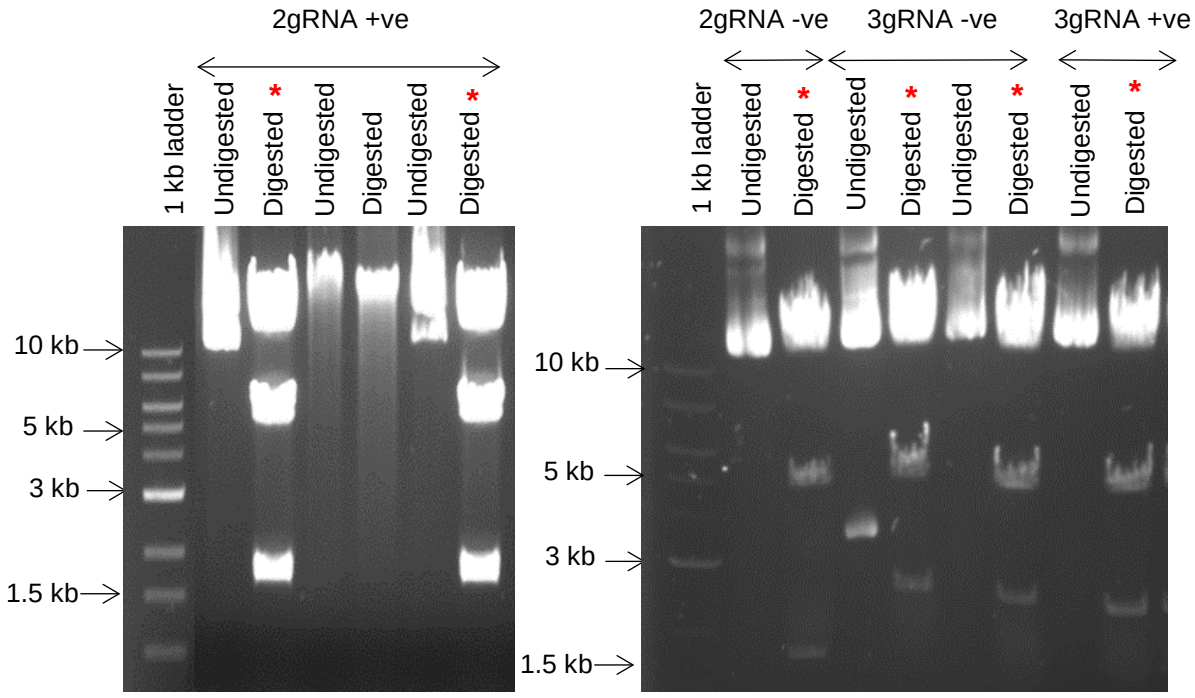

Figure 38: Restriction Digestion of Final CRISPR-Cas9 Construct Using XbaI. Positive constructs are indicated by red asterisk. DNA ladder (1 kb) was used to compare product size.

Final CRISPR Cas9 positive construct for targeting *SIP68* gene consists of plant codon optimized pcoCas9 under CaMV 35s promoter, and gRNA under AtU6 promotor. Upon binding of gRNA to Cas9, Cas9 gets activated and searches for target sequence (Kiani et al. 2015). Cas9 endonuclease recognizes protospacer adjacent motif (PAM) (NGG) present around target site (Anders et al. 2014). When the gRNA sequence (SIP68) matches the target sequence present in *SIP68* gene (tobacco genome), Cas9 nuclease activity is triggered and double stand breaks introduced near PAM sequence and SIP68 will be disrupted. While in case of negative constructs, it can recognize the PAM sequence present in *SIP68* gene but lack of target sequence fails to trigger nuclease activity of Cas9 and *SIP68* will remain unaffected. This construct containing tobacco plant will act as a negative control.

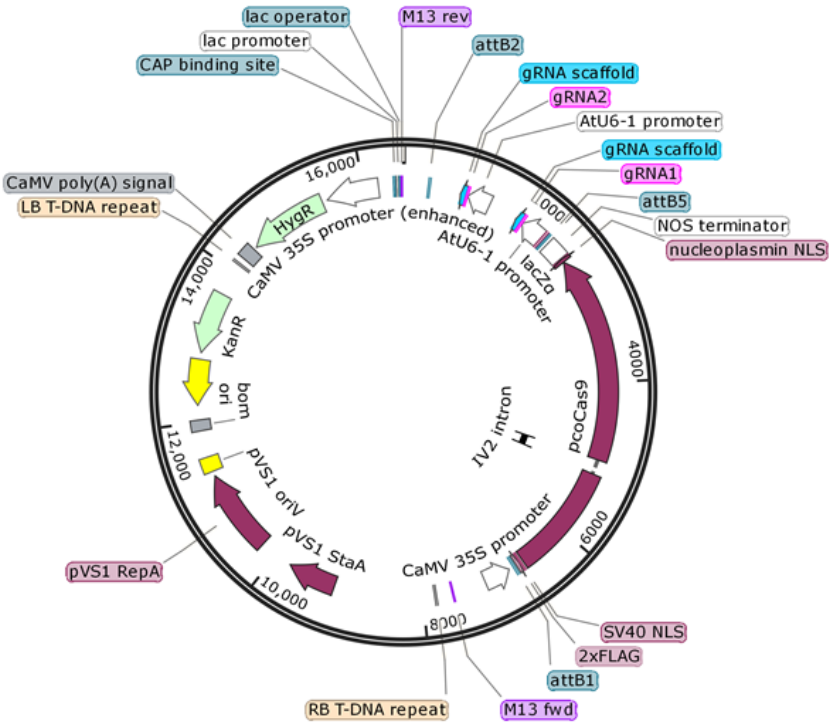

Figure 39: Final 2gRNA Positive Construct Showing gRNA Insertion Site, AtU6 Promotor Cas9, CaMV 35S Promoter, and Other Features

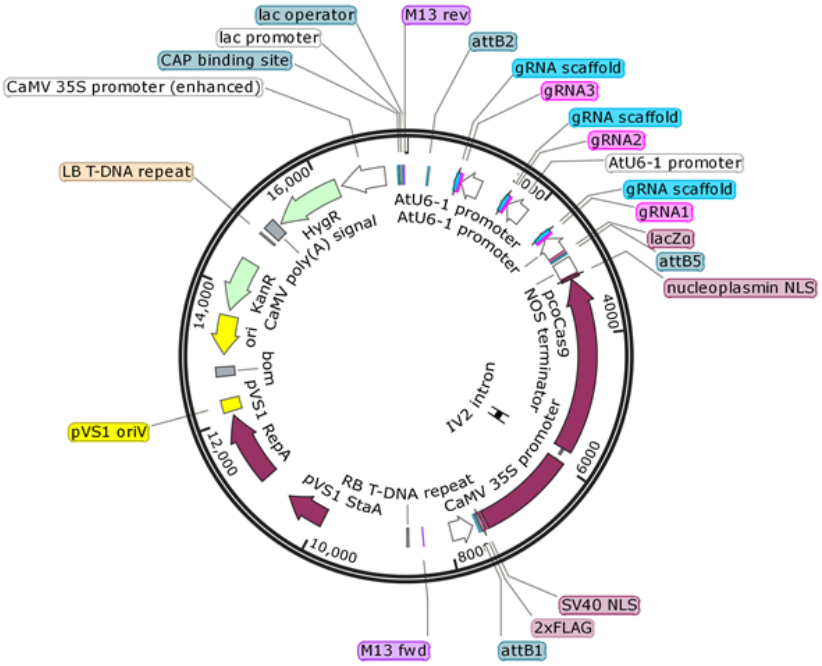

Figure 40: Final 3gRNA Positive Construct Showing gRNA Insertion Site, AtU6 Promotor Cas9, CaMV 35S Promoter, and Other Features

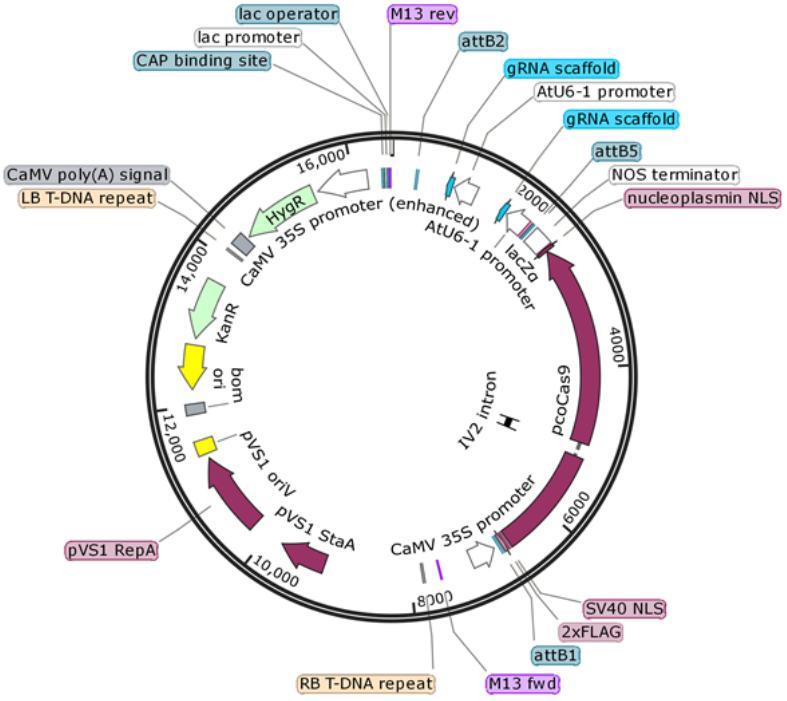

Figure 41: Final 2gRNA Negative Construct Showing, AtU6 Promotor Cas9, CaMV 35S Promoter, and Other Features

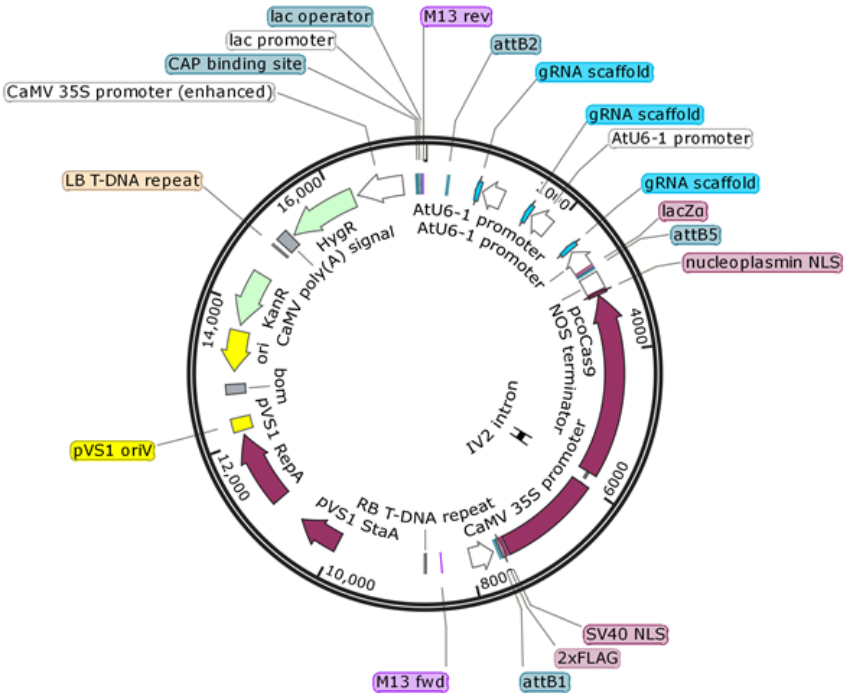

Figure 42: Final 3gRNA Negative Construct Showing AtU6 Promotor Cas9, CaMV 35S Promoter, and Other Features

Transformation of Final CRISPR-Cas9 Construct into *A. tumefaciens LBA4404*

Nucleotide sequence-verified positive CRISPR-Cas9 clones were transformed into *A. tumefaciens LBA4404* for plant transformation. Colony PCR was performed to confirm transformation into *Agrobacterium* using vector specific primer M13 (reverse), and gRNA specific primers (Table#1) DK746 forward for 2gRNA construct and DK748 forward for 3gRNA construct (Figure 43). Some unspecific amplification seen may be due to nonspecific binding of primers in *Agrobacterium* genome. No amplification on the negative construct is due to using gRNA specific forward primers. As all the negative construct lacks gRNA sequence, PCR amplification using gRNA specific primer resulted in no amplification.

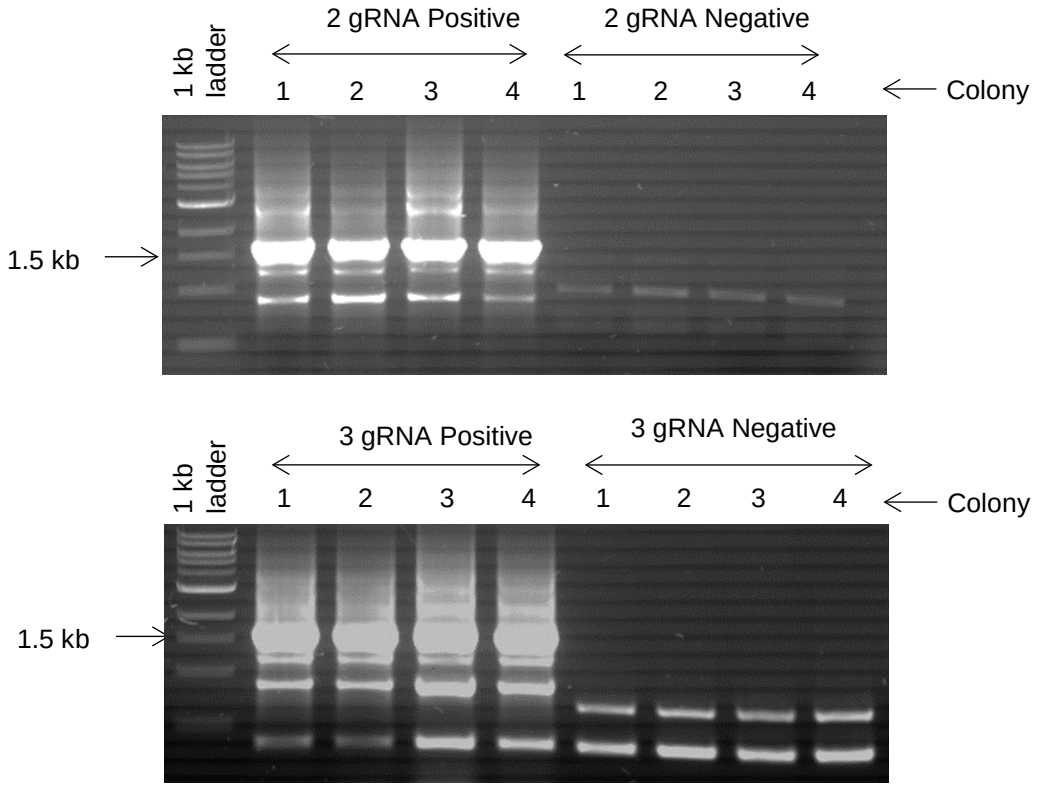

Figure 43: *Agrobacterium LBA4404* Transformation of Final CRISPR-Cas9 Construct. Ethidium bromide stained 0.8% agarose gel of colony PCR of final CRISPR construct in Agrobacterium. DNA ladder (1 kb) was used to compare the product size (~1644bp).

Screening of CRISPR Cas9 Transgenic Line

CRISPR Cas9 targets the genomic DNA at the specific site and causes a double strand break resulting in a mutated gene. The CRISPR Cas9 system used in this research was designed in such a way that it targets the two sites and three sites at *SIP68* gene by 2gRNA positive and 3gRNA positive construct, respectively. Being unable to amplify genomic DNA, an alternative approach of measuring mRNA was used to screen the transgenic line. Briefly, total RNA was extracted, and cDNA was synthesized using RT-PCR as described in the methods section. DK643 and DK644 were used to amplify SIP68 (Figure 44). As compared to wild-type, SIP68 mRNA level

was significantly decreased in the transgenic line (Figure 45). The 3gRNA construct had a considerably lower level of mRNA as compare to 2gRNA construct. Complete knockout of *SIP68* gene was not observed in T1 generation. This might be the due to present of heterozygote genotype that requires multi-generational breeding for uniform germline transmission to obtain a homozygous mutant (Aslan et al. 2017).

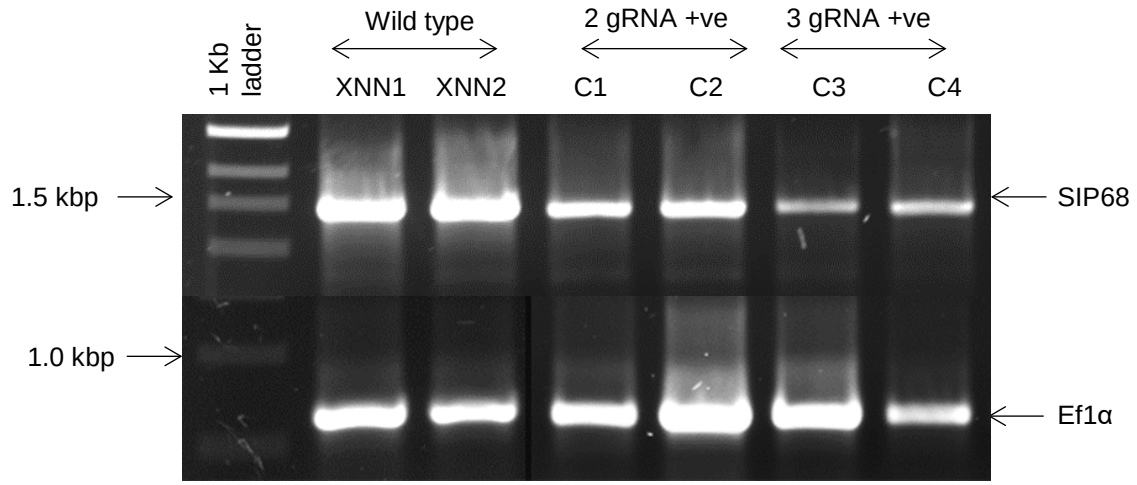

Figure 44: SIP68 mRNA Expression in CRISPR-Cas9 Transgenic Lines. Ethidium bromide stained 0.8% agarose gel showing SIP68 expression in wild type and transgenic line. DNA ladder (1 kb) was used to compare the product size (~1491 bp).

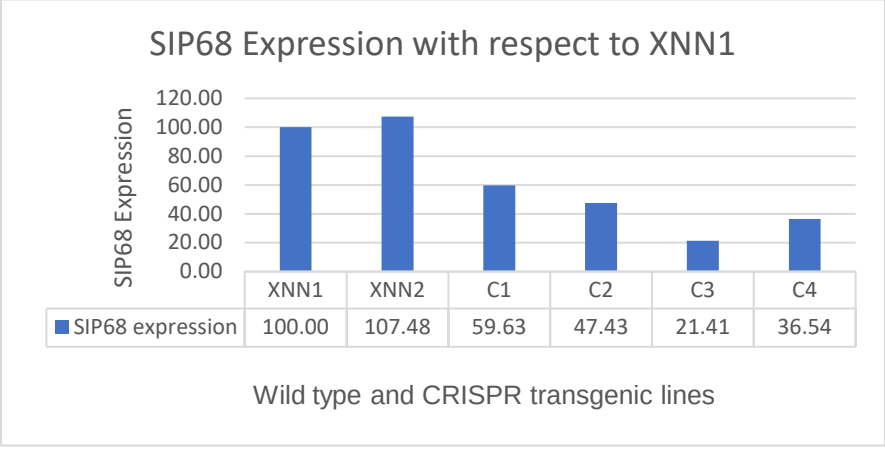

Figure 45: Densitometric Analysis of SIP68 Expression in Wild Type and Transgenic Lines. Signal is normalized to Ef1α intensity in each lane.

CHAPTER 4

DISCUSSION

Plants are sessile organisms which limits their ability to defend against adverse environmental conditions. Therefore, they have evolved in such a way that they can organize their defenses and exhibit tolerance against biotic and abiotic stresses. This involves gene regulation, involvement of enzyme like glucosyltransferase in modifying plant secondary product like flavonoids (Gachon et al. 2005), complex signaling pathways and crosstalk between different plant hormones such as ABA, JA, SA and ET (von Saint Paul et al. 2011), and other low-molecular-weight metabolites (LMWMs) such as antioxidants, biopolymer precursors, vitamins, spices, poisons etc (reviewed in Franz Hadacek and Gert Bachmann 2015). SA is undoubtedly one of the most important plant hormones that exhibits diverse functions from controlling different physiological process to defense against biotic and abiotic stresses. One of the important hallmark functions of SA is its role in SAR (Ryals et al. 1996). It is universally accepted that SA plays the central role in SAR. During pathogen invasion, the level of SA is increased in both local as well as distal parts of the plant (Métraux et al. 1990). Accumulated SA in the primary infected site is converted to its inactive but mobile form, MeSA. MeSA then travels through the phloem to other systemic tissue where the methylesterase activity of SABP2 converts it back to SA thereby inducing SAR (Kumar and Klessig 2003; Park et al. 2007). Increased SA level changes the cellular redox potential that then reduces oligomeric NPR1 protein into the monomeric form which travels and gets accumulated in the nucleus and activates expression of defense genes (Mou et al. 2003). In a study by Kumar and Klessig (2003), in SABP2-silenced transgenic tobacco plants, SA-induced *PR-1* expression was suppressed, and the transgenic line was compromised in

inducing local and systemic resistance to TMV (Kumar and Klessig 2003). Furthermore, in another study by Tripathi et al (2010), silenced-SABP2 transgenic tobacco plants failed to express the PR-1 protein, and SAR was compromised when treated with acibenzolar-S-methyl (ASM), a functional analog of SA (Tripathi et al. 2010). These results suggest a critical role of SABP2 in SAR and expression of defense-related genes. To learn more about the role of SABP2 in plant defense signaling, a yeast-two hybrid was performed to identify the SABP2-interacting protein (SIP) using SABP2 as bait protein and tobacco leaf proteins as prey. Several SIP proteins were discovered, and SIP68 is one of them (Odesina 2015).

Bioinformatic analysis of SIP68 revealed that SIP68 is encoded by tobacco *NtGT4* gene with a 1491 bp coding sequence. It has a C-terminal domain consensus sequence, the PSPG box, characteristic of plant glycosyltransferase proteins (Odesina, 2015). Biochemical characterization using radiolabelled assay and HPLC confirmed SIP68 as a flavonoid: glucosyltransferase protein (Odesina, 2015).

Our aim is to further characterize the SIP68 protein and to know its biological functions. Subcellular localization is one crucial aspect of protein functional analysis to assess its biological function. Glycosyltransferase proteins have been shown to play a role in some basic physiological functions in the plants (Vogt and Jones 2000; Daniel et al. 2011). It is now also characterized to play role in plant defense mechanism (Vogt and Jones 2000). They are also involved in various physiological funtions in plants including biosynthesis and modification of plant secondary metabolites (Gachon et al. 2005). Glycosylation enhances the properties of the compound for storage, transport, and stability (Reviewed in Tiwari et al. 2016). Many toxic compounds are glycosylated

for storage and later upon decompartmentation, exposure to glycosidases release biologically active molecules to defend against pathogens (Vogt and Jones 2000). Glycosylation is an important modification of protein that occurs in the Golgi apparatus, the endoplasmic reticulum, and the cytoplasm (Jaeken and Carchon 2009). In general plant UGTs are cytoplasmic enzymes (Li et al. 2001; Lim and Bowles 2004). Because SIP68 is a glucosyltransferase, it is arguable that it is likely to be active in the cytoplasm. *In silico* analysis revealed SIP68 as a signal peptide lacking protein (Figure 10-12). Proteins lacking signal peptide are suggested to localize in the cytoplasm (Moraga et al. 2009).

To precisely determine the localization of SIP68, it was tagged with enhanced Green Fluorescent Protein (eGFP) at the N-terminal using pSITE-2CA vector. GFP imparts stability to the fusion protein and, when observed under a certain wavelength it fluoresces, enabling visualization of protein localization (March et al. 2003). The pSITE-2CA-SIP68 construct was transiently expressed in *N. benthamiana* using *A. tumefaciens LBA4404* for confocal microscopy. When plants are infiltrated with *Agrobacterium* containing external genetic material, plant immune systems try to suppress expressions. RNAi silencing is the common method used by the plant to defend against external genetic material while viruses use antisilencing strategies to overcome the plant's suppressing mechanism (Baulcombe 2004). Similarly, upon infection with *Agrobacterium*, host cells produce small interfering RNAs (siRNAs) against the external genetic materials to mediate RNA silencing, this results in the reduction or even elimination of transient expression of T-DNA (Ding and Voinnet 2007). To overcome this plant suppressing mechanism and to enhance and prolong transient

expression, plant viral silencing suppressors such as p19 from tomato bushy stunt virus (TBSV) or helper component proteinase (HCPro) from the member of genus *potyvirus* (Peyret and Lomonossoff 2015) are used. pSITE-2CA-SIP68 was expressed with and without HCPro for seven days to determine the expression pattern of SIP68-eGFP (Figure 19). SIP68+eGFP started expressing detectable amounts of protein after three days post-infiltration. Co-infiltration with HCPro enhanced and prolonged the expression as compared to without HCPro where SIP68+eGFP expression started decreasing after 5 DPI (Figure 19).

pSITE-2CA has a cauliflower mosaic virus (CaMV 35S) promotor and, along with HCPro, SIP68+eGFP was constitutively expressed for seven days. To know whether transiently overexpressed SIP68+eGFP can be used for biotic stress (basal and systemic acquired resistance) experiments, PR1 protein expression at different time points was measured in *LBA4404* only, HCPro in *LBA4404*, and SIP68+eGFP with and without HCPro in *LBA4404* was evaluated (Figure 20). Because the level of PR1 induced was significantly high (Figure 21) it was not used for biotic stress experiments as the level of resistance that might be observed (due to the expression of *PR1* gene) would be hard to infer whether it was due to SIP68 overexpression or due *LBA4404* bacteria itself.

Subcellular localization using confocal microscopy, despite having certain limitations in determining the precise location of the molecules, is the most commonly used approach at this time (Hayashi et al. 2012). *N. benthamiana* leaves after five days post infiltration with pSITE-2CA-SIP68 with and without HCPro were used for confocal microscopy. Confocal microscopy focuses a laser beam on the surface of samples, and

a high-resolution image is generated by collecting photons emitted from the fluorescent probe in the sample (Rigby and Goldie 1999). Comparison of the SIP68 confocal images to those from other published flavonoid glucosyltransferase protein shows a similar pattern of distribution of the fluorescent protein. (Sun et al. 2016; Dai et al. 2017). The fluorescent protein was seen diffused towards the edges of the cell and nucleus (Figure 22 and 23).

According to the result published on subcellular localization of *Freesia hybrida* flavonoid 3-0- glucosyltransferase 1 (Fh3GT1) fused to the C terminus of GFP, expressed in Arabidopsis, it was suggested to be localized in the cytosol and the nuclei (Sun et al. 2016). A similar result of cytoplasm and nucleus localization was reported for flavonoid 7-O-glucosyltransferase (CsUGT75L12) in *Camellia sinensis* (Dai et al. 2017). While others have reported that glucosyltransferase protein UGT71C5 of Arabidopsis tagged with GFP localized in cytoplasm only (Liu et al. 2015). It is important to consider the properties of GFP in nuclear localization studies as to some extent, GFP could diffuse into the nucleus on its own. The fluorescence intensities in the cytoplasm and nucleus should be quantified carefully especially with smaller protein fusions (Seibel et al. 2007). In the confocal image, green patches around the nucleus and green fluorescence of nuclei may be the degraded product of SIP68+eGFP concentrated around it as the nuclear envelope allows free movement of protein less than 50 kD between the cytoplasm and nucleus (Cooper GM 2000).

Due to the large size of the vacuole in the tobacco cell, the cytoplasm and its contents are compressed towards the plasma membrane, resulting in thin layer of cytoplasm in-between the plasma membrane and the tonoplast (Kost and Chua 2002)

Because the fluorescent signals are diffused toward the edges of cell, it is likely that the signals are coming from cytoplasm rather than plasma membrane or tonoplast which could have given sharp undiffused signals around the edge of the cell.

To precisely determine SIP68 localization, western blot analysis on cellular fractions was performed. Results from the western blot analysis suggested that SIP68+eGFP is localized in the cytosolic fraction (Figure 24) which suggests SIP68 enzyme activity in the cytoplasm. Similar, cytosolic activity was observed in isovitexin 7-O-glucosyltransferase from subcellular fractionation of barley protoplasts was reported suggesting its localization in the cytoplasm (Blume et al.1979). Also, UDP-glucose is a cytosolic compound (Ramirez-Estrada et al. 2017), and flavonoid biosynthesis takes place in the cytoplasm (Winkel-Shirley 2001). Because both the substrates of SIP68 are localized in the cytoplasm, this further supports the idea of SIP68 being localized and functional in the cytoplasm.

Glycosyltransferase enzymes serve various functions in living organisms. Due to advancement of genome annotation large number of genes has been annotated as UGT that only denotes as its ability to transfer glucose molecule to acceptor substrate (von Saint Paul et al. 2011). But this annotation does not tell about its native substrates and vast majority of gene products are still orphan enzymes whose biological characteristics still need to be explored (von Saint Paul et al. 2011). One of the important aspects of glycosyltransferase enzymes is their role in plant defense signaling. Several UGTs genes are induced during abiotic and biotic stresses. For examples in *Arabidopsis, UGT85V1* and *UGT85U1/2* were involved in oxidative stress and salt tolerance (Ahrazem et al. 2015).*UGT73B3* and *UGT73B5* of *Arabidopsis* have

been reported as necessary for resistance against *Pseudomonas syringae* (Langlois-Meurinne et al. 2005) while *UGT76B1* knockout line and *UGT74F1* and *UGT76B1* double mutant had the opposite effect (von Saint Paul et al. 2011; Noutoshi et al. 2012). Similarly, in gymnosperms, the role of UGTs in defense against insects has been reported (Mageroy et al. 2017). Another aspect of this research was to generate a silenced line of SIP68 and assess its role in biotic stress.

RNAi and CRISPR Cas9 are the most common silencing/gene editing technique used to date. RNAi relies on homology-dependent degradation of a target mRNA controlled by RNA induced silencing complex (RISC) (Almeida and Allshire 2005). Exogenously supplied or stably expressed double-stranded RNA (dsRNA) complementary to a target mRNA is cleaved by the nuclease, Dicer into small interfering RNA (siRNA) of 21-23 bp which is loaded to RISC. In RISC, argonaute unwinds double strand siRNA and releases the passenger strand, leading to activation of RISC which then cleaves the target mRNA (Almeida and Allshire 2005). T1 generation transgenic *Nicotiana tabacum* silenced lines using RNAi generated previously (Kumar et al. 2017 unpublished) were screened for SIP68 silencing. Four lines showing the significant level of silencing as compared to the wild-type plant was identified (Figure 25 and 26). Those SIP68 silenced transgenic tobacco lines were grown for seed collection and were further screened in T2 generation using antibiotic selection in tissue culture. Three out of 4 lines growing in an antibiotic selection medium were further screened using RT-PCR which showed more than 92% (Except E#8) SIP68 silencing as compared to the wild-type plant (Figure 27-30). These lines upon infection with pathogen will help to

assess the role of SIP68 in biotic stress. Also, seeds from those lines can be used for abiotic stress experiment.

CRISPR Cas9 is an efficient technology used to target, modify, and regulate genomic loci of organisms (Zhang et al. 2014). It uses endonuclease Cas9 that introduce a double-strand break in DNA in a site-specific manner using guide RNA (specific to a gene) (Doudna and Charpentier 2014). Upon binding the guide RNA to the Cas9 protein, conformational changes are induced that activates the protein which stochastically searches for target DNA. Upon finding the target region, two nuclease domains of Cas9, RuvC and HNH cuts the DNA 3-4 bp upstream of the Protospacer Adjacent Motif (PAM) (Anders et al. 2014; Nishimasu et al. 2014). The double strand break thus produced is repaired by either homologous recombination or error-prone non-homologous end joining (NHEJ) pathway that introduces a mutation thereby disrupting the gene (Lieber 2010). To generate SIP68 knock out transgenic lines, CRISPR Cas9 system with some modification as described by Lowder et al. 2015 was used.

One of the important steps of the CRISPR Cas9 system is to design single specific guide RNA (sgRNA) having no off-target effect. For this, the online platform CRISPRdirect (https://crispr.dbcls.jp) was used to design unique sgRNA targeting *SIP68* gene only. Three unique sites in the *SIP68* gene were selected and targeted at 2 and 3 sites by 2gRNAs and 3gRNAs in the final pMDC32-Cas9 construct, respectively. While designing sgRNA an additional G (guanine) was added in the 5' end in case there was a target site that did not start with guanine, as U6 promoter strongly prefer guanine for the expression (Doench et al. 2014) and additional C (cytosine) at 3' end of

the complementary sequence. An additional step of dephosphorylation of Golden Gate entry plasmids (pYPQ131A, 132A, and 133A), digested by BsmBI restriction enzyme, was performed prior to ligation of annealed sgRNA oligos to minimize circularization of the digested vector (Ukai et al. 2002) As sgRNA oligos are phosphorylated by the T4 kinase, dephosphorylated linear golden gate entry plasmids will still be able to re-circularize and incorporate sgRNA oligos. Another additional step of PCR screening of ligation of sgRNA oligos into golden gate entry plasmids was performed to minimize empty plasmids being sent for sequencing.

Initial screening by amplification of *SIP68* gene in genomic DNA was unsuccessful, and an alternative approach of measuring SIP68 mRNA using RT-PCR was done. As compared to the wild-type, SIP68 mRNA level was significantly decreased in the transgenic lines (Figure 44 and 45). The 3gRNAs construct has a considerably lower level of SIP68 mRNA as compare to the 2gRNAs construct. Complete knock out was not observed in screened plants. Failure to obtain complete knock out in the T1 generation might be due to the “mosaic” effect of CaMV 35s promoter having weak activity in the germ line cells (Osakabe et al. 2016). Different types of genomic modification such as homozygous, heterozygous and bi-allelic or intermingling of these types of mutations (mosaic) have been observed in plant CRISPR/Cas9 system (Osakabe et al. 2016). Mosaicism has been observed in many other organisms up to 80% generated by CRISPR (Yen et al. 2014) and requires multi-generational breeding for uniform germline transmission to obtain a homozygous mutant (Aslan et al. 2017). While screening successive generations, care should be taken to screen Cas9 free mutants to obtain inherited mutation from the parent plant rather than

the continuous activity of Cas9 due to the CRISPR construct being present in successive generations (Gao et al. 2016).

Future Directions

Subcellular localization of SIP68 adds to the limited knowledge that has been known so far in understanding SIP68. Thus far, it is known that SIP68 is a flavonoid glucosyltransferase protein (Odesina, 2015) and it is localized in the cytoplasm. Transgenic tobacco plants silenced in SIP68 using RNAi and altered SIP68 expression transgenic line using CRISPR Cas9 were also generated and should be used for further analysis.

To further understand SIP68, biochemical characterization of SIP68 is one of the important aspects. Enzyme kinetic studies should be performed to understand how glucosyltransferase activity of recombinant SIP68 is affected in various conditions such as changes in pH, presence of various metals ions and amino acid interacting compounds. Study should be done in presence and absence of His tag present in recombinant SIP68 to understand tag's effect on enzyme activity. Enzyme kinetic studies will help us to know the catalytic mechanism of SIP68 and how its activity is controlled. Also, glucosyltransferase activity of recombinant SIP68 in presence of SABP2 should be tested to understand how SABP2 interferes with the glucosyltransferase activity of SIP68.

The SIP68 localization under normal condition was determined but its localization studies under various stress conditions (biotic and abiotic) will help to know how its localization is affected. This will help to connect its role in defense signaling in

the plant. During transient expression of SIP68, tobacco leaves should be co-infiltrated with pathogenic bacteria *Pseudomonas syringae pv. tabaci* and confocal microscopy and subcellular fractionation should be performed to understand pattern of SIP68 localization under biotic stress. Also, experiment under abiotic stress conditions can be performed by growing plant under abiotic stressors like mannitol, sodium chloride etc.

Similarly, the generated SIP68 transgenic lines should be used for abiotic and biotic stress tests which will help to understand the SIP68 role in defense signaling in the plant. For abiotic stress experiment, SIP68 silenced plants should be grown in different concentration of stressors like mannitol and sodium chloride and bleaching effect should be compared with wild-type grown in same condition. For the biotic stress experiment, both basal resistance and SAR experiment should be performed. Simple representation for performing basal resistance and SAR experiment is described in the Figure 47 and Figure 48. In case of basal resistance, if the number of bacterial colonies is significantly high in transgenic line as compared to the wild type than it could be inferred that SIP68 lacking plants are more susceptible to pathogen infection. Similarly, in case of the SAR experiment, if TMV necrotic lesion size is significantly bigger than that of the wild type than it could be inferred that SIP68 lacking plants are compromised in mounting systemic acquired resistance.

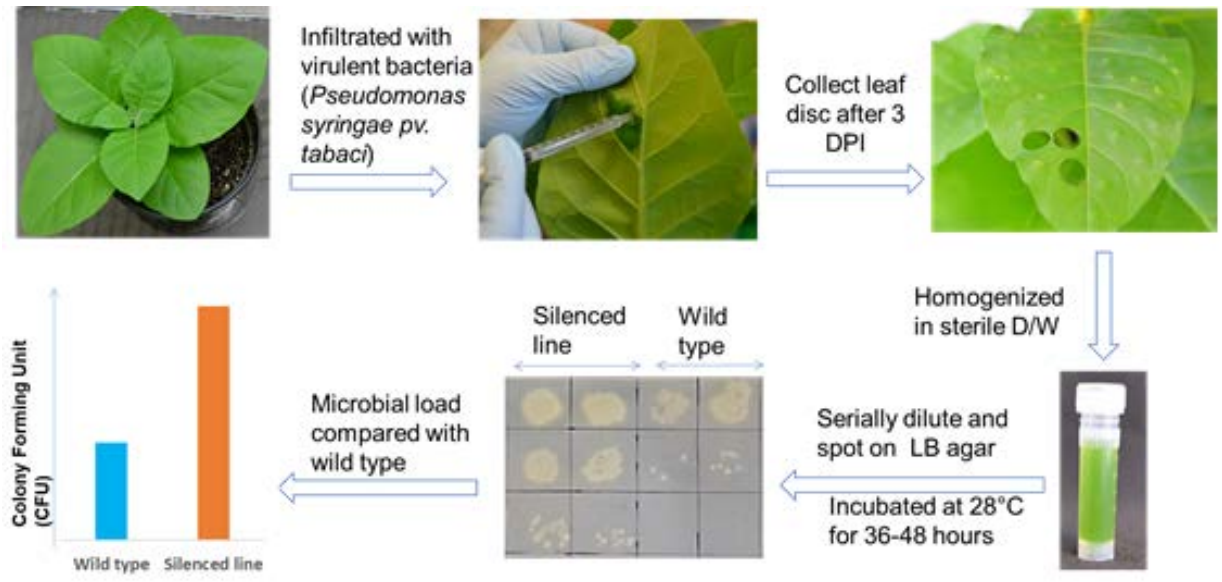

Figure 46: Basal Resistance Experiment Procedure

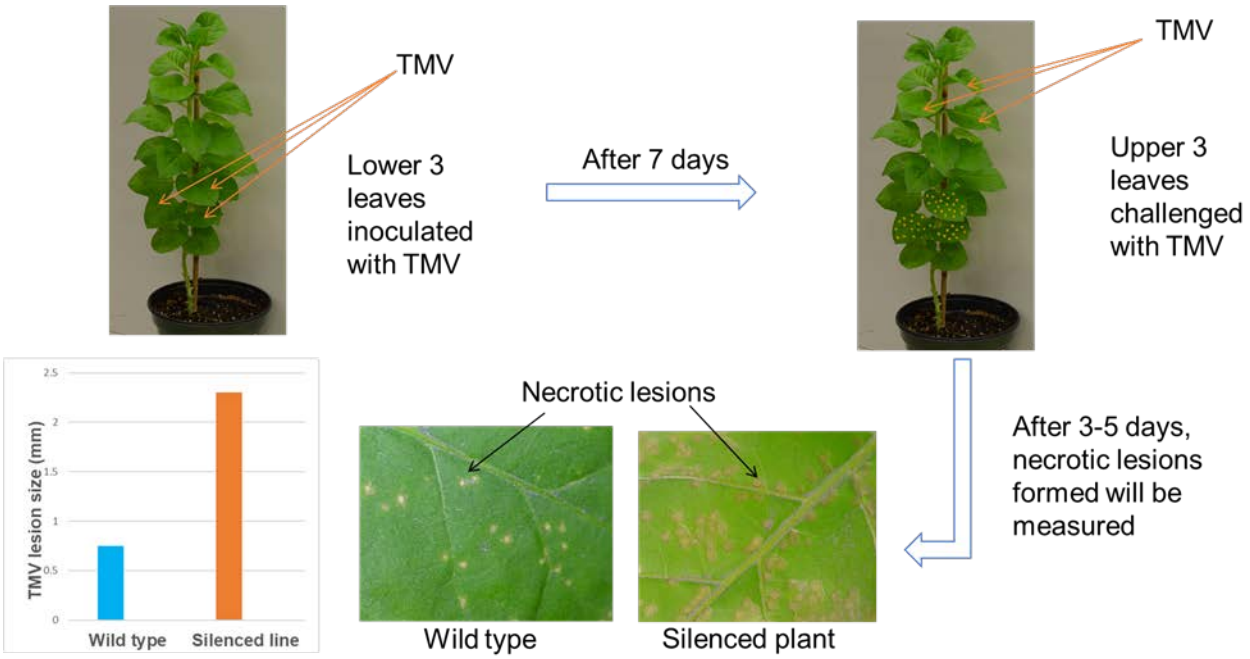

Figure 47: Systemic Acquired Resistance Experiment Procedure

REFERENCES

Ahrazem O, Rubio-Moraga A, Trapero-Mozos A, Climent MF, Gómez-Cadenas A, Gómez-Gómez L. 2015. Ectopic expression of a stress-inducible glycosyltransferase from saffron enhances salt and oxidative stress tolerance in Arabidopsis while alters anchor root formation. Plant Sci 234:60-73.

Alazem M, Lin NS. 2017. Antiviral Roles of Abscisic Acid in Plants. Front Plant Sci 8:1760.

Almeida R, Allshire RC. 2005. RNA silencing and genome regulation. Trends Cell Biol 15(5):251-8.

Anders C, Niewoehner O, Duerst A, Jinek M. 2014. Structural basis of PAM-dependent target DNA recognition by the Cas9 endonuclease. Nature 513(7519):569-73.

Anderson JP, Gleason CA, Foley RC, Thrall PH, Burdon JB, Singh KB. 2010. Plants versus pathogens: an evolutionary arms race. Funct Plant Biol 37(6):499-512.

Aslan Y, Tadjuidje E, Zorn AM, Cha SW. 2017. High-efficiency non-mosaic CRISPR-mediated knock-in and indel mutation in F0. Development 144(15):2852-2858.

Bari R, Jones JD. 2009. Role of plant hormones in plant defence responses. Plant Mol Biol 69(4):473-88.

Baulcombe D. 2004. RNA silencing in plants. Nature 431(7006):356-63.

Bleecker AB, Kenyon WH, Somerville SC, Kende H. 1986. Use of monoclonal antibodies in the purification and characterization of 1-aminocyclopropane-1-carboxylate synthase, an enzyme in ethylene biosynthesis. Proc Natl Acad Sci U S A 83(20):7755-9.

Blume DE, Jaworski JG, McClure JW. 1979. Uridinediphosphate-glucose: Isovitexin 7-O-glucosyltransferase from barley protoplasts: Subcellular localization. Planta 146(2):199-202.

Bock KW. 2016. The UDP-glycosyltransferase (UGT) superfamily expressed in humans, insects and plants: Animal-plant arms-race and co-evolution. Biochem Pharmacol 99:11-7.

Boss PK, Davies C, Robinson SP. 1996. Expression of anthocyanin biosynthesis pathway genes in red and white grapes. Plant Mol Biol 32(3):565-9.

Caarls L, Pieterse CM, Van Wees SC. 2015. How salicylic acid takes transcriptional control over jasmonic acid signaling. Front Plant Sci 6:170.

Campbell JA, Davies GJ, Bulone V, Henrissat B. 1997. A classification of nucleotide-diphospho-sugar glycosyltransferases based on amino acid sequence similarities. Biochem J 326 (Pt 3):929-39.

Cantarel BL, Coutinho PM, Rancurel C, Bernard T, Lombard V, Henrissat B. 2009. The Carbohydrate-Active EnZymes database (CAZy): an expert resource for Glycogenomics. Nucleic Acids Res 37(Database issue):D233-8.

Cao H, Bowling SA, Gordon AS, Dong X. 1994. Characterization of an Arabidopsis Mutant That Is Nonresponsive to Inducers of Systemic Acquired Resistance. Plant Cell 6(11):1583-1592.

Cao H, Li X, Dong X. 1998. Generation of broad-spectrum disease resistance by overexpression of an essential regulatory gene in systemic acquired resistance. Proc Natl Acad Sci U S A 95(11):6531-6.

Chaturvedi R, Krothapalli K, Makandar R, Nandi A, Sparks AA, Roth MR, Welti R, Shah J. 2008. Plastid omega3-fatty acid desaturase-dependent accumulation of a systemic acquired resistance inducing activity in petiole exudates of Arabidopsis thaliana is independent of jasmonic acid. Plant J 54(1):106-17.

Chen F, D'Auria JC, Tholl D, Ross JR, Gershenzon J, Noel JP, Pichersky E. 2003. An Arabidopsis thaliana gene for methylsalicylate biosynthesis, identified by a biochemical genomics approach, has a role in defense. Plant J 36(5):577-88.

Chen SL, Yu H, Luo HM, Wu Q, Li CF, Steinmetz A. 2016. Conservation and sustainable use of medicinal plants: problems, progress, and prospects. Chin Med 11:37.

Chen Y, Shen H, Wang M, Li Q, He Z. 2013. Salicyloyl-aspartate synthesized by the acetyl-amido synthetase GH3.5 is a potential activator of plant immunity in Arabidopsis. Acta Biochim Biophys Sin (Shanghai) 45(10):827-36.

Chen Z, Zheng Z, Huang J, Lai Z, Fan B. 2009. Biosynthesis of salicylic acid in plants. Plant Signal Behav 4(6):493-6.

Chisholm ST, Coaker G, Day B, Staskawicz BJ. 2006. Host-microbe interactions: shaping the evolution of the plant immune response. Cell 124(4):803-14.

Clarke JD, Volko SM, Ledford H, Ausubel FM, Dong X. 2000. Roles of salicylic acid, jasmonic acid, and ethylene in cpr-induced resistance in arabidopsis. Plant Cell 12(11):2175-90.

Cooper, GM. The Cell: A Molecular Approach. 2nd edition. Sunderland (MA): Sinauer Associates; 2000. The Nuclear Envelope and Traffic between the Nucleus and Cytoplasm. Available from:https://www.ncbi.nlm.nih.gov/books/NBK9927

Dai X, Zhuang J, Wu Y, Wang P, Zhao G, Liu Y, Jiang X, Gao L, Xia T. 2017. Identification of a Flavonoid Glucosyltransferase Involved in 7-OH Site Glycosylation in Tea plants (Camellia sinensis). Sci Rep 7(1):5926.

Dancer J, Neuhaus HE, Stitt M. 1990. Subcellular compartmentation of uridine nucleotides and nucleoside-5' -diphosphate kinase in leaves. Plant Physiol 92(3):637-41.

Daniel JJ, Owens DK, McIntosh CA. 2011. Secondary product glucosyltransferase and putative glucosyltransferase expression during Citrus paradisi (c.v. Duncan) growth and development. Phytochemistry 72(14-15):1732-8.

De Vleesschauwer D, Xu J, Höfte M. 2014. Making sense of hormone-mediated defense networking: from rice to Arabidopsis. Front Plant Sci 5:611.

Dean JV, Delaney SP. 2008. Metabolism of salicylic acid in wild-type, ugt74f1 and ugt74f2 glucosyltransferase mutants of Arabidopsis thaliana. Physiol Plant 132(4):417-25.

Delaney TP, Uknes S, Vernooij B, Friedrich L, Weymann K, Negrotto D, Gaffney T, Gut-Rella M, Kessmann H, Ward E et al. . 1994. A central role of salicylic Acid in plant disease resistance. Science 266(5188):1247-50.

Dempsey DA, Klessig DF. 2017. How does the multifaceted plant hormone salicylic acid combat disease in plants and are similar mechanisms utilized in humans? BMC Biol 15(1):23.

Dempsey DA, Vlot AC, Wildermuth MC, Klessig DF. 2011. Salicylic Acid biosynthesis and metabolism. Arabidopsis Book 9:e0156.

Ding SW, Voinnet O. 2007. Antiviral immunity directed by small RNAs. Cell 130(3):413-26.

Doench JG, Hartenian E, Graham DB, Tothova Z, Hegde M, Smith I, Sullender M, Ebert BL, Xavier RJ, Root DE. 2014. Rational design of highly active sgRNAs for CRISPR-Cas9-mediated gene inactivation. Nat Biotechnol 32(12):1262-7.

Doudna JA, Charpentier E. 2014. Genome editing. The new frontier of genome engineering with CRISPR-Cas9. Science 346(6213):1258096.

Du H, Klessig DF. 1997. Identification of a Soluble, High-Affinity Salicylic Acid-Binding Protein in Tobacco. Plant Physiol 113(4):1319-1327.

Effmert U, Saschenbrecker S, Ross J, Negre F, Fraser CM, Noel JP, Dudareva N, Piechulla B. 2005. Floral benzenoid carboxyl methyltransferases: from in vitro to in planta function. Phytochemistry 66(11):1211-30.

Ellinger D, Naumann M, Falter C, Zwikowics C, Jamrow T, Manisseri C, Somerville SC, Voigt CA. 2013. Elevated early callose deposition results in complete penetration resistance to powdery mildew in Arabidopsis. Plant Physiol 161(3):1433-44.

Fang Y, Ramasamy RP. 2015. Current and Prospective Methods for Plant Disease Detection. Biosensors (Basel) 5(3):537-61.

Finkelstein R. 2013. Abscisic Acid synthesis and response. Arabidopsis Book 11:e0166.

Finkelstein RR, Rock CD. 2002. Abscisic Acid biosynthesis and response. Arabidopsis Book 1:e0058.

Forouhar F, Yang Y, Kumar D, Chen Y, Fridman E, Park SW, Chiang Y, Acton TB, Montelione GT, Pichersky E et al. . 2005. Structural and biochemical studies

identify tobacco SABP2 as a methyl salicylate esterase and implicate it in plant innate immunity. Proc Natl Acad Sci U S A 102(5):1773-8.

Frampton RA, Pitman AR, Fineran PC. 2012. Advances in bacteriophage-mediated control of plant pathogens. Int J Microbiol 2012:326452.

Frank K, Sippl MJ. 2008. High-performance signal peptide prediction based on sequence alignment techniques. Bioinformatics 24(19):2172-6.

Gachon CM, Langlois-Meurinne M, Saindrenan P. 2005. Plant secondary metabolism glycosyltransferases: the emerging functional analysis. Trends Plant Sci 10(11):542-9.

Gaffney T, Friedrich L, Vernooij B, Negrotto D, Nye G, Uknes S, Ward E, Kessmann H, Ryals J. 1993. Requirement of salicylic Acid for the induction of systemic acquired resistance. Science 261(5122):754-6.

Gao QM, Zhu S, Kachroo P, Kachroo A. 2015. Signal regulators of systemic acquired resistance. Front Plant Sci 6:228.

Gao X, Chen J, Dai X, Zhang D, Zhao Y. 2016. An Effective Strategy for Reliably Isolating Heritable and Cas9-Free Arabidopsis Mutants Generated by CRISPR/Cas9-Mediated Genome Editing. Plant Physiol 171(3):1794-800.

Glazebrook J. 2005. Contrasting mechanisms of defense against biotrophic and necrotrophic pathogens. Annu Rev Phytopathol 43:205-27.

Gelvin SB. 2003. Agrobacterium-mediated plant transformation: the biology behind the "gene-jockeying" tool. Microbiol Mol Biol Rev 67(1):16-37, table of contents.

Godfray HC, Beddington JR, Crute IR, Haddad L, Lawrence D, Muir JF, Pretty J, Robinson S, Thomas SM, Toulmin C. 2010. Food security: the challenge of feeding 9 billion people. Science 327(5967):812-8.

Grubb CD, Zipp BJ, Ludwig-Müller J, Masuno MN, Molinski TF, Abel S. 2004. Arabidopsis glucosyltransferase UGT74B1 functions in glucosinolate biosynthesis and auxin homeostasis. Plant J 40(6):893-908.

Guo, Y. Ren X, Yu S, and Zhao J. 2016. Application of tobacco glycosyl transferase gene NtGT4 in regulation of plant cell differentiation. CN105567727A.

Hayashi T, Hayashi E, Fujimoto M, Sprong H, Su TP. 2012. The lifetime of UDP-galactose:ceramide galactosyltransferase is controlled by a distinct endoplasmic reticulum-associated degradation (ERAD) regulated by sigma-1 receptor chaperones. J Biol Chem 287(51):43156-69.

Hsu PD, Lander ES, Zhang F. 2014. Development and applications of CRISPR-Cas9 for genome engineering. Cell 157(6):1262-78.

Imam J, Singh PK, Shukla P. 2016. Plant Microbe Interactions in Post Genomic Era: Perspectives and Applications. Front Microbiol 7:1488.

Iqbal N, Khan NA, Ferrante A, Trivellini A, Francini A, Khan MIR. 2017. Ethylene Role in Plant Growth, Development and Senescence: Interaction with Other Phytohormones. Front Plant Sci 8:475.

Jaeken, J., and H. Carchon. 2009. Glycosylation: General Overview. Encyclopedia of Neuroscience, PP 935-942, Academic Press, ISBN 9780080450469.

Jones JB, Vallad GE, Iriarte FB, Obradović A, Wernsing MH, Jackson LE, Balogh B, Hong JC, Momol MT. 2012. Considerations for using bacteriophages for plant disease control. Bacteriophage 2(4):208-214.

Jones JD, Dangl JL. 2006. The plant immune system. Nature 444(7117):323-9.

Jones P, Vogt T. 2001. Glycosyltransferases in secondary plant metabolism: tranquilizers and stimulant controllers. Planta 213(2):164-74.

Jourdan PS, McIntosh CA, Mansell RL. 1985. Naringin Levels in Citrus Tissues : II. Quantitative Distribution of Naringin in Citrus paradisi MacFad. Plant Physiol 77(4):903-8.

Kende H. 1989. Enzymes of ethylene biosynthesis. Plant Physiol 91(1):1-4.

Klessig DF, Malamy J. 1994. The salicylic acid signal in plants. Plant Mol Biol 26(5):1439-58.

Kiani S, Chavez A, Tuttle M, Hall RN, Chari R, Ter-Ovanesyan D, Qian J, Pruitt BW, Beal J, Vora S et al. . 2015. Cas9 gRNA engineering for genome editing, activation and repression. Nat Methods 12(11):1051-4.

Kost B, Chua NH. 2002. The plant cytoskeleton: vacuoles and cell walls make the difference. Cell 108(1):9-12.

Kumar D. 2014. Salicylic acid signaling in disease resistance. Plant Sci 228:127-34.

Kumar D, Chapagai D, Dean P, Mackenzie D. 2014. Biotic and Abiotic Stress Signaling Mediated by Salicylic Acid. Elucidation of Abiotic Stress Signaling in Plants, pp 329-346. Springer, New York.

Kumar D, Haq I, Chapagai D, Tripathi D, Donald D, Hossain M, Devaiahs S. 2014. Hormonal Signaling: Current Perspective on the Role of Salicylic Acid and its

Derivatives in Plants". Recent Advances in Phytochemistry, Springer, ISBN: 978-3-319-20397-3.

Kumar D, Klessig DF. 2003. High-affinity salicylic acid-binding protein 2 is required for plant innate immunity and has salicylic acid-stimulated lipase activity. Proc Natl Acad Sci U S A 100(26):16101-6.

Kumar D, Klessig DF. 2008. The search for the salicylic acid receptor led to discovery of the SAR signal receptor. Plant Signal Behav 3(9):691-2.

Lairson LL, Henrissat B, Davies GJ, Withers SG. 2008. Glycosyltransferases: structures, functions, and mechanisms. Annu Rev Biochem 77:521-55.

Langlois-Meurinne M, Gachon CM, Saindrenan P. 2005. Pathogen-responsive expression of glycosyltransferase genes UGT73B3 and UGT73B5 is necessary for resistance to Pseudomonas syringae pv tomato in Arabidopsis. Plant Physiol 139(4):1890-901.

Lawton K, Weymann K, Friedrich L, Vernooij B, Uknes S, Ryals J. 1995. Systemic acquired resistance in Arabidopsis requires salicylic acid but not ethylene. Mol Plant Microbe Interact 8(6):863-70.

Lawton KA, Friedrich L, Hunt M, Weymann K, Delaney T, Kessmann H, Staub T, Ryals J. 1996. Benzothiadiazole induces disease resistance in Arabidopsis by activation of the systemic acquired resistance signal transduction pathway. Plant J 10(1):71-82.

Le Roy J, Huss B, Creach A, Hawkins S, Neutelings G. 2016. Glycosylation Is a Major Regulator of Phenylpropanoid Availability and Biological Activity in Plants. Front Plant Sci 7:735.

Leon-Reyes A, Van der Does D, De Lange ES, Delker C, Wasternack C, Van Wees SC, Ritsema T, Pieterse CM. 2010. Salicylate-mediated suppression of jasmonate-responsive gene expression in Arabidopsis is targeted downstream of the jasmonate biosynthesis pathway. Planta 232(6):1423-32.

Lepak A, Gutmann A, Kulmer ST, Nidetzky B. 2015. Creating a Water-Soluble Resveratrol-Based Antioxidant by Site-Selective Enzymatic Glucosylation. Chembiochem 16(13):1870-1874.

Leung J, Giraudat J. 1998. ABSCISIC ACID SIGNAL TRANSDUCTION. Annu Rev Plant Physiol Plant Mol Biol 49:199-222.

Li X, Shin S, Heinen S, Dill-Macky R, Berthiller F, Nersesian N, Clemente T, McCormick S, Muehlbauer GJ. 2015. Transgenic Wheat Expressing a Barley UDP-Glucosyltransferase Detoxifies Deoxynivalenol and Provides High Levels of Resistance to Fusarium graminearum. Mol Plant Microbe Interact 28(11):1237-46.

Li Y, Baldauf S, Lim EK, Bowles DJ. 2001. Phylogenetic analysis of the UDP-glycosyltransferase multigene family of Arabidopsis thaliana. J Biol Chem 276(6):4338-43.

Lieber MR. 2010. The mechanism of double-strand DNA break repair by the nonhomologous DNA end-joining pathway. Annu Rev Biochem 79:181-211.

Lim EK, Bowles DJ. 2004. A class of plant glycosyltransferases involved in cellular homeostasis. EMBO J 23(15):2915-22.

Liu Z, Yan JP, Li DK, Luo Q, Yan Q, Liu ZB, Ye LM, Wang JM, Li XF, Yang Y. 2015. UDP-glucosyltransferase71c5, a major glucosyltransferase, mediates abscisic acid homeostasis in Arabidopsis. Plant Physiol 167(4):1659-70.

Lorenzo O, Solano R. 2005. Molecular players regulating the jasmonate signalling network. Curr Opin Plant Biol 8(5):532-40.

Lowder LG, Zhang D, Baltes NJ, Paul JW, Tang X, Zheng X, Voytas DF, Hsieh TF, Zhang Y, Qi Y. 2015. A CRISPR/Cas9 Toolbox for Multiplexed Plant Genome Editing and Transcriptional Regulation. Plant Physiol 169(2):971-85.

Luna E, Bruce TJ, Roberts MR, Flors V, Ton J. 2012. Next-generation systemic acquired resistance. Plant Physiol 158(2):844-53.

Ma J, Wang D, She J, Li J, Zhu JK, She YM. 2016. Endoplasmic reticulum-associated N-glycan degradation of cold-upregulated glycoproteins in response to chilling stress in Arabidopsis. New Phytol 212(1):282-96.

Mageroy MH, Jancsik S, Man Saint Yuen M, Fischer M, Withers SG, Paetz C, Schneider B, Mackay J, Bohlmann J. 2017. A Conifer UDP-Sugar Dependent Glycosyltransferase Contributes to Acetophenone Metabolism and Defense against Insects. Plant Physiol 175(2):641-651.

Malamy J, Carr JP, Klessig DF, Raskin I. 1990. Salicylic Acid: a likely endogenous signal in the resistance response of tobacco to viral infection. Science 250(4983):1002-4.

Malamy J, Hennig J, Klessig DF. 1992. Temperature-Dependent Induction of Salicylic Acid and Its Conjugates during the Resistance Response to Tobacco Mosaic Virus Infection. Plant Cell 4(3):359-366.

March JC, Rao G, Bentley WE. 2003. Biotechnological applications of green fluorescent protein. Appl Microbiol Biotechnol 62(4):303-15.

Marinova K, Kleinschmidt K, Weissenböck G, Klein M. 2007. Flavonoid biosynthesis in barley primary leaves requires the presence of the vacuole and controls the activity of vacuolar flavonoid transport. Plant Physiol 144(1):432-44.

Maskos Z, Rush JD, Koppenol WH. 1990. The hydroxylation of the salicylate anion by a Fenton reaction and T-radiolysis: a consideration of the respective mechanisms. Free Radic Biol Med 8(2):153-62.

McIntosh CA, Latchinian L, Mansell RL. 1990. Flavanone-specific 7-O-glucosyltransferase activity in Citrus paradisi seedlings: Purification and characterization. Archives of Biochemistry and Biophysics 282(1):50-57.

Moraga AR, Mozos AT, Ahrazem O, Gómez-Gómez L. 2009. Cloning and characterization of a glucosyltransferase from Crocus sativus stigmas involved in flavonoid glucosylation. BMC Plant Biol 9:109.

Mou Z, Fan W, Dong X. 2003. Inducers of plant systemic acquired resistance regulate NPR1 function through redox changes. Cell 113(7):935-44.

Mur LA, Kenton P, Atzorn R, Miersch O, Wasternack C. 2006. The outcomes of concentration-specific interactions between salicylate and jasmonate signaling include synergy, antagonism, and oxidative stress leading to cell death. Plant Physiol 140(1):249-62.

Métraux JP, Signer H, Ryals J, Ward E, Wyss-Benz M, Gaudin J, Raschdorf K, Schmid E, Blum W, Inverardi B. 1990. Increase in salicylic Acid at the onset of systemic acquired resistance in cucumber. Science 250(4983):1004-6.

Naito Y, Hino K, Bono H, Ui-Tei K. 2015 CRISPRdirect: software for designing CRISPR/Cas guide RNA with reduced off-target sites. Bioinformatics. 31: 1120-1123.

Nicolopoulou-Stamati P, Maipas S, Kotampasi C, Stamatis P, Hens L. 2016. Chemical Pesticides and Human Health: The Urgent Need for a New Concept in Agriculture. Front Public Health 4:148.

Niki T, Mitsuhara I, Seo S, Ohtsubo N, Ohasshi Y, 1998. Antagonistic effect of salicylic acid andjasmonic acid on the expression of pathogenesis-related (PR) protein genes in wounded maturetobacco leaves. Plant Cell Physiol 39: 500–507.

Nishimasu H, Ran FA, Hsu PD, Konermann S, Shehata SI, Dohmae N, Ishitani R, Zhang F, Nureki O. 2014. Crystal structure of Cas9 in complex with guide RNA and target DNA. Cell 156(5):935-49.

Noutoshi Y, Okazaki M, Kida T, Nishina Y, Morishita Y, Ogawa T, Suzuki H, Shibata D, Jikumaru Y, Hanada A et al. . 2012. Novel plant immune-priming compounds identified via high-throughput chemical screening target salicylic acid glucosyltransferases in Arabidopsis. Plant Cell 24(9):3795-804.

Odesina AO. 2015. Characterization of SIPB68: A Putative Tobacco Glucosyltransferase Protein and its Role in Plant Defense Mechanisms. Electronic Thesis and Dissertations. Paper 2598, ETSU.

Osakabe Y, Watanabe T, Sugano SS, Ueta R, Ishihara R, Shinozaki K, Osakabe K. 2016. Optimization of CRISPR/Cas9 genome editing to modify abiotic stress responses in plants. Sci Rep 6:26685.

Park SW, Kaimoyo E, Kumar D, Mosher S, Klessig DF. 2007. Methyl salicylate is a critical mobile signal for plant systemic acquired resistance. Science 318(5847):113-6.

Petersen TN, Brunak S, von Heijne G, Nielsen H. 2011. SignalP 4.0: discriminating signal peptides from transmembrane regions. Nat Methods 8(10):785-6.

Peyret H, Lomonossoff GP. 2015. When plant virology met Agrobacterium: the rise of the deconstructed clones. Plant Biotechnol J 13(8):1121-35.

Pieterse CM, Van Loon LC. 2004. NPR1: the spider in the web of induced resistance signaling pathways. Curr Opin Plant Biol 7(4):456-64.

Pitzschke A, Hirt H. 2010. New insights into an old story: Agrobacterium-induced tumour formation in plants by plant transformation. EMBO J 29(6):1021-32.

Poppenberger B, Berthiller F, Lucyshyn D, Sieberer T, Schuhmacher R, Krska R, Kuchler K, Glössl J, Luschnig C, Adam G. 2003. Detoxification of the Fusarium mycotoxin deoxynivalenol by a UDP-glucosyltransferase from Arabidopsis thaliana. J Biol Chem 278(48):47905-14.

Poppenberger B, Fujioka S, Soeno K, George GL, Vaistij FE, Hiranuma S, Seto H, Takatsuto S, Adam G, Yoshida S et al. . 2005. The UGT73C5 of Arabidopsis thaliana glucosylates brassinosteroids. Proc Natl Acad Sci U S A 102(42):15253-8.

Proietti S, Bertini L, Timperio AM, Zolla L, Caporale C, Caruso C. 2013. Crosstalk between salicylic acid and jasmonate in Arabidopsis investigated by an integrated proteomic and transcriptomic approach. Mol Biosyst 9(6):1169-87.

Ramirez-Estrada K, Castillo N, Lara JA, Arró M, Boronat A, Ferrer A, Altabella T. 2017. Tomato UDP-Glucose Sterol Glycosyltransferases: A Family of Developmental and Stress Regulated Genes that Encode Cytosolic and Membrane-Associated Forms of the Enzyme. Front Plant Sci 8:984.

Rehman HM, Nawaz MA, Shah ZH, Ludwig-Müller J, Chung G, Ahmad MQ, Yang SH, Lee SI. 2018. Comparative genomic and transcriptomic analyses of Family-1 UDP glycosyltransferase in three Brassica species and Arabidopsis indicates stress-responsive regulation. Sci Rep 8(1):1875.

Ridgway RL, Tinney JC, MacGregor JT, Starler NJ. 1978. Pesticide use in agriculture. Environ Health Perspect 27:103-12.

Rigby PJ, Goldie RG. 1999. Confocal microscopy in biomedical research. Croat Med J 40(3):346-52.

Rivas-San Vicente M, Plasencia J. 2011. Salicylic acid beyond defence: its role in plant growth and development. J Exp Bot 62(10):3321-38.

Ryals JA, Neuenschwander UH, Willits MG, Molina A, Steiner HY, Hunt MD. 1996. Systemic Acquired Resistance. Plant Cell 8(10):1809-1819.

Salazar C, Hernández C, and Teresa M.p. 2015. Plant water stress: Associations between ethylene and abscisic acid response. Chilean J. Agric. Res. vol.75 supl.1 Chillán ago.

Santner A, Calderon-Villalobos LI, Estelle M. 2009. Plant hormones are versatile chemical regulators of plant growth. Nat Chem Biol 5(5):301-7.

Sasaki Y, Asamizu E, Shibata D, Nakamura Y, Kaneko T, Awai K, Amagai M, Kuwata C, Tsugane T, Masuda T et al. . 2001. Monitoring of methyl jasmonate-

responsive genes in Arabidopsis by cDNA macroarray: self-activation of jasmonic acid biosynthesis and crosstalk with other phytohormone signaling pathways. DNA Res 8(4):153-61.

Savary S, Ficke A, Aubertot J.-N, Hollier C, 2012. Crop losses due to diseases and their implications for global food production losses and food security. Food Secur 4: 519–537.

Seibel NM, Eljouni J, Nalaskowski MM, Hampe W. 2007. Nuclear localization of enhanced green fluorescent protein homomultimers. Anal Biochem 368(1):95-9.

Seo PJ, Lee AK, Xiang F, Park CM. 2008. Molecular and functional profiling of Arabidopsis pathogenesis-related genes: insights into their roles in salt response of seed germination. Plant Cell Physiol 49(3):334-44.

Shah J. 2003. The salicylic acid loop in plant defense. Curr Opin Plant Biol 6(4):365-71.

Shen HB, Chou KC. 2007. Signal-3L: A 3-layer approach for predicting signal peptides. Biochem Biophys Res Commun 363(2):297-303

Speth EB, Imboden L, Hauck P, He SY. 2009. Subcellular localization and functional analysis of the Arabidopsis GTPase RabE. Plant Physiol 149(4):1824-37.

Strobel GA, Hess WM. 1997. Glucosylation of the peptide leucinostatin A, produced by an endophytic fungus of European yew, may protect the host from leucinostatin toxicity. Chem Biol 4(7):529-36.

Shulaev V, Silverman P, and Ilya R. 1997. Airborne signaling by methyl salicylate in plant pathogen resistance. Nature (385):718-721.

Sun W, Liang L, Meng X, Li Y, Gao F, Liu X, Wang S, Gao X, Wang L. 2016. Biochemical and Molecular Characterization of a Flavonoid 3-O-

glycosyltransferase Responsible for Anthocyanins and Flavonols Biosynthesis in Freesia hybrida. Front Plant Sci 7:410.

Tiwari P, R. S. Sangwan, and N. S. Sangwan. 2016. Plant secondary metabolism linked glycosyltransferases: An update on expanding knowledge and scopes. Biotechnol Adv 34 (5):714-739.

Tognetti VB, Van Aken O, Morreel K, Vandenbroucke K, van de Cotte B, De Clercq I, Chiwocha S, Fenske R, Prinsen E, Boerjan W et al. . 2010. Perturbation of indole-3-butyric acid homeostasis by the UDP-glucosyltransferase UGT74E2 modulates Arabidopsis architecture and water stress tolerance. Plant Cell 22(8):2660-79.

Ton J, Flors V, Mauch-Mani B. 2009. The multifaceted role of ABA in disease resistance. Trends Plant Sci 14(6):310-7.

Tripathi D, Jiang YL, Kumar D. 2010. SABP2, a methyl salicylate esterase is required for the systemic acquired resistance induced by acibenzolar-S-methyl in plants. FEBS Lett 584(15):3458-63.

Truman W, Bennett MH, Kubigsteltig I, Turnbull C, Grant M. 2007. Arabidopsis systemic immunity uses conserved defense signaling pathways and is mediated by jasmonates. Proc Natl Acad Sci U S A 104(3):1075-80.

Ukai H, Ukai-Tadenuma M, Ogiu T, Tsuji H. 2002. A new technique to prevent self-ligation of DNA. J Biotechnol 97(3):233-42.

van Loon LC, Geraats BP, Linthorst HJ. 2006. Ethylene as a modulator of disease resistance in plants. Trends Plant Sci 11(4):184-91.

Verberne MC, Hoekstra J, Bol JF, Linthorst HJ. 2003. Signaling of systemic acquired resistance in tobacco depends on ethylene perception. Plant J 35(1):27-32.

Vick BA, Zimmerman DC. 1984. Biosynthesis of jasmonic Acid by several plant species. Plant Physiol 75(2):458-61.

Vlot AC, Dempsey DA, Klessig DF. 2009. Salicylic Acid, a multifaceted hormone to combat disease. Annu Rev Phytopathol 47:177-206.

Vogt T, Jones P. 2000. Glycosyltransferases in plant natural product synthesis: characterization of a supergene family. Trends Plant Sci 5(9):380-6.

von Saint Paul V, Zhang W, Kanawati B, Geist B, Faus-Kessler T, Schmitt-Kopplin P, Schäffner AR. 2011. The Arabidopsis glucosyltransferase UGT76B1 conjugates isoleucic acid and modulates plant defense and senescence. Plant Cell 23(11):4124-45.

Wang J, Ma XM, Kojima M, Sakakibara H, Hou BK. 2011. N-glucosyltransferase UGT76C2 is involved in cytokinin homeostasis and cytokinin response in Arabidopsis thaliana. Plant Cell Physiol 52(12):2200-13.

Wang KL, Li H, Ecker JR. 2002. Ethylene biosynthesis and signaling networks. Plant Cell 14 Suppl:S131-51.

Wasternack C. 2007. Jasmonates: an update on biosynthesis, signal transduction and action in plant stress response, growth and development. Ann Bot 100(4):681-97.

Winkel-Shirley B. 2001. Flavonoid biosynthesis. A colorful model for genetics, biochemistry, cell biology, and biotechnology. Plant Physiol 126(2):485-93.

Wu B, Gao L, Gao J, Xu Y, Liu H, Cao X, Zhang B, Chen K. 2017. Genome-Wide Identification, Expression Patterns, and Functional Analysis of UDP

Glycosyltransferase Family in Peach (Prunus persica L. Batsch). Front Plant Sci 8:389.

Yasuda M, Ishikawa A, Jikumaru Y, Seki M, Umezawa T, Asami T, Maruyama-Nakashita A, Kudo T, Shinozaki K, Yoshida S et al. . 2008. Antagonistic interaction between systemic acquired resistance and the abscisic acid-mediated abiotic stress response in Arabidopsis. Plant Cell 20(6):1678-92.

Yauk YK, Ged C, Wang MY, Matich AJ, Tessarotto L, Cooney JM, Chervin C, Atkinson RG. 2014. Manipulation of flavour and aroma compound sequestration and release using a glycosyltransferase with specificity for terpene alcohols. Plant J 80(2):317-30.

Yen ST, Zhang M, Deng JM, Usman SJ, Smith CN, Parker-Thornburg J, Swinton PG, Martin JF, Behringer RR. 2014. Somatic mosaicism and allele complexity induced by CRISPR/Cas9 RNA injections in mouse zygotes. Dev Biol 393(1):3-9.

Yuliar, Nion YA, Toyota K. 2015. Recent trends in control methods for bacterial wilt diseases caused by Ralstonia solanacearum. Microbes Environ 30(1):1-11.

Zabel F, Putzenlechner B, Mauser W. 2014. Global agricultural land resources--a high resolution suitability evaluation and its perspectives until 2100 under climate change conditions. PLoS One 9(9):e107522.

Zhang F, Wen Y, Guo X. 2014. CRISPR/Cas9 for genome editing: progress, implications and challenges. Hum Mol Genet 23(R1):R40-6.

Zhang M, Smith JA, Harberd NP, Jiang C. 2016. The regulatory roles of ethylene and reactive oxygen species (ROS) in plant salt stress responses. Plant Mol Biol 91(6):651-9.

APPENDICES

Appendix A: Abbreviations

ABA: Abscisic Acid

ACC: 1-Aminocyclopropane-1Carboxylic acid

ACO: ACC Oxidase

APS: Ammonium Persulfate

ASM: Acibenzolar-S-Methyl

CAZy: Carbohydrate-Active enZymes

CRISPR: Clustered Regularly Interspaced Short Palindromic Repeats

DEPC: Diethylpyrocarbonate

DTT: Dithiothreitol

eGFP: enhanced Green Fluorescent Protein

ET: Ethylene

EtBr: Ethidium Bromide

ETI: Effector-Triggered Immunity

ETS: Effector Triggered Susceptibility

HCPro: Helper Component Proteinase

IAA: Indole-3-Acetic Acid

IBA: Indole-3-Butyric Acid

ICS: Isochorismate Synthase

IPTG: Isopropyl β-D-1-Thiogalactopyranoside

JA: Jasmonic Acid

KDa: Kilo Dalton

LMW: Low Molecular Weight

MeSA: Methyl Salicylate

MEP: 2-C-Methyl-D-Erythritol-4-Phosphate

MS: Murashige Skoog

MES: Morpholinoethanesulfonic acid

NB-LRR: Nucleotide Binding Leucine Rich Repeat

Ni-NTA: Nickel-Nitrilotriacetic Acid

NPR1: Nonexpresser of Pathogenesis-Related protein 1

OD: Optical Density

PAL: Phenylalanine Ammonia Lyase

PAM: Protospacer Adjacent Motif

PAMPs: Pathogen Associated Molecular Patterns

PCR: Polymerase Chain Reaction

PMSF: Phenylmethylsulfonyl Fluoride

PTI: PAMP-Triggered Immunity

PVDF: Polyvinylidene Fluoride

ROS: Reactive Oxygen Species

RNAi: RNA Interference

RT-PCR: Reverse Transcriptase- Polymerase Chain Reaction

SA: Salicylic Acid

SA-Asp: Salicylocyl-L-Aspartate

SABP2: Salicylic Acid Binding protein 2

SAG: Salicylic Acid beta-Glucoside

SAM: S-Adenosyl-Methionine

SAMT: Salicylic Acid Methyl Transferase

SAR: Systemic Acquired Resistance

SDS: Sodium Dodecyl Sulfate

SDS-PAGE: Sodium Dodecyl Sulfate Polyacrylamide Gel Electrophoresis

SGE: Salicylate Glucose Ester

SIP: SABP2 Interacting Protein

SIP68: SABP2 Interacting Protein 68

TBSV: Tomato Bushy Stunt Virus

TEMED: Tetramethylethylenediamine

UGT: UDP-Glycosyltransferase

mA: Milli-ampere

β-ME: β-mercaptoethanol

µg: Microgram

µM: Micromole

µl: Microlitre

mg/ml: Milligram/Milliliter

ng/µl: Nanogram/Microliter

Appendix B: Buffers and Reagents

0.8% Agarose Gel

1x TAE Buffer= 50 ml

Agarose= 0.4 g

Add the agarose in 1X TAE buffer and heat in the microwave for 60 seconds.

Place the mixture in water bath ~ 55^{o}C for 10-15 minutes

Add 2.5 µl (10 mg/mL) ethidium bromide to the mixture and cast the gel in the tray with required comb size.

70% Ethanol (100 ml)

Add 30 ml of water in 70 ml of ethanol

20% APS (Ammonium persulfate) (0.5 ml)

Milli-Q Water= 0.5 ml

Ammonium persulfate= 0.1g

0.1% DEPC treated water (100 ml)

Milli-Q Water= 100 ml

Diethyl pyrocarbonate= 0.1 ml

Mix the solution properly and incubate the mixture for ~12 hours at 37 ^{o}C and then autoclave for 20 minutes at 121 ^{o}C and 15 psi atmospheric pressure.

2X SDS-PAGE Loading Dye (100 ml)

SDS= 0.4g, final concentration 0.4% (v/v)

Bromophenol blue= 0.2 g, final concentration 0.2% (v/v)

1M Tris-Cl, pH 6.8 = 10ml, final concentration 100mM

Glycerol= 20 ml, final concentration 20% (v/v)

Add 5% of βME before use

10X SDS-PAGE Running Buffer (1 L)

Glycine (M.W: 75.07 g/mol) = 144 g

Tris base (M.W: 121.1 g/mol) = 30 g

SDS = 10 g

1X SDS-PAGE Running Buffer (500 ml)

Add 50 ml of 10X SDS-PAGE Running Buffer in 450 ml of Milli-Q water

10X Phosphate Buffer Saline (PBS) (1 L)

Sodium Phosphate monobasic (M.W: 119.96 g/mol) = 4.1 g, final concentration = 30 mM

Sodium Phosphate dibasic (M.W: 141.96 g/mol) = 10 g, final concentration: 70 mM

Sodium Chloride (M.W: 58.44 g/mol) = 76 g, final concentration: 1.3M

1X Phosphate Buffer Saline (PBS) (1 L)

Add 100 ml of 10X PBS in 900 ml of Milli-Q Water

1X PBS plus 0.3% Tween Twenty (1 L)

Add 100ml of 10X PBS in 897 ml of milli-Q water and then add 3 ml of Tween twenty

10X Western Blotting Transfer Buffer (1 L)

Glycine (M.W: 75.07 g/mol) = 72.06 g, final concentration 960 mM

Tris base (M.W: 121.1 g/mol) = 30.3 g, final concentration 125 mM

1X Western Blotting Transfer Buffer (1 L)

10X Western Blotting Transfer Buffer = 100 ml

Methanol = 100 ml

Cold Milli-Q Water = 800 ml

Western Blotting Blocking Buffer (100 ml)

BSA= 3 g, final concentration 3%

Dry Milk = 1 g, final concentration 1%

1X PBS = 100 ml

50X Tris Acetate EDTA (TAE) Buffer (500 ml)

Glacial acetic acid = 28.55 ml

0.5 M EDTA (pH 8.0) = 50.0 ml

Tris base (M.W: 121.1 g/mol) = 121.0 g

Add milli-Q water to make final volume 500 ml

1X TAE Buffer (1 L)

Dissolve 20 ml of 50X TAE buffer in 980 ml of milli-Q water.

Ponceau S Stain (100 ml)

Acetic acid = 5 ml, final concentration = 5%

Ponceau S = 0.1 g, final concentration = 0.1%

Milli-Q Water = 95 ml

Coomassie brilliant blue destaining solution (1 L)

Acetic acid = 100 ml

Methanol = 400 ml

Milli-Q Water = 500 ml

Coomassie Brilliant Blue staining solution (1 L)

Acetic Acid = 100 ml

Methanol = 500

Milli-Q Water = 400 ml

Dissolve 1 g of Coomassie Brilliant Blue in the solution

STE Buffer (100 ml)

STE Buffer is composed of 10m M Tris-HCl, 100 mM NaCl, 1 mM EDTA.

Tris = 0.121 g

NaCl = 0.584 g

EDTA = 0.029 g

Adjust the pH with HCl to 8.0 and store in 4 ^{o}C.

STET solution (100 ml)

To STE buffer add 5% Triton X-100 and store in 4 ^{o}C.

Grinding Buffer (1 L)

EDTA (0.42g), M.W. = 416.20g/mol, final concentration = 1mM

Glycine (0.75g), M.W. = 75.07g/mol, final concentration = 10mM

Mannitol (60.12g), M.W. = 182.17g/mol, final concentration = 0.33M

MOPS (4.19g), M.W. = 209.26g/mol, final concentration = 20mM

Adjust pH to 7.2 with NaOH

Sterilized the solution by autoclaving for 20 minutes at 121 ^{o}C and 15 psi atmospheric pressure. Let the solution cool down at 4 ^{o}C and add 2 g of BSA and 5 g of PVP and mix well.

Prior to grinding plant tissue, add β-mercaptoethanol (0.02% final concentration) and PMSF (1mM final concentration). Two grams of deveined leaf was ground in 10 ml grinding buffer.

GunHCl buffer

4 M Guanine thiocyanate

5 mM Sodium Citrate pH 7.0

0.5% Sarkosyl

20 mg/ml X-Gal stock solution

Add 20 mg of X-Gal to 1 ml of Dimethylformamide (DMF). Vortex to dissolve X-Gal. Wrap the tube properly with aluminum foil and store at -20 ^{o}C.

LB Broth (100 ml)

Add 2.5 g of LB media in milli-Q water to make a final volume of 100 ml. Sterilized the solution by autoclaving for 20 minutes at 121 ^{o}C and 15 psi atmospheric pressure.

LB agar Media (100 ml)

Add 2.5 g of LB media and 1.5 g of agar in milli-Q water to make a final volume of 100 ml. Sterilized the solution by autoclaving for 20 minutes at 121 ^{o}C and 15 psi atmospheric pressure.

SOC Medium (100ml)

Bacto tryptone = 2 gm

Yeast Extract = 0.5 gm

Glucose = 0.4 gm

NaCl (5 M) = 0.2 ml

KCl (1 M) = 0.25 ml

$MgSO_4$ (1 M) = 1 ml

$MgCl_2$ (1 M) = 1 ml

Adjust the volume to 100 ml with milli-Q water and sterilized the solution by autoclaving for 20 minutes at 121 ^oC and 15 psi atmospheric pressure. Store the solution in 4 ^oC.

Half Strength MS Media (1 L)

MS Salt = 2.155 g

Sucrose = 1 g

Adjust pH with 1 M KOH to 5.9

Add 0.9% of Agar and adjust the volume to 1L with milli-Q water and sterilized the solution by autoclaving for 20 minutes at 121 ^oC and 15 psi atmospheric pressure.

Shoot Inducing Media (SIM) (1 L)

MS Salt = 4.31 g

Sucrose = 3 g

Adjust pH with 1 M KOH to 5.9

Add 0.9% of Agar and adjust the volume to 1L with milli-Q water and sterilized the solution by autoclaving for 20 minutes at 121 ^oC and 15 psi atmospheric pressure. Place the mixture in water bath ~55 ^oC for 10-15 minutes. Add 1 ml of 1000X Vitamins solution, 1 ml of 1mg/l BAP, alpha NAA to final concentration of 0.1mg/l before pouring.

Root Inducing Media (RIM)

MS Salt = 4.31 g

Sucrose = 1 g

Adjust pH with 1 M KOH to 5.9

Add 0.9% of Agar and adjust the volume to 1L with milli-Q water and sterilized the solution by autoclaving for 20 minutes at 121 ^{o}C and 15 psi atmospheric pressure. Place the mixture in water bath ~55 ^{o}C for 10-15 minutes. Add 1 ml of 1000X Vitamins solution, 1 ml of 1mg/l BAP and alpha NAA to a final concentration of 0.1mg/l before pouring.

Appendix C: DNA sequencing Analysis of Final CRISPR Cas9 Construct

3gRNA Positive Construct

(1) For First gRNA

Blue represent gRNA oligos sequence

```
Vector              TTAAGCTATTAACAATCTTCAAAAGTACCACAGCGCTTAGGTAAAGAAAGCAGCTGAGTT
Sequenced_Data      ttaagctattaacaatcttcaaaagtaccacagcgcttaggtaaagaaagcagctgagtt
                    ************************************************************

Vector              TATATATGGTTAGAcACGAAGTAGTGATTGTGAGCAAATCAGATTAGCCGGTTTTAGAGC
Sequenced_Data      tatatatggttagacacgaagtagtgattgtgagcaaatcagattagccggttttagagc
                    ************************************************************

Vector              TAGAAATAGCAAGTTAAAATAAGGCTAGTCCGTTATCAACTTGAAAAAGTGGCACCGAGT
Sequenced_Data      tagaaatagcaagttaaaataaggctagtccgttatcaacttgaaaaagtggcaccgagt
                    ************************************************************
```

(2) For Second gRNA

Blue represent gRNA oligos sequence

```
Vector          CAATCTTCAAAAGTACCACAGCGCTTAGGTAAAGAAAGCAGCTGAGTTTATATATGGTTA
Sequenced       caatcttcaaaagtaccacagcgcttaggtaaagaaagcagctgagtttatatatggtta
                ************************************************************

Vector          GAcACGAAGTAGTGATTGCATGCTTCCTTCTCTTGACTGTTTTAGAGCTAGAAATAGCAA
Sequenced       gacacgaagtagtgattgcatgcttccttctcttgactgttttagagctagaaatagcaa
                ************************************************************

Vector          GTTAAAATAAGGCTAGTCCGTTATCAACTTGAAAAAGTGGCACCGAGTCGGTGCTTTTTT
Sequenced       gttaaaataaggctagtccgttatcaacttgaaaaagtggcaccgagtcggtgctttttt
                ************************************************************
```

(3) For Last gRNA (Reverse sequence used)

Blue represent gRNA oligos sequence

```
Vector              AAAAAAGCACCGACTCGGTGCCACTTTTTCAAGTTGATAACGGACTAGCCTTATTTTAAC
Sequenced_DATA      aaaaaagcaccgactcggtgccacttttcaagttgataacggactagccttattttaac
                    ************************************************************

Vector              TTGCTATTTCTAGCTCTAAAACAGTCAAGAGAAGGAAGCATGCAATCACTACTTCGTgTC
Sequenced_DATA      ttgctatttctagctctaaaacagtcaagagaaggaagcatgcaatcactacttcgtgtc
                    ************************************************************

Vector              TAACCATATATAAACTCAGCTGCTTTCTTTACCTAAGCGCTGTGGTACTTTTGAAGATTG
Sequenced_DATA      taaccatatataaactcagctgctttctttacctaagcgctgtggtacttttgaagattg
                    ************************************************************
```

(4) For Cas9

Purple represent Cas9 sequence

```
Vector              ttgctgatgctaaccttgataaggttctttctgcttacaacaagcacagagataagccaa
Sequenced_DATA      ttgctgatgctaaccttgataaggttctttctgcttacaacaagcacagagataagccaa
                    ************************************************************

Vector              tcagagagcaggctgagaacatcatccacctttcacccttaccaaccttggtgctccag
Sequenced_DATA      tcagagagcaggctgagaacatcatccacctttcacccttaccaaccttggtgctccag
                    ************************************************************

Vector              ctgctttcaagtacttcgataccaccatcgatagaaaaagatacacctctaccaaggagg
Sequenced_DATA      ctgctttcaagtacttcgataccaccatcgatagaaaaagatacacctctaccaaggagg
                    ************************************************************

Vector              ttcttgatgctacccttatccaccagtctatcaccggactttacgagaccagaatcgatc
Sequenced_DATA      ttcttgatgctacccttatccaccagtctatcaccggactttacgagaccagaatcgatc
                    ************************************************************

Vector              tttctcagcttggaggagataagagaccagctgctaccaagaaggctggacaggctaaga
Sequenced_DATA      tttctcagcttggaggagataagagaccagctgctaccaagaaggctggacaggctaaga
                    ************************************************************

Vector              agaagaagtgagacgtccgatcgttcaaacatttggcaataaagtttcttaagattgaat
Sequenced_DATA      agaagaagtgagacgtccgatcgttcaaacatttggcaataaagtttcttaagattgaat
                    ************************************************************
```

For 2gRNA Positive Construct

(1) For First gRNA

Blue represent gRNA oligos sequence

```
Vector              GGCCCATTTAAGCTATTAACAATCTTCAAAAGTACCACAGCGCTTAGGTAAAGAAAGCAG
Sequenced_Data      ggcccatttaagctattaacaatcttcaaaagtaccacagcgcttaggtaaagaaagcag
                    ************************************************************

Vector              CTGAGTTTATATATGGTTAGAcACGAAGTAGTGATTGTGAGCAAATCAGATTAGCCGGTT
Sequenced_Data      ctgagtttatatatggttagacacgaagtagtgattgtgagcaaatcagattagccggtt
                    ************************************************************

Vector              TTAGAGCTAGAAATAGCAAGTTAAAATAAGGCTAGTCCGTTATCAACTTGAAAAAGTGGC
Sequenced_Data      ttagagctagaaatagcaagttaaaataaggctagtccgttatcaacttgaaaaagtggc
                    ************************************************************
```

(2) For Last gRNA (Reverse sequence used)

Blue represent gRNA oligos sequence

```
Vector              ACAGATGAAGAAAAAATCTGAAAATTTTTGCCAAAAAAAAGCACCGACTCGGTGCCACTTT
Sequenced_DATA      acagatgaagaaaaaatctgaaaatttttgccaaaaaaaagcaccgactcggtgccacttt
                    ************************************************************

Vector              TTCAAGTTGATAACGGACTAGCCTTATTTTAACTTGCTATTTCTAGCTCTAAAACTTTGA
Sequenced_DATA      ttcaagttgataacggactagccttattttaacttgctatttctagctctaaaacttttga
                    ************************************************************

Vector              CAGGCACCTTCACACAATCACTACTTCGTgTCTAACCATATATAAACTCAGCTGCTTTCT
Sequenced_DATA      caggcaccttcacacaatcactacttcgtgtctaaccatatataaactcagctgctttct
                    ************************************************************

Vector              TTACCTAAGCGCTGTGGTACTTTTGAAGATTGTTAATAGCTTAAATGGGCCTATTTTAGA
Sequenced_DATA      ttacctaagcgctgtggtacttttgaagattgttaatagcttaaatgggcctattttaga
                    ************************************************************
```

(3) For Cas9

Purple represent Cas9 sequence

```
Vector              ttgatgagatcatcgagcaaatctctgagttctctaagagagttatccttgctgatgcta
Sequenced_Data      ttgatgagatcatcgagcaaatctctgagttctctaagagagttatccttgctgatgcta
                    ************************************************************

Vector              accttgataaggttctttctgcttacaacaagcacagagataagccaatcagagagcagg
Sequenced_Data      accttgataaggttctttctgcttacaacaagcacagagataagccaatcagagagcagg
                    ************************************************************

Vector              ctgagaacatcatccacctttcacccttaccaaccttggtgctccagctgctttcaagt
Sequenced_Data      ctgagaacatcatccacctttcacccttaccaaccttggtgctccagctgctttcaagt
                    ************************************************************

Vector              acttcgataccaccatcgatagaaaaagatacacctctaccaaggaggttcttgatgcta
Sequenced_Data      acttcgataccaccatcgatagaaaaagatacacctctaccaaggaggttcttgatgcta
                    ************************************************************

Vector              cccttatccaccagtctatcaccggactttacgagaccagaatcgatctttctcagcttg
Sequenced_Data      cccttatccaccagtctatcaccggactttacgagaccagaatcgatctttctcagcttg
                    ************************************************************

Vector              gaggagataagagaccagctgctaccaagaaggctggacaggctaagaagaagaagtgag
Sequenced_Data      gaggagataagagaccagctgctaccaagaaggctggacaggctaagaagaagaagtgag
                    ************************************************************
```

3gRNA Negative Construct

(1) For first gRNA position

Green represent first gRNA Position

```
Vector              CTAAAATAGGCCCATTTAAGCTATTAACAATCTTCAAAAGTACCACAGCGCTTAGGTAAA
Sequenced_DATA      ctaaaataggcccatttaagctattaacaatcttcaaaagtaccacagcgcttaggtaaa
                    ************************************************************

Vector              GAAAGCAGCTGAGTTTATATATGGTTAGAcACGAAGTAGTGATTGgagacgagatctagt
Sequenced_DATA      gaaagcagctgagtttatatatggttagacacgaagtagtgattggagacgagatctagt
                    ************************************************************

Vector              ctgagtcgaccgtctctGTTTTAGAGCTAGAAATAGCAAGTTAAAATAAGGCTAGTCCGT
Sequenced_DATA      ctgagtcgaccgtctctgttttagagctagaaatagcaagttaaaataaggctagtccgt
                    ************************************************************

Vector              TATCAACTTGAAAAAGTGGCACCGAGTCGGTGCTTTTTTTGGCAAAAATTTTCAGATTTT
Sequenced_DATA      tatcaacttgaaaaagtggcaccgagtcggtgctttttttggcaaaaattttcagatttt
                    ************************************************************
```

(2) For last gRNA position (reverse sequence used)

Green represent last gRNA Position

```
Vector              AGAAAAAATCTGAAAATTTTTGCCAAAAAAAGCACCGACTCGGTGCCACTTTTTCAAGTT
Sequenced_Data      agaaaaaatctgaaaatttttgccaaaaaaagcaccgactcggtgccacttttttcaagtt
                    ************************************************************

Vector              GATAACGGACTAGCCTTATTTTAACTTGCTATTTCTAGCTCTAAAACagagacggtcgac
Sequenced_Data      gataacggactagccttattttaacttgctatttctagctctaaaacagagacggtcgac
                    ************************************************************

Vector              tcagactagatctcgtctcCAATCACTACTTCGTgTCTAACCATATATAAACTCAGCTGC
Sequenced_Data      tcagactagatctcgtctccaatcactacttcgtgtctaaccatatataaactcagctgc
                    ************************************************************

Vector              TTTCTTTACCTAAGCGCTGTGGTACTTTTGAAGATTGTTAATAGCTTAAATGGGCCTATT
Sequenced_Data      tttctttacctaagcgctgtggtacttttgaagattgttaatagcttaaatgggcctatt
                    ************************************************************
```

(3) For Cas9

Purple represent Cas9 sequence

```
Vector              ctgcttacaacaagcacagagataagccaatcagagagcaggctgagaacatcatccacc
Sequenced_Data      ctgcttacaacaagcacagagataagccaatcagagagcaggctgagaacatcatccacc
                    ************************************************************
```

```
Vector              ttttcacccttaccaaccttggtgctccagctgctttcaagtacttcgataccaccatcg
Sequenced_Data      ttttcacccttaccaaccttggtgctccagctgctttcaagtacttcgataccaccatcg
                    ************************************************************

Vector              atagaaaaagatacacctctaccaaggaggttcttgatgctacccttatccaccagtcta
Sequenced_Data      atagaaaaagatacacctctaccaaggaggttcttgatgctacccttatccaccagtcta
                    ************************************************************

Vector              tcaccggactttacgagaccagaatcgatctttctcagcttggaggagataagagaccag
Sequenced_Data      tcaccggactttacgagaccagaatcgatctttctcagcttggaggagataagagaccag
                    ************************************************************

Vector              ctgctaccaagaaggctggacaggctaagaagaagaagtgagacgtccgatcgttcaaac
Sequenced_Data      ctgctaccaagaaggctggacaggctaagaagaagaagtgagacgtccgatcgttcaaac
                    ************************************************************
```

For 2gRNA Negative Construct

(1) For first gRNA position

Green represent the position of First gRNA

```
Vector              ATTAACAATCTTCAAAAGTACCACAGCGCTTAGGTAAAGAAAGCAGCTGAGTTTATATAT
Sequenced_DATA      attaacaatcttcaaaagtaccacagcgcttaggtaaagaaagcagctgagtttatatat
                    ************************************************************

Vector              GGTTAGAcACGAAGTAGTGATTGgagacgagatctagtctgagtcgaccgtctctGTTTT
Sequenced_DATA      ggttagacacgaagtagtgattggagacgagatctagtctgagtcgaccgtctctgtttt
                    ************************************************************

Vector              AGAGCTAGAAATAGCAAGTTAAAATAAGGCTAGTCCGTTATCAACTTGAAAAAGTGGCAC
Sequenced_DATA      agagctagaaatagcaagttaaaataaggctagtccgttatcaacttgaaaaagtggcac
                    ************************************************************
```

(2) For last gRNA position (Reverse sequence used)

Green represent last gRNA Position

```
Vector              TGAAAATTTTTGCCAAAAAAAGCACCGACTCGGTGCCACTTTTTCAAGTTGATAACGGAC
Sequenced_DATA      tgaaaatttttgccaaaaaaagcaccgactcggtgccacttttttcaagttgataacggac
                    ************************************************************

Vector              TAGCCTTATTTTAACTTGCTATTTCTAGCTCTAAAACagagacggtcgactcagactaga
Sequenced_DATA      tagccttattttaacttgctatttctagctctaaaacagagacggtcgactcagactaga
                    ************************************************************

Vector              tctcgtctcCAATCACTACTTCGTgTCTAACCATATATAAACTCAGCTGCTTTCTTTACC
Sequenced_DATA      tctcgtctccaatcactacttcgtgtctaaccatatataaactcagctgctttctttacc
                    ************************************************************
```

```
Vector              TAAGCGCTGTGGTACTTTTGAAGATTGTTAATAGCTTAAATGGGCCTATTTTAGAAAAAG
Sequenced_DATA      taagcgctgtggtacttttgaagattgttaatagcttaaatgggcctatttagaaaaag
                    ************************************************************
```

(3) For Cas9

Purple represent Cas9 sequence

```
Vector_Map          atgctaaccttgataaggttctttctgcttacaacaagcacagagataagccaatcagag
Sequenced_Data      atgctaaccttgataaggttctttctgcttacaacaagcacagagataagccaatcagag
                    ************************************************************

Vector_Map          agcaggctgagaacatcatccacctttcacccttaccaaccttggtgctccagctgctt
Sequenced_Data      agcaggctgagaacatcatccacctttcacccttaccaaccttggtgctccagctgctt
                    ************************************************************

Vector_Map          tcaagtacttcgataccaccatcgatagaaaaagatacacctctaccaaggaggttcttg
Sequenced_Data      tcaagtacttcgataccaccatcgatagaaaaagatacacctctaccaaggaggttcttg
                    ************************************************************

Vector_Map          atgctacccttatccaccagtctatcaccggactttacgagaccagaatcgatctttctc
Sequenced_Data      atgctacccttatccaccagtctatcaccggactttacgagaccagaatcgatctttctc
                    ************************************************************

Vector_Map          agcttggaggagataagagaccagctgctaccaagaaggctggacaggctaagaagaaga
Sequenced_Data      agcttggaggagataagagaccagctgctaccaagaaggctggacaggctaagaagaaga
                    ************************************************************

Vector_Map          agtgagacgtccgatcgttcaaacatttggcaataaagtttcttaagattgaatcctgtt
Sequenced_Data      agtgagacgtccgatcgttcaaacatttggcaataaagtttcttaagattgaatcctgtt
                    ************************************************************
```

Appendix D: Molecular Weight Calculation of Subcellular Fractionation

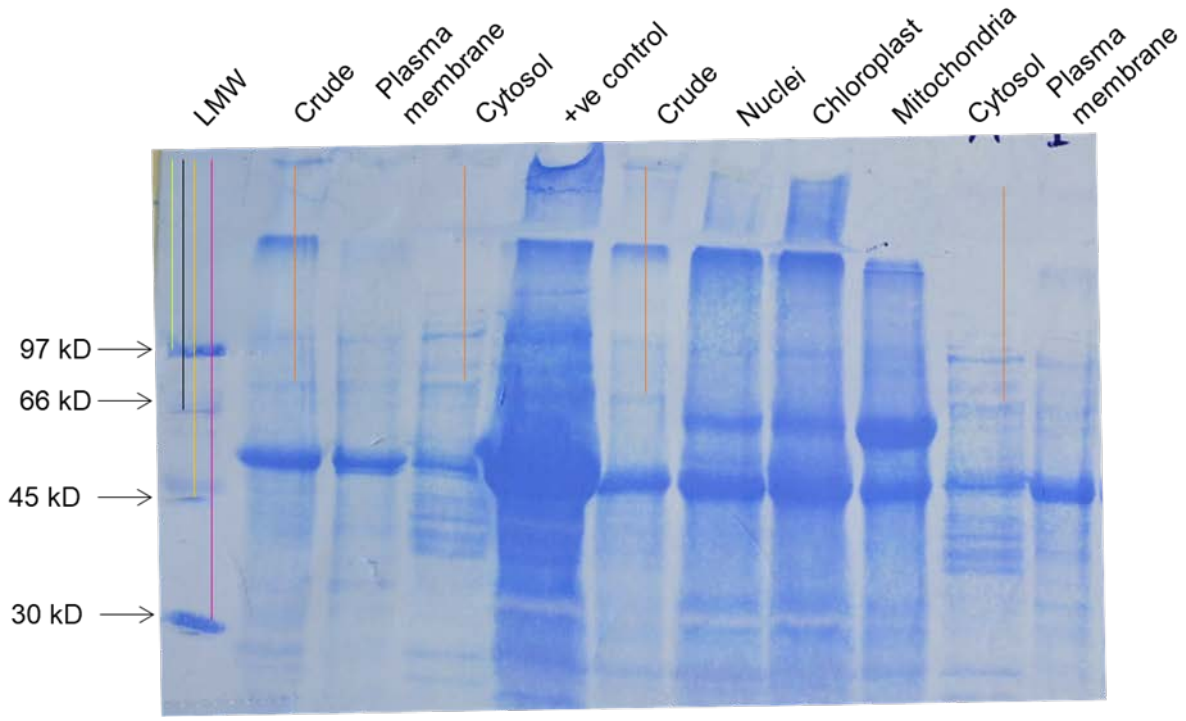

Figure 48: Relative Migration Distance (Rf) of Maker and SIP68+eGFP.

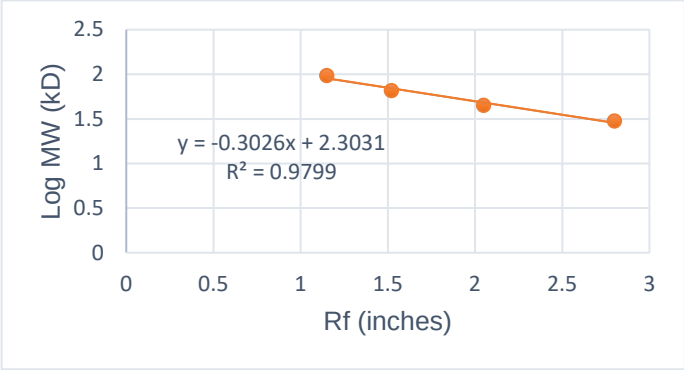

Molecular Weight	Log MW (kD)	Rf (inches)
97 kD	1.9868	1.15
66 kD	1.8195	1.52
45 kD	1.6532	2.05
30 kD	1.4771	2.08
Sip68+eGFP	1.9097	1.3

Log molecular weight of SIP68+eGFP

= -0.3026x+ 2.3031

= 1.9097 kD

Antilog$_{10}$(1.9097) = 81.2269 kD

VITA

SAROJ CHANDRA LOHANI

Education: East Tennessee State University, Johnson City, TN, USA,

MS, Biology, 2018

Tri-Chandra Multiple Campus, Kathmandu, Nepal

MSc, Medical Microbiology, 2014

Tri-Chandra Multiple Campus, Kathmandu, Nepal

BSc, Microbiology, 2010

Professional Experience: Graduate Teaching Assistant, East Tennessee State University, Department of Biological Sciences, Johnson City, TN, USA, 2016-2018

Assistant Research Fellow, Nepal Academy of Science and Technology, Khumaltar, Lalitpur, Nepal, July 2015-July 2016

Adjunct Faculty member, Department of Microbiology, Tri Chandra Multiple Campus, Kathmandu, Nepal, January 2016- July 2016

Presentations: Lohani S, Odesina A, and Kumar D. (2018). SIP68, a Glucosyltransferase Protein and its Role in SABP2

Signaling Pathway, Oral Presentation, American Society of Plant Biologists, New Orleans, Louisiana.

Lohani S, Odesina A, and Kumar D. (2018). SIP68, a Glucosyltransferase Protein and its role in plant Defense Mechanism. Oral Presentation, Appalachian Student Research Forum, Johnson City, TN.

Lohani S, Odesina A, and Kumar D. (2017). Characterization of SIP68 for its Role in SA Mediated Stress Signaling in Plants. Poster presentation, Phytochemical Society of North America, University of Missouri, Columbia.

Lohani S, Odesina A, and Kumar D. (2017). Characterization of SIP68, a Glucosyltransferase Protein and its role in Plant Stress Signaling. Poster presentation, Appalachian Student Research Forum, Johnson City, TN.

Honors and Awards:

Best poster MS Category, 56th Annual meeting of the Phytochemical Society of North America, University of Missouri, Columbia (2017).

Frank and Mary Loewus Travel Award by the Phytochemical Society of North America (2017).

Assistant Research Fellow (ARF), Nepal Academy of Science and Technology (2015).